Addis Ababa University

Addis Ababa University Institute of Technology (AAiT)

School of Electrical and Computer Engineering

# FUZZY AND PLL BASED MPPT SYSTEM DESIGN FOR ENERGY EFFICIENCY OF PV SYSTEM:WITH A CASE STUDY IN SAMARA UNIVERSITY

A thesis Submitted to the Addis Ababa Institute of Technology, School of Graduate Studies, Addis Ababa University in partial Fulfillment of the Requirement for the Degree of Master of Science in Electrical and Computer Engineering (**CONTROL ENGINEERING**)

**By KIROS ABAYE BADASE**

**Advisor: Dr. Dereje Shiferaw**

**January, 2020**

**Addis Ababa, Ethiopia**

Addis Ababa University

Addis Ababa University Institute of Technology

School of Electrical and Computer Engineering

# FUZZY AND PLL BASED MPPT SYSTEM DESIGN FOR ENERGY EFFICIENCY OF PV SYSTEM:WITH A CASE STUDY IN SAMARA UNIVERSITY

**Submitted By:** Kiros Abaye Badase __________ _________

Student Signature Date

**APPROVED BY BOARD OF EXAMINERS**

_____________________________________ ____________ _____________

Chairman, Department of Graduate Committee Signature Date

Dr. Dereje Shiferaw ______________ ___________

Advisor Signature Date

________________________ ___________ ____________

Internal Examiner Signature Date

______________________ ___________ ___________

External Examiner Signature Date

# DECLARATION

I, the undersigned, declare that this thesis is my original work, and has not been presented for a degree in this or other universities, and all sources of materials used for this thesis work have been fully acknowledged.

Name: Kiros Abaye Badase

Signature:_____________

Place: Addis Ababa Institute of Technology, Addis Ababa University, Addis Ababa Ethiopia

This thesis has been submitted for examination with my approval as a university advisor

| Dr.Dereje Shiferaw | _______________ | _____________ |
|---|---|---|
| Advisor | Signature | Date |

# ACKNOWLEDGMENTS

I want to start expressing a sincere acknowledgement to my advisor, **Dr. Dereje Shiferaw** for giving me the opportunity to research under his guidance and supervision. I received motivation, comments, encouragement and continuous guidance from him during my graduate studies.

And to the **Almighty GOD**, may you continue to give me strength and vision that I may follow your path…..to eternal salvation.

Last but not least, I would like to thank my wife for her great encouragement from day to day during my study.

# ABSTRACT

Maximum power point tracking plays an important role for Photovoltaic systems because it optimize the power output from a Pholovoltaic system for a given set of conditions. This thesis presents a maximum power point tracker using artificial intelligence(Fuzzy controller) and Phase locked loop for a Grid Connected Photovoltaic system. The aim of this paper is to improve the dynamic performance of the available photovoltaic (PV) system and maximizing the power obtained from it by the use of cascaded converters with intelligent control techniques. Fuzzy logic based maximum power point technique have embedded in the first conversion stage to obtain the maximum power from the available PV array. The cascading of second converter which is needed to maintain the terminal voltage at grid potential. The soft-switching region of the three-stage converter is increased with the proposed phase-locked loop leads to a reduction in the ripple content, rating of components, and switching losses. The PV array is mathematically modeled and the results will be analyzed. This thesis lead to accomplishing maximum power and improved reliability for the same insolation of the PV system. After designed and sized the proposed system components, each System elements are individually modelled in MATLAB/SIMULINK and then connected to assess performance under different environmental conditions. The system consists of modeled PV Array, Boost converter model, TSSSBC, modeled fuzzy controller, Phase locked loop, inverter, and low pass filter is applied to generate a 24.22kW power by using a boost converter as a supporter for maximum power point traking algorithm by adjusting the duty cycle of the boost converter to maximize the output signal of the solar PV array was optimized using boost converter. The performance of the proposed controllers for energy efficiency of PV system is evaluated through simulation studies. The simulation results show that the efficiency of the photovoltaic system with the fuzzy logic controller is 99.2%, where as the same without any controller is found to be 87%.

**Keywords**: Maximum Power Point Traking (MPPT), Artificial intelligent (AI) , Fuzzy logic (FL), Three stage soft switching boost converter (TSSBC),Phase looked loop(PLL), Photovoltaic (PV).

# Contents

**ACKNOWLEDGMENTS** ..... ii

**ABSTRACT** ..... iii

**List of Figures** ..... viii

**List of Table** ..... xi

**LIST OF SYMBOLS AND ABBREVIATIONS** ..... xii

**CHAPTER ONE** ..... 1

**1. INTRODACTION** ..... 1

**1.1 Background** ..... 1

**1.2 Photovoltaic system** ..... 3

**1.3 Problem statement** ..... 3

**1.4 Research Objectives** ..... 4

**1.4.1 General Objectives** ..... 4

**1.4.2 The Specific Objectives** ..... 4

**1.5 Scope and significance of the thesis** ..... 4

**1.6 Methodology** ..... 5

**1.7 Thesis outlines** ..... 6

**CHAPTER TWO** ..... 7

**CONTROL OF MAXIMUM POWER POINT TRACKING FOR ENERGY EFFICIENCY OF PHOTOVOLTAIC SYSTEM** ..... 7

**2.1 Maximum Power point Tracking (MPPT) System** ..... 7

**2.1.1 Performance specifications of MPPT controller** ..... 8

**2.1.2 DC-DC converter for photovoltaic system** ..... 8

**2.1.3 Step-up (boost) converter** ..... 11

**2.1.4 Cuk (buck-boost) converter** ..... 13

**2.2 Design of Three-Stage Soft-Switching Boost Converter** ..... 16

**2.3 DC-AC converter for photovoltaic system** ..... 17

**2.3.1 Three phase inverter topology** ..... 18

**2.3.2 Sinusoidal pulse widith Modulation in Three-Phase Voltage Source Inverters** ..... 21

**2.3.3 Six Step Voltage Source Inverter** ..... 22

**2.4 Output Filters for photo voltaic system** ..... 24

**2.4.1 L-filter** ..... 25

**2.4.2 LC filter** ........ 25
**2.4.3 LCL filter** ........ 25
**2.5 MPPT Controller algorithms** ........ 26
**2.5.1 Simple panel load matching** ........ 26
**2.5.2 Load switching technique** ........ 27
**2.5.3 Constant voltage method (CV)** ........ 27
**2.5.4 Perturb and observe (P&O) algorithm** ........ 28
**2.5.5 Intelligent control techniques** ........ 29
**2.5.3 Artificial Neural Network** ........ 30
**2.6 Grid Synchronization** ........ 31
**2.6.1 Phase Locked Loop** ........ 31
**CHAPTER THREE** ........ 32
**MODELLING AND DESIGN OF MAXIMUM POWER POINT TRACKING FOR ENERGY EFFICIENCY OF PV SYSTEM** ........ 32
**3.1 Photovoltaic system design** ........ 32
**3.1.1 Photovoltaic cells** ........ 32
**3.1.4 Basic Types of PV cells** ........ 34
**3.2 Simple solar cell modeling** ........ 35
**3.3 General solar cell Modeling** ........ 36
**3.3.1 Module I-V characterstics** ........ 40
**3.3.2 Factors that affecting Solar PV System Performance** ........ 41
**3.3.3 Photovoltaic arrays** ........ 43
**3.4 Design of DC-DC boost converter** ........ 46
**3.4.1 Three-Stage Soft-Switching Boost Converter** ........ 47
**3.4.2 DC Link Design** ........ 49
**3.4.3 Three phase full-bridge inverter design and interfaceing** ........ 49
**3.4.1 Photovoltaic Array – Inverter Interface** ........ 50
**3.4.2 Inverter – load interface** ........ 51
**3.4.3 LCL low pass filter design** ........ 51
**CHAPTER FOUR** ........ 54
**DESIGN OF CONTROLLERS FOR ENERGY EFFICIENCY OF PV SYSTEM** ........ 54
**4.1 Fuzzy logic controller** ........ 54
**4.1.1 Fuzzy logic controller structure** ........ 54

**4.1.2 Knowledge Base** ........ 55
**4.1.3 Fuzzy interface procedure** ........ 55
**4.1.4 Fuzzy logic controller for Energy efficiency of PV system** ........ 57
**4.2 Phase-Locked Loop Controller** ........ 60
**CHAPTER FIVE** ........ 62
**SIMULATION STUDIES AND ANALYSIS OF RESULTS** ........ 62
**5.1 Photovoltaic System modelling using Simulink** ........ 62
**5.1.1 Boost converter modelling** ........ 66
**5.1.2 Three-Stage Soft-Switching Boost Converter Modelling** ........ 67
**5.1.2 DC to AC converter modelling** ........ 69
**5.1.3 LCL Low pass filter modelling** ........ 69
**5.2 Simulink Model of controllers for Energy efficiency of PV system** ........ 70
**5.2.1 Fuzzy logic controller simulink model for Energy efficiency of PV system** ........ 70
**5.2.1 Phase-Locked Loop Controller simulink model for Energy efficiency of PV system** ........ 71
**5.3 Energy efficiency of PV system with and without controllers** ........ 72
**5.3.1 Energy efficiency of PV system simulation without any controller** ........ 73
**5.3.1 Energy efficiency of PV system simulation using fuzzy logic and Phase locked loop controller** ........ 75
**5.4 Performance analysis of controllers** ........ 77
**CHAPTER SIX** ........ 78
**CONCLUSIONS,RECOMMENDATIONS AND FUTUIRE WORKS** ........ 78
**6.1 Conclusions** ........ 78
**6.2 Recommendations** ........ 79
**6.3 Suggestions for future work** ........ 79
**7. References** ........ 80
**APPENDIX A** ........ 85
**A.1 MATLAB functions and scripts of PV panel** ........ 85
**A.1.1 MATLAB Function of the module specifications** ........ 85
**APPENDIX B** ........ 86
**B.1 MATLAB simulation of the PV system** ........ 86
**APPENDIX C** ........ 88
**C.1 Artificial Intelligent MPPT Controllers MATLAB Simulation** ........ 88
**C.1.1 FIS of FLC based MPPT of Energy efficiency of PV system MATLAB SIMULINK** ........ 88

**APPENDIX D** ........................................................ 90

D.1 Artificial Intelligent Fuzzy controller Data From Pv Panel. ........................................................ 90

# List of Figures

Figure 1. 1 General methodology flow chart ... 5
Figure 2. 1 Converter acting as a Maximum Power Point Tracker...7
Figure 2. 2 step-down Buck converter ... 9
Figure 2. 3 Buck converter wave form ... 10
Figure 2. 4 Step-up boost converter ... 11
Figure 2. 5 Step-up converter wave form of the inductor current and voltage in continuous current ... 12
Figure 2. 6 Cuk converter ... 13
Figure 2. 7 cuk converter wave form ... 14
Figure 2. 8 Equivalent circuit diagram of SSSSBC for various modes of operation... 16
Figure 2. 9 Inverter block diagram ... 17
Figure 2. 10 Three-phase full –Bridge Inverter ... 18
Figure 2. 11 PWM illustration by the sine-triangle comparison method... 21
Figure 2. 12 pulse generated by 2-level PWM in Three-Phase VSI ... 22
Figure 2. 13 180° mode Generation of the switching signals for (a) top devices, (b) bottom devices... 23
Figure 2. 14 180° conduction mode six step inverter line voltage (Vab, Vbc & Vca) ... 24
Figure 2. 15 LCL-filter ... 25
Figure 2. 16 Schematic block diagram of the load-switching method ... 27
Figure 2. 17 Voltage feed back MPPT method with constant voltage reference ... 28
Figure 2. 18 perturbs and observes technique... 28
Figure 3. 1 schematic diagram of the proposed model...32
Figure 3. 2 Hole-electron pairs created by photons in p-n junction of PV cell ... 33
Figure 3. 3 connecting solar cells with a load and conducting current... 33
Figure 3. 4 Photovoltaic Hierarch... 34
Figure 3. 5 Mono-crystalline PV cell... 34
Figure 3. 6 Poly-crystalline PV cell. ... 34
Figure 3. 7 Amorphous PV cell. ... 35

Figure 3. 8 simple equivalent circuit of PV cell ........ 35
Figure 3. 9 open circuit and short circuit ........ 36
Figure 3. 10 Equivalent circuit of a general solar cell ........ 36
Figure 3. 11 solar cell I-V characteristics curve ........ 40
Figure 3. 12 (a) V-P (b) V-I characteristics at constant ambient temperature (STD)........ 42
Figure 3. 13 (a) V-I characteristics (b) V-P characteristics of PV module at fixed irradiance level........ 43
Figure 3. 14 The proposed real PV array series parallel structure........ 45
Figure 3. 15 Proposed Boost converter........ 46
Figure 3. 16 Circuit diagram for three-stage soft-switching boost converter. ........ 48
Figure 3. 17 The proposed three phase full bridge PWM inverter ........ 50
Figure 3. 18 LCL proposed Filter ........ 52
Figure 4. 1 General diagram of a fuzzy controller........54
Figure 4. 2 Schematic diagram of the proposed FLC MPPT based Energy Efficiency of PV system. ........ 57
Figure 4. 3 Schematic diagram of the proposed PLL based Energy Efficiency of PV system. ... 60
Figure 4. 4 Block diagram of phase-locked loop. ........ 60
Figure 5. 1 Connection of Eleven PV array in parallel........62
Figure 5. 2 Embedded PV Array or PV panel SIMULINK model. ........ 63
Figure 5. 3 Simulink model for data collecting system of PV array........ 64
Figure 5. 4 V-I and V-P characteristics of the PV array at standard irradiation level. ........ 65
Figure 5. 5 V-I and V-P characteristics of PV array at standard temperature ........ 66
Figure 5. 6 Simulation model of DC-DC Boost converter ........ 66
Figure 5. 7 Boost converter one block representation ........ 67
Figure 5. 8 Simulation circuit of three-stage soft-switching boost converter........ 68
Figure 5. 9 TSSSBC one block representation ........ 68
Figure 5. 10 Simulink models of three phase inverter........ 69
Figure 5. 11 Simulink model of LCL filter........ 69
Figure 5. 12 SIMULINK block of fuzzy logic controller........ 70
Figure 5. 13 SIMULINK block of phase locked loop controller........ 71
Figure 5. 14 General Simulink model of the PV systems........ 72
Figure 5. 15 Different level of solar irradiation and temperature values for testing system performance ........ 73
Figure 5. 16 PV array output current at different environments........ 73
Figure 5. 17 PV array output voltage at different condition. ........ 74
Figure 5. 18 The PV panel output power in direct connection systems ........ 74

Figure 5. 19 The output three phase voltage and current of the PV system at different conditions ........................................................................................................................... 75
Figure 5. 20 Duty cycle signal output of FLC for different level of temperatures and irradiations ........................................................................................................................... 75
Figure 5. 21 Boost output voltage based on FLC PV systems.................................................... 75
Figure 5. 22 Boost current based on FLC and Direct connection PV systems........................... 76
Figure 5. 23 Output power in KW based on FLC PV systems.................................................. 76
Figure 5. 24 Three phase output voltage based on PLL controller.............................................. 76

# List of Table

Table 2. 1 Current and voltage equations of SSSSBC for various modes .................................. 17
Table 2. 2 Eight state of three phase inverter .................................................................. 19
Table 2. 3 Characteristics of different MPPT techniques .................................................... 31
Table 3. 1Polycrystalline PV module specifications at standard test conditions-----------------------------39
Table 3. 2 The proposed module and array value ................................................................ 46
Table 3. 3 Boost converter parameters. ................................................................................ 47
Table 3. 4 Specifications of the components. ...................................................................... 49
Table 3. 5 Specifications of three phase H-bridge inverter .................................................. 51
Table 3. 6 LCL filter specification ........................................................................................ 53
Table 4. 1 fuzzy rule base table............................................................................................59
Table 5. 1 The proposed module and array value……………………….........................................................63
Table 5. 2 Fuzzy logic controller parameter ........................................................................ 70
Table 5. 3 phase locked loop parameter ................................................................................ 71
Table 5. 4 The controller output at different level of environmental condition .......................... 77
Table 5. 5 Performance compression of Fuzzy logic controller and direct connection ............... 77
Table D.1. 1 The data set collected for Fuzzy logic controller---------------------------------------------------90

# LIST OF SYMBOLS AND ABBREVIATIONS

| | |
|---|---|
| ANFIS | Artificial Neuro Fuzzy Inference System |
| AC | Alternating Current |
| ANFISC | Artificial neuro Fuzzy Inference System controller |
| ANN | Artificial Neural Network |
| Cb | Boost capacitor |
| Cf | Filter capacitance |
| COG | Centre of Gravity |
| D | Duty cycle |
| DC | Direct Current |
| FIS | Fuzzy Interface System |
| FL | Fuzzy Logic |
| FLC | Fuzzy Logic Control |
| Ꞙo | Resonant frequency |
| G | Photovoltaic cell‟s operating irradiation |
| Imp | Maximum power point voltage at reference condition |
| Ipv | Output current of the solar cell |
| Isc | Short Circuit current |
| LCL | Inductor capacitor inductor low pass filter |
| Lb | Boost inductor |
| INC | Incremental conductance |
| INR | Incremental resistance |
| ISSBC | Interleaved soft Switching boost converter |
| MPP | maximum power point |
| MPPT | maximum power point tracking |
| MOM | Mean of maximum method |
| ɳ | Tracking efficiency |

| | |
|---|---|
| NP | Number of connected PV cells in parallel |
| NS | Number of connected PV cells in series |
| Pinv | Rated output power of inverter. |
| Pmax | Maximum power point |
| Pout | Output power of the converter |
| Ppv | Output power of the solar cell |
| PIC | Programing logic control |
| PLL | Phase locked loop |
| PV | Photovoltaic |
| PWM | pulse width modulation |
| RMS | Root mean square |
| Rs | Series resistance of the photovoltaic cell |
| Rsh | Shunt resistance of the photovoltaic cell |
| T | Photovoltaic cell"s operating temperature |
| Tc | Photovoltaic cell"s operating temperature in kelvin |
| Toff | Off period of converter switch |
| Ton | On period of converter switch |
| Ts | DC/DC converter switching period |
| TSSSBC | Three stage soft switching boost converter |
| Vdc | Output voltage of the boost converter |
| Vmp | Voltage at maximum power of the PV array |
| Voc | Open Circuit voltage |
| Vpv | Output voltage of the solar cell |

# CHAPTER ONE

# 1. INTRODACTION

## 1.1 Background

The steady increase in demand for power supply with overexploited decreasing conventional sources increases the necessity for alternative energy sources. Energy has the great importance for our life and economy. The energy demand has greatly increased due to the industrial revolution. Fossil fuels have been started to be gradually depleted. The sustainability of our civilization is seriously threatened. Photovoltaic (PV) array, using solar energy as a source, is a better option as it provides a pollution-free, easily available, clean energy source[1].

For a grid area application, PV array can be used as a source of energy in conjunction with the existing conventional source[1]. A PV system converts photon energy from sunlight into electricity. With PV panel prices dropping and the desire to “go green” expanding, demand for PV power is improving. As the efficiency of a PV array is much less, it becomes imperative to extract the maximum available power out of it. Various maximum power point tracking (MPPT) techniques are available to extract maximum power available from the solar energy. According to the maximum power transfer theorem, if the source impedance is equal to the load impedance, maximum energy can be transferred from the source to the load. The inclusion of DC-DC converter with MPPT technique varies the equivalent impedance, thereby matching the load resistance to achieve maximum power transfer. The DC power from solar array is boosted and fed to an inverter which gives AC to the inverter that drives the Energy efficiency of pv system[2]. The output power of a Photovoltaic (PV) array varies according to the sunlight conditions such as solar irradiation, shading and temperature. To obtain maximum power from photovoltaic array, photovoltaic power system usually requires maximum power point tracking (MPPT) controller [3]. The perturb and observe (P&O) method is the simplest method. Maximum power control is achieved by forcing the derivative of the power to be equal to zero under power feedback control. But this method produces oscillations closer to the maximum power point, thereby raising the response time. Incremental conductance process traces the maximum power by observing the conductance. It uses $dI/dV$ and compares it with $I/V$, thereby adjusting the step size to track the maximum power point of PV array. Incremental resistance (INR) is similar to INC except that it compares *dV*/*dI* with *V*/*I* for tracking maximum power point[4-7]. Fuzzy logic control is an artificial intelligence technique which can be used to track the maximum power point ,to improve the performance of the system. As there is fuzziness in the input for PV array like change in insolation, temperature, and shading effects during the entire day, this logic is more suitable than the other methods for tracking maximum power point. In addition, this system does not require the knowledge of the exact model. To transmit the power at the required voltage and current level from the PV array to the load, boost converter is used. The interleaved soft switching boost converter (ISSBC) shares the input current all along each phase, thereby decreasing the current rating of the switching device[8-9].

The ripple content present in the input current and the output voltage and the size of the passive components are also reduced in this converter. The problems caused due to switching loss, and diode recovery loss can be overcome by using the resonant soft-switching technique. This technique does have certain limitations. The fidelity of the PWM signal to the analog input is determined by the linearity of the ramp-wave signal. The performance of the comparator determines speed, accuracy.

Phase locked loops (PLL) synchronize a local voltage-controlled oscillator (VCO) to an external frequency input by means of an electronic servo loop. It is used with converter to achieve constant operating frequency over a wide output voltage range, eliminating the dependence of switching frequency on duty cycle or voltage conversion range. In the present work, to improve the dynamic performance of the PV system, cascaded converter topology is used with intelligent power tracker and modified control strategy. The first conversion stage uses the fuzzy logic controller to track the maximum power. The phase-locked loop is used in the cascaded three-stage converter to extend the soft-switching region to minimize the losses. The interleaved soft-switching technique available in the literature is extended in the present work for a three-stage converter for improved efficiency. In addition, the power handling capability is improved and the ripple content of the output is reduced. The PLL control scheme prevents the operating frequency of the circuit from being lower than the resonant frequency[10-11].

Therefore in this thesis an artificial intelligent control technique associated with MPPT controller are used to improve energy conversion efficiency of the photovoltaic system. The proposed intelligent process comprises of expert knowledge which extracts maximum power from a PV module under varying solar irradiation and temperature[5]. . In this work, phase-locked loop is implemented to maintain the required frequency of operation with reduced ripple and to increase the soft-switching range of operation. The PV array was mathematically modeled using the basic equations to match the actual parameters of the nonlinear model.

### 1.2 Photovoltaic system

The photovoltaic system consists of interconnected components designed in a way to achieve the specific target of delivering the desired electricity from a small device to the load. Photovoltaic systems are categorized by the main categories of grid connected, standalone systems and hybrid system which comprises different sources of energy such as PV arrays, diesel generators and wind generators. In the grid connected and the stand-alone systems, storage elements such as batteries or super capacitors may be adopted to store the energy during the day time when there is enough sunshine. Hybrid and stand-alone systems are used increasingly in rural areas. Therefore, the PV system considered in this thesis is a grid connected system to fulfil the urgent needs of people in the rural locations. The power from the photovoltaic array in the grid connected system is directly fed to the load with connection to the utility system.

## 1.3 Problem statement

The need for renewable energy sources is on the rise because of the acute energy crisis in Samara University. There is an inherent tracking-oscillations trade-off problem in Perturb and Observe (P&O) maximum power point tracking (MPPT) technique for photovoltaic (PV) system. The P & O method of maximum power point tracking (MPPT) and INC method are simple and easy to be implemented. However, P & O method yields two weaknesses namely power oscillation at maximum power point (MPP) and divergence of MPP under rapid atmospheric change. The INC method also yields the same problem as P & O MPPT method. Hence in this thesis, Fuzzy logic controller method will yield fast convergence to MPP and minimal oscillation around MPP.

## 1.4 Research Objectives

### 1.4.1 General Objectives

The main objective of this thesis is to design Fuzzy and PLL based on MPPT system design for energy efficiency of PV system.

### 1.4.2 The Specific Objectives

To achive the the general objectivies of the thesis the following specific objectives will be done:

- To design a PLL and FUZZY logic controller for MPPT of a PV system.
- To implement the designed controller using MATLAB/SIMULINK.
- To analyze the performance of the FUZZY controller.

## 1.5 Scope and significance of the thesis

The scope of this thesis is to investigate how to improve the MPPT based PV system, fuzzy and PLL based MPPT system design for energy efficiency of PV system controller, then implement the system using the available mathematical computation tools MATLAB /SIMULINK to evaluate the performance. In this thesis the application of artificial intelligence controller is signify in a time of hard non-linear systems occur to control a system like a linear one and the thesis up grades the detail knowledge of internal characteristics of maximum power point tracking (MPPT) in different techniques. This study also increases the penetration of PV energy which is a renewable and environmental friendly energy source.

## 1.6 Methodology

The methodologies that we followed in this thesis are listed by the following chart.

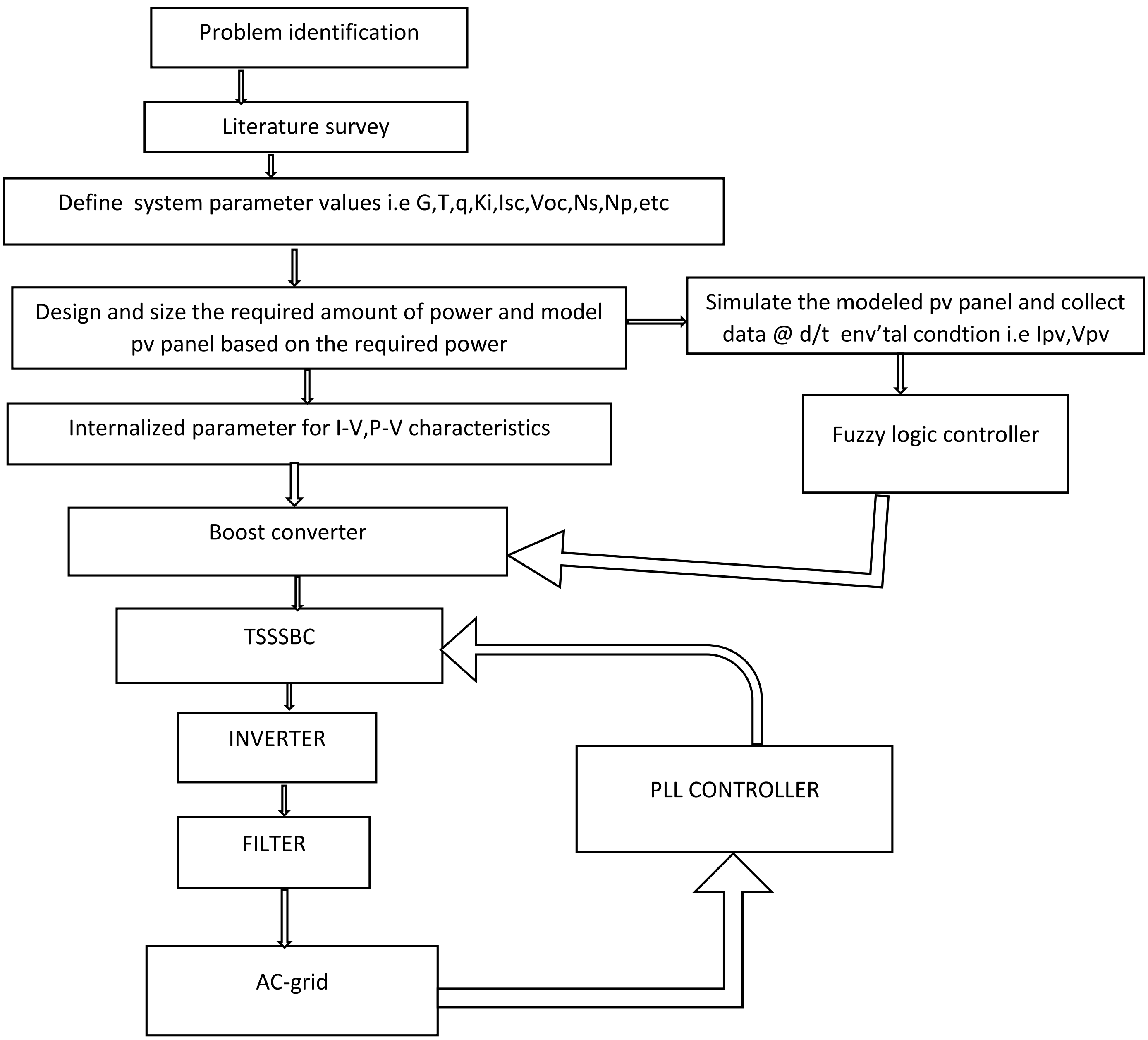


Figure 1. 1 General methodology flow chart

## 1.7 Thesis outlines

This thesis contains totally six chapters and the content of each chapters are disused below.

Chapter one is an introductory chapter and presents an overview of the thesis background, objectives, scope and significance and a brief summary of the thesis. It presents a brief introduction to PV energy, and how to increasing the Energy efficiency of PV systems attractive and economically viable in remote locations.

Chapter two provides a review of the literature on some components of Energy Efficiency of PV systems and the MPPT algorithms with controlling techniques and Performance specifications of MPPT control algorithm techniques are presented and briefly explained.

Chapter three contains the modeling and design the Energy efficiency of PV System. In this chapter the design of MPPT for Energy Efficiency of PV system and the modelling of the whole components of the PV system and its operation is discussed detail is done.

Chapter four introduces the design of controllers for Grid system. In this chapter discussed detail in artificial intelligent controller techniques and Phase locked loop controller. It provides a fuzzy logic control development and applications, and illustrates its basic structure and the working principles. This chapter also provides a brief explanation of the working principles of the PLL. it gives brief explanation and working principles of ANFIS controller and finally discussion of each control based MPPT method for the Energy Efficiency of PV system is presented.

Chapter Five presents the MATLAB/SIMULINK implementation results of the system and describes each of the subsystems in detail. This chapter also discusses and compares the MATLAB results for the proposed maximum power-point tracking algorithms applied for energy efficiency of photovoltaic system. It also shows the behavior and performance of each method under similar conditions of temperature and irradiation and

chapter six conclusions and contribution summary of the thesis are presented. Moreover, potential research ideas for future work in this field are proposed.

# CHAPTER TWO

# CONTROL OF MAXIMUM POWER POINT TRACKING FOR ENERGY EFFICIENCY OF PHOTOVOLTAIC SYSTEM

## 2.1 Maximum Power point Tracking (MPPT) System

MPPT is basic for photovoltaic generation to operate the system at high power efficiency by ensuring that, the system is always working at the peak power point in a time of changes weather conditions. In other words transfer the maximum power to the load by matching the source impedance with the load impedance. To confirm that, an MPPT system has been implemented, which enables the maximum power to be delivered during the operation of the solar array and which tracks the variations in maximum power caused by the changes in the atmospheric conditions. The MPPT system is basically an electronic device inserted between the PV array and the load. A DC-DC switching power converter or DC-AC inverter along with an MPPT control algorithm to operate the PV system in such way it can transfer the maximum capable power to the load.As the solar panel outputs power, maximum generated power changes with the atmospheric conditions and the electrical characteristic of the load may also vary. The main objective of the MPPT is to match these two parameters by adjusting the duty ratio of the power converter [7]. The matching of MPP illustrate as the following Fig.

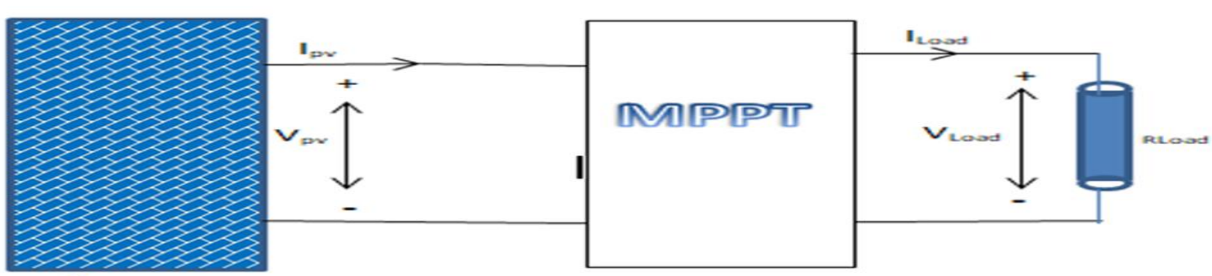


PV array

Figure 2. 1 Converter acting as a Maximum Power Point Tracker

### 2.1.1 Performance specifications of MPPT controller

The dynamic response, steady-state error and tracking efficiency would be considered for a successful design when evaluating the performance of a new or modified MPPT control algorithms [7].

## The dynamic response

The Response of a MPPT control algorithm needs to be fast to track the MPP during the rapid changes in the atmospheric conditions. The higher the tracking speed of the MPPT algorithm, the lower the loss in solar energy in the system

## Steady-state error

MPPT control algorithm should stop tracking, once the MPP is located and should force the system to maintain operation at this optimal operating point as long as possible. However, this is impossible to achieve practically in an actual MPPT system because of the active perturbation process in MPPT algorithms and the continuous variation in solar insolation and temperature. This phenomenon has a negative impact on the PV system efficiency.

## Tracking efficiency

The tracking efficiency is a very important step, to quantify how successfully an MPPT control algorithm tracks the MPP and to what extent it contributes to increase the overall performance of the PV system compared to other methods. According to [8] the tracking efficiency is defined as the ratio between the actual power of the PV array and the theoretical power during the same time period. To calculate the tracking efficiency we have use the following equation

$$\eta mppt=\frac{1}{n}\sum_{i}^{n}\frac{Pactual,i}{Pmax,i} \qquad (2.1)$$

### 2.1.2 DC-DC converter for photovoltaic system

The switch mode DC-DC converter is considered the main part of a MPPT system. These are widely used to convert unregulated DC inputs into a controlled DC output at a desired voltage and current levels in DC power supplies or as input of the inverte [9]. The same converter is used for a MPPT to provide load matching for the maximum power transfer by regulating the input voltage at the PV array MPP by controlling the duty ratio (D). DC-DC converters are used to interface the photovoltaic module with an inverter, in order to ensure the photovoltaic module is always operating at the maximum power point to get the desired input voltage level to the inverter. This is done by controlling the converter duty ratio (D) with maximum power point tracking algorithms (MPPT). Generally, converters are categorized into two types: isolated and non-isolated converters. In the isolated topologies a small high frequency electrical isolation transformer is used to provide the DC isolation between the input and output of the DC converter; and step up or down of the output voltage is achieved by changing the transformer turns ratio.

Non-isolated converters are classified into three types: step up (boost), step down (buck), and step up & step down (buck-boost).

### 2.1.2.1 Step-down (buck) converter

In this type of DC-DC converter, the average output voltage Vo produced is always lower than the DC input voltage. The buck converter is used for voltage step-down in PV applications, such as for charging batteries and in water pumping systems.

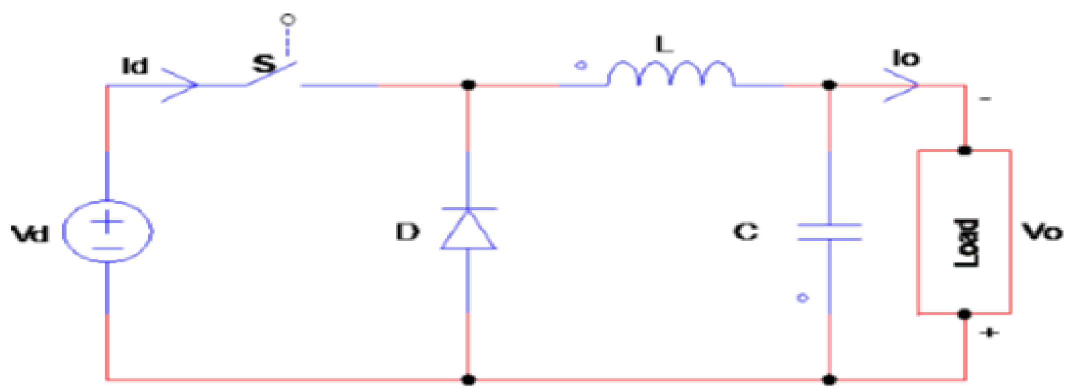


Figure 2. 2 step-down Buck converter

The diode (d) is used to enhance the output filtering effect and prevent the switch from absorbing or dissipating the inductive energy because this would lead to overheating the switch. In addition to that, there is an inductor and capacitor at the output of the converter which forms a low-pass filter to attenuate the output voltage fluctuation. Thus the diode enables the converter to convert stored energy in the inductor to the load. This is a reason why we have higher efficiency in a DC-DC Converters as compared to a linear regulator. When the switch closes, the current rises linearly. When the switch opens, the freewheeling diode causes a linear decrease in current. The function of the inductor is to limit the current slew rate (current in rush) through the power switch when the circuit is ON. The current through the inductor cannot change suddenly. When the current through an inductor tends to fall, the inductor tends to maintain the current by acting as a source. The key advantage is when the inductor is used to drop voltage, it stores energy. Also the inductor controls the percent of the ripple and determines whether or not the converter is operating in the continuous conduction mode. The smaller inductor value enables a faster transient response; it also results in larger current ripple, which causes higher conduction losses in the switches, inductor, and parasitic resistances. Also the smaller inductor value requires a larger filter capacitor to decrease the output voltage ripple.

The capacitor provides the filtering action by providing a path for the harmonic currents away from the load. Output capacitance (across the load) is required to minimize the voltage overshoot and ripple present at the output of a step-down converter.

The capacitor is large enough so that its voltage does not have any noticeable change during the time of switch is off [9].

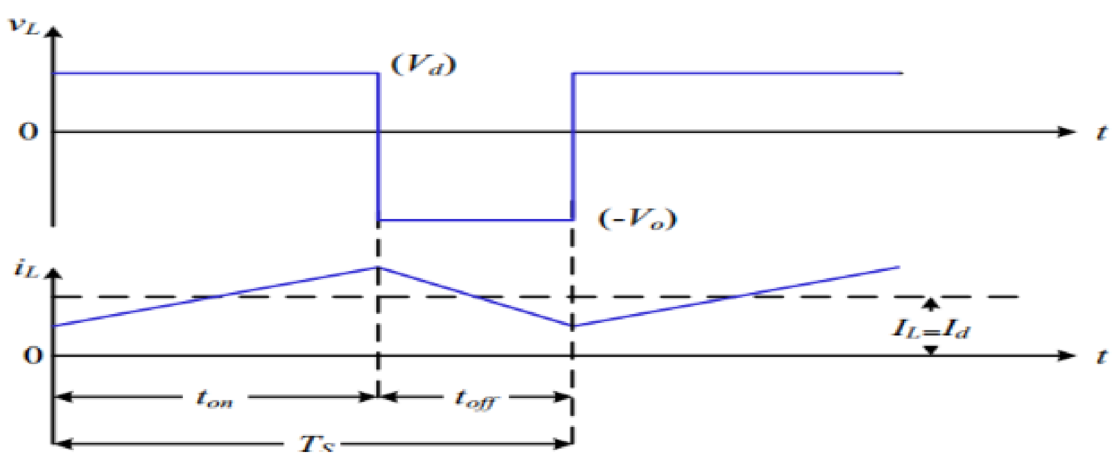


Figure 2. 3 Buck converter wave form

During the steady-state condition the relation between the output voltage Vo and the duty ratio of the converter can be defined by the following equation.

$$\frac{Vo}{Vd} = \frac{D}{1-D} \qquad (2.2)$$

From the above equation the output voltage could be higher or lower than the input voltage according to the value of the duty ratio. For the duty ratio condition D > 0.5, the output is higher than the input as in a boost converter. If D < 0.5 the output is lower than the input as in a buck converter.

$$L = \frac{(1-D)^2 R}{2Fs} \quad (2.3)$$

$$C = \frac{D}{RFs(\frac{\Delta Vo}{Vo})} \quad (2.4)$$

### 2.1.3 Step-up (boost) converter

The applications of boost converter operation and in regulated DC power supplies. In this type of converter the output voltage is always greater than the input voltage. Therefore the step up converter can be applied to MPPT systems where the output voltage needs to be greater than the input voltage. Such as in a grid-connected system where the boost converter maintains a high output voltage even if the PV array voltage falls to low values.

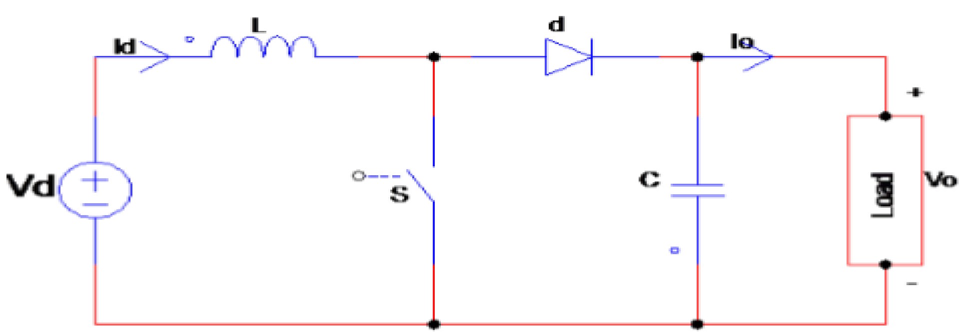


Figure 2. 4 Step-up boost converter

When the switch S is on the diode d is reverse based. Consequently, the current in the inductor L rises linearly due to the input voltage source, and in this case the output stage is isolated and the capacitor (C) is partially discharged supplying the current load. When the switch is off during the second interval the diode is conducting, and during this time the output stage receives energy from both the inductor and the input source. The wave form of the inductor current during continuous conduction mode is shown below, where the inductor current flows continuously, i.e. IL(t) > 0 [9].

A dual stage power electronic system comprising a boost type dc-dc converter and an inverter is used to feed the power generated by the PV array to the load. To maintain the load voltage constant a DC-DC step up converter is introduced between the PV array and the inverter. The DC-DC converter is considered the main part of a MPPT system. These are widely used to convert unregulated DC inputs into a controlled DC output at a desired voltage and current levels in DC power supplies. The voltage across the DC-DC converter is fed to a three-phase, sine wave six step inverter a three-phase fixed amplitude and fixed frequency supply is obtained to feed an inverter as input. When the converter is operating at steady-state condition, the duty ratio (D), can be expressed by Equation

$$D = 1 - \frac{Vd{-}min}{Vout}\eta \qquad (2.5)$$

Where D denotes the duty ratio, (assume $\eta \approx 1$ )efficiency, Vd and Vout denotes the input and the output voltages of the converter, respectively. From the above equation it can be seen that, the increase in the duty ratio D will increase the value of the output voltage, Vout. In addition the change in the duty ratio results in change in the input and the output current of the converter.

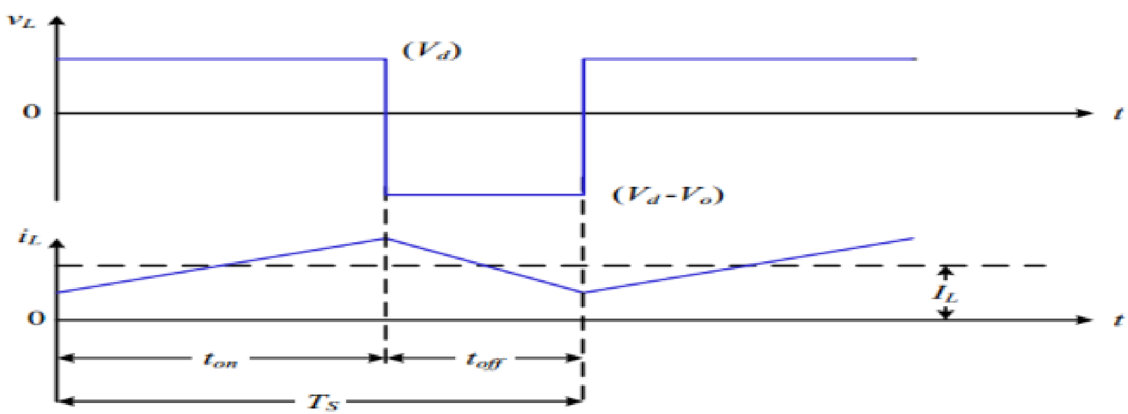


Figure 2. 5 Step-up converter wave form of the inductor current and voltage in continuous current

The filter inductor and capacitor to oprate the converter in the continuous conduction mode can be calculated by the following equations:-

$$\boldsymbol{L = \frac{Vd\,min}{\Delta ILFs}D} \qquad \textbf{(2.6)}$$

$$C=\frac{Io}{\Delta VoFs}D \qquad (2.7)$$

Where Fs is switching frequency, Io and Iin is output and input current respectively.

### 2.1.4 Cuk (buck-boost) converter

The Cuk converter can be obtained by using the duality principle on the circuit of a BuckBoost topology.. It is clear that the input circuit of Cuk converter is a Boost converter and the output circuit is seen to be a Buck converter. Hence the Cuk converter is similar to the BuckBoost converter, it provides a negative polarity regulated output voltage with respect to its terminal of the input voltage [9, 10].

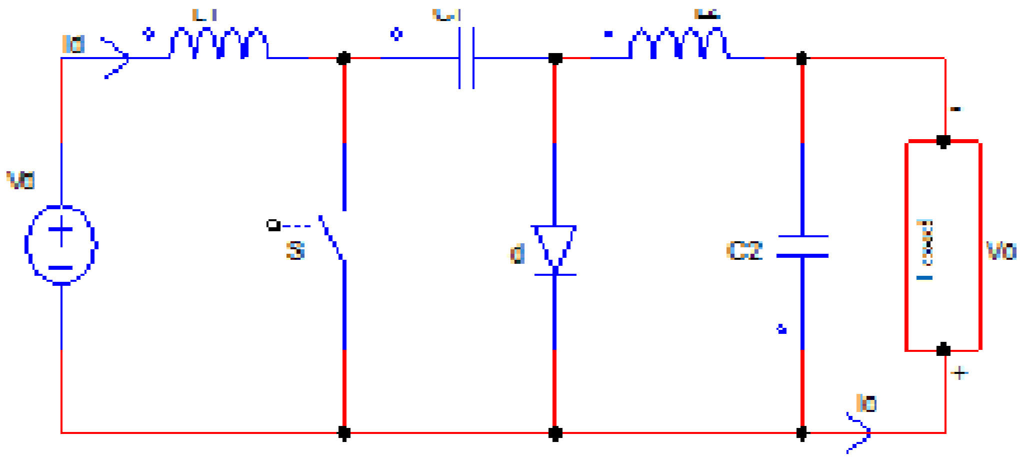


Figure 2. 6 Cuk converter

In steady-state operation, the average voltage of the inductor is zero, therefore by applying Kirchoff‟s voltage law to the circuit.

$$Vc1 = Vd + Vo \qquad (2.8)$$

Cuk converter shows two different operating modes. The first mode obtained when the switch S is off. In this case the diode d is conducting. Therefore, the capacitor C1 is charged by the input Vd through the inductor L1. The energy stored in the inductor L2 feeds the load. Hence, the following relationship is obtained [11].

$$Ic1 = Il1 \qquad (2.9)$$

The second mode of operation exists when the switch S is on. The diode d is not conducting because it is reverse-based due to C1. The capacitor C1 discharges through the switch S, transferring its energy to the load and L2. Assume the inductor currents are ripple free, because the inductors are large enough. Therefore, the following relationship is obtained.

$$-Ic1 = Il2 \quad (2.10)$$

For one time period of operation, the average capacitor current is zero. Therefore, by rearranging the above two equation

$$[Ic1_{sON}]DTs + [Ic1_{sOFF}][1-D]Ts = 0 \quad (2.11)$$

$$[I_{L2}]DTs + [I_{L1}][1-D]Ts = 0 \quad (2.12)$$

$$\frac{I_{L1}}{I_{L2}} = \frac{D}{D-1} \quad (2.13)$$

Where D is the duty ratio of the converter and it is the ratio of the conduction time ton to the switching period TS. The value of D changes between 0 and 1 [9]. Assuming the converter is ideal in other words there are no losses. Therefore, the input power of the converter Pin is equal to the output power Pout.

$$Pin = Pout \quad (2.14)$$

$$V_d I_{L1} = Vo_{Il2} \quad (2.15)$$

$$\frac{I_{L1}}{I_{L2}} = \frac{V_o}{V_d} \quad (2.16)$$

Then finally;

$$\frac{V_o}{V_d} = \frac{D}{D-1} \quad (2.17)$$

- ❖ If 0< $D < 0.5$ the output is smaller than the input.
- ❖ If D=0.5 the output is the same as input.
- ❖ If 0.5< $D < 1$ the output is larger than the input.

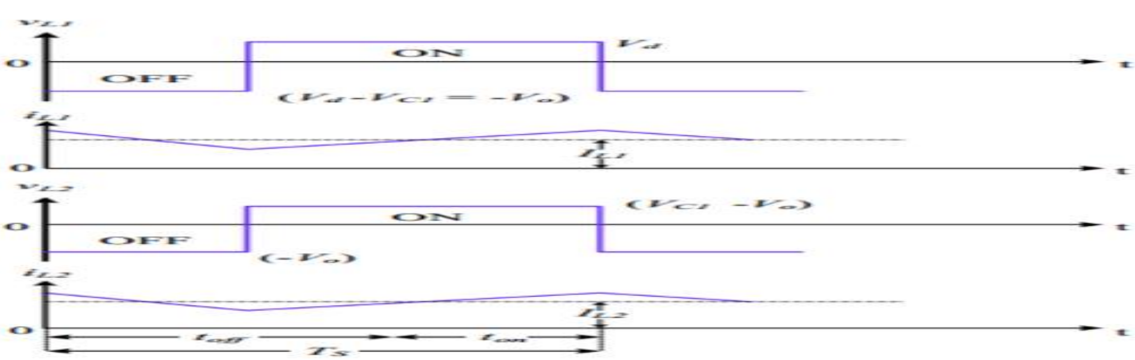


Figure 2. 7 cuk converter wave form

In the literature, many types of DC-DC converters have been studied to see which converter is suitable for the MPPT stage of the PV system. In the literature [9,11], a comparative analysis from different viewpoints has been made between some commonly used topologies to track the maximum power of the PV array. Reference [12] showed that, the Buck-Boost converter has the advantage over individual Buck and Boost converters of following the MPP at all times, under any conditions of solar global radiation, cell temperature and connected load. However, the individual Boost and Buck types are the most efficient converters for a given price. The author in [13] found that each topology has its pros and cons in comparison to the others. For example, some of them present low current ripple such as SEPIC and Cuk converter and may provide input-output isolation. For water pumping systems, the output voltage needs to be stepped down or step-up so that Buck and Boost converter is suitable. The Cuk and SEPIC converters have the advantage that their input current is continuous, and they can draw ripple free current from a PV array [14]. However, Cuk, SEPIC and BuckBoost converters have a higher number of passive components and high current, voltage and switched power stresses in the switch or transistor compared to the Boost converter. This also affects the whole system efficiency [15], since the switched current and voltage are higher for the same output power as an individual buck or boost.And also it needs the higer Voltages to feed the inverter inorder to get the desired AC voltages which is supply to the Ac machins. Boost converters developed to maximize the energy harvest for photovoltaic systems. Transformers used for voltage conversion at mains frequencies of 50–60 Hz must be large and heavy for powers exceeding a few watts. This makes them expensive, and they are subject to energy losses in their windings and due to eddy currents in their cores. Boost techniques that use transformer‟s work at much higher frequencies, requiring only muchsmaller, lighter, and cheaper wound components. Therefore, in this work it was decided to use a boost converter because the DC-DC boost converter is an important stage in the PV inverter system because it increases the overall efficiency of the system. In fact, the operating with higher input voltage leads to lower input current required for a given power and hence reduces the losses. It is responsible to regulate and boost the DC output voltage of the PV system. In this work, a boost converter operating in continuous conduction mode has been designed to step up the voltage of the PV system to a higher constant voltage of 500V to feed an inverter.

## 2.2 Design of Three-Stage Soft-Switching Boost Converter

Based on the working of single switch soft switching boost converter (SSSSBC), the three-stage soft switching boost converter (TSSSBC) has been developed and analyzed with eight modes. Figure shows the equivalent circuit diagram for various modes of operation of SSSSBC. For TSSSBC,the same is applicable with aphase shift of 120∘ for the MOSFETgate pulse in each arm. The formula for $i$ L($t$ ), $i\ L\ r\ (t\ )$,$V\ C\ r\ \ (t\ )i_{L(t),}$, and $V\ C\ a\ \ (t\ )$ during various modes of operation are summarized in Table.By introducing soft-switching technique, the switching loss is minimized. Hence, the total loss is minimized with the TSSSBC.Figure below  Equivalent circuit diagram of SSSSBC for various modes of operation.The circuit diagram for three-stage soft-switching boost converter (TSSSBC) is shown in Figure below. In the proposed TSSSBC, the three main inductors ($L$ 1, $L$ 2, and $L$ 3) and resonant inductors($L\ r$ 1,$L\ r$ 2,and $L\ r$ 3)of reduced magnitudes (1/3rd of the original values) are considered. Driving pulses for the three switches were phase shifted by120°. By introducing soft-switching technique, the switching loss is minimized. Hence,the total loss is minimized with the TSSSBC.

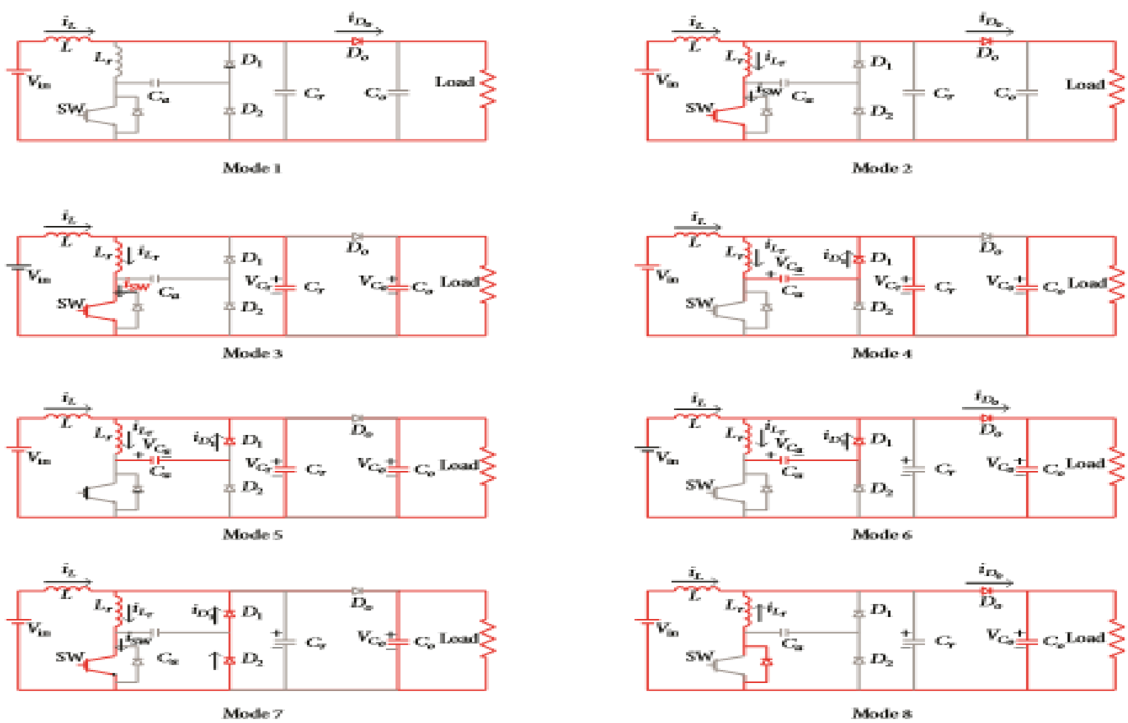


Figure 2. 8 Equivalent circuit diagram of SSSSBC for various modes of operation.

Table 2. 1 Current and voltage equations of SSSSBC for various modes

| modes | $i_L(t)$ | $i_{Lr}(t)$ | $v_{cr}(t)$ | $v_{ca}(t)$ |
|---|---|---|---|---|
| Mode 1 | $i_L(to) - \frac{(v_o - v_{in})}{L} t$ | 0 | $v_0$ | 0 |
| Mode 2 | $i_1 - \frac{(v_o - v_{in})}{L} t$ | $\frac{(v_o)}{L_r}t$ | $v_0$ | 0 |
| Mode 3 | $i_{min}$ | 0 | $i_{\min} + \left(\frac{v_o}{z_r} \sin w_r t\right)$ | $(v_o) cos w_r t$ |
| Mode 4 | $i_{min} + \frac{(v_{in})}{L} t$ | $i_2$ | 0 | 0 |
| Mode 5 | $i_{max}$ | $(i_2) cos w_a t$ | $\frac{(i_2)}{c_a}$ | $z_r (i_2) sin w_a t$ |
| Mode 6 | $i_3 - \frac{(v_o - v_{in})}{L} * t$ | $(i_2) cos w_a t$ | $v_0$ | $z_r (i_2) sin w_a t$ |
| Mode 7 | $i_3 - \frac{(v_o - v_{in})}{L} * t$ | $\left(\frac{v_o}{z_a} - i_2\right) \sin w_a t$ | $v_0$ | $v_2$ |
| Mode 8 | $i_4 - \frac{(v_o - v_{in})}{L} * t$ | $i_s - \frac{(v_o)}{L_r} * t$ | $v_0$ | 0 |

## 2.3 DC-AC converter for photovoltaic system

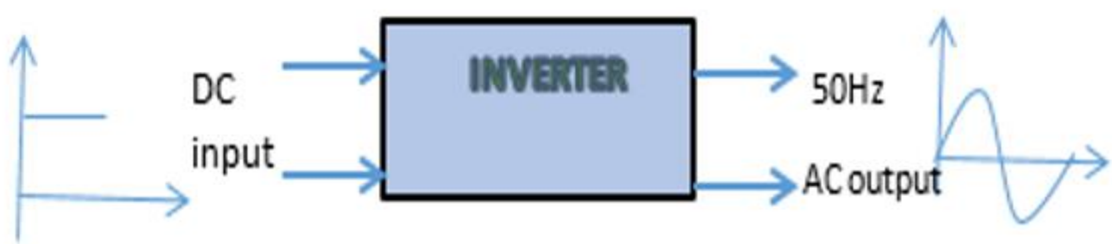


Figure 2. 9 Inverter block diagram

An inverter is a device that changes DC voltage into AC voltage. A direct current (DC) is a current that flows in only one direction, while an alternating current (AC) is that which flows in both positive and negative directions. There are two basic types of inverters based on type of sources input; Voltage source(VSI) and Current Source(CSI). Voltage/current source implies that the voltage/current level doesn"t change instantly as the result of switching. Photovolatic source and Battries source can be used as voltage sources. It is difficult to get ideal voltage or current sources. In practice voltage sources are simulated by voltage stiff (power supply with shunt capacitor) and hence voltage stiff inverter. Similarly, current sources are simulated by current stiff (power supply with serious inductor). In the other way Inverter may be single-phase (hafe bridge, full bridge) or three phase( hafe bridge, full bridge) but single-phase half and full bridge voltage source inverter cover low-range power applications. The main purpose of these topologies is to provide a three-phase voltage source, where the amplitude, phase and frequency of the voltages can be controlled.in this worke I have to discused three phase inverters with the controling techniques and select the best one based on the performance parametres.

### 2.3.1 Three phase inverter topology

There are many three phase inverter types ,but for coparation I have desccused some of them. Three phase inverters are often used to supply three-phase loads, such as ac motors. The basic structure of a three-phase inverter is shown in Figure below. Each of the three legs produces an output which is displaced by 120◦ with respect to each other. The output of each leg depends on the status of the switch and the input voltage, Vdc. Since one of the two switches in each leg is always on, the output voltage is independent of the output load current.

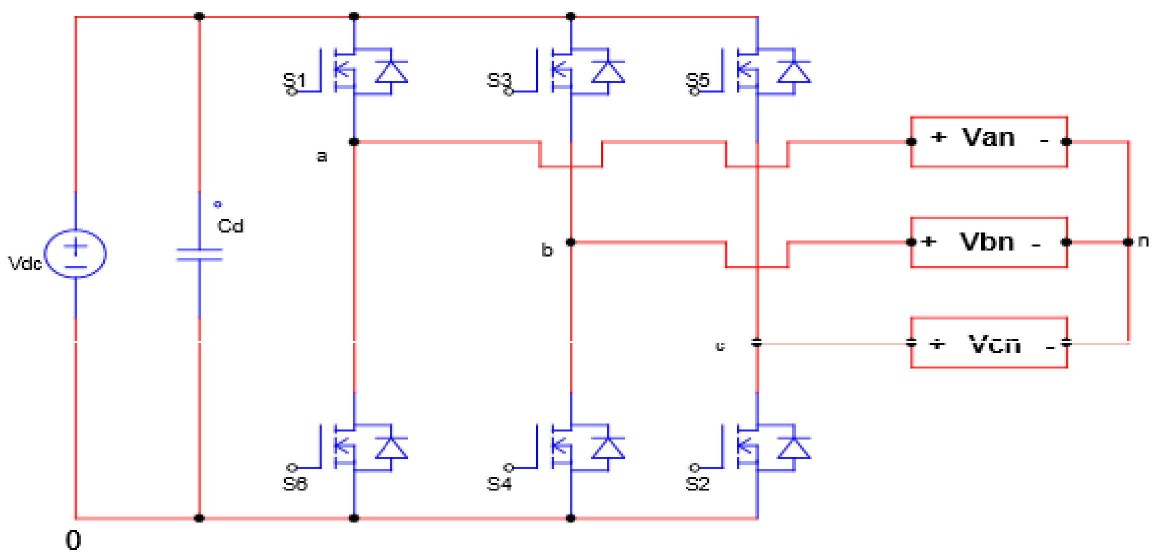


Figure 2. 10 Three-phase full –Bridge Inverter

The standard three-phase VSI topology is shown in Fig.2.10 And the eight valid switch states are given in Table 2.2. As in single-phase VSIs, the switches of any leg of the inverter (S1 and S4, S3 and S6, or S3 and S2) cannot be switched on simultaneously because this would result in a short circuit across the dc link voltage supply. Similarly, in order to avoid undefined states in the VSI, and thus undefined ac output line voltages, the switches of any leg of the inverter cannot be switched off simultaneously as this will result in voltages that will depend upon the respective line current polarity. As explained earlier in order that the circuit satisfies the KVL and the KCL,thus the nature of the two switches in the same leg is complementary [16].

$$S1 + S6 = 1 \quad (2.18)$$

$$S3 + S4 = 1 \quad (2.19)$$

$$S5 + S2 = 1 \quad (2.20)$$

Table 2. 2 Eight state of three phase inverter

| | S1 | S3 | S5 | $V_{ab}$ | $V_{bc}$ | $V_{ca}$ |
|---|---|---|---|---|---|---|
| 1 | 0 | 0 | 0 | 0 | 0 | 0 |
| 2 | 0 | 0 | 1 | 0 | $-V_{dc}$ | $V_{dc}$ |
| 3 | 0 | 1 | 0 | $-V_{dc}$ | $V_{dc}$ | 0 |
| 4 | 0 | 1 | 1 | $-V_{dc}$ | 0 | $-V_{dc}$ |
| 5 | 1 | 0 | 0 | $V_{dc}$ | 0 | $-V_{dc}$ |
| 6 | 1 | 0 | 1 | $V_{dc}$ | $-V_{dc}$ | 0 |
| 7 | 1 | 1 | 0 | 0 | $V_{dc}$ | $-V_{dc}$ |
| 8 | 1 | 1 | 1 | 0 | 0 | 0 |

Among the eight valid states, two of them produce zero ac line voltages. In this case, the ac line currents freewheel through either the upper or lower components. The remaining states produce non-zero ac output voltages. In order to generate a given voltage wave form, the inverter moves from one state to another. Thus the resulting ac output line voltages consist of discrete values of voltages that are Vdc , 0, and -Vdc for the topology shown above. The selection of the states in order to generate the given waveform is done by the modulating technique that should ensure the use of only the valid states[16].

$$\frac{V_{dc}}{2}(S1 - S6) = V_{an} + V_{no} \quad (2.21)$$

$$\frac{V_{dc}}{2}(S3 - S4) = V_{bn} + V_{no} \quad (2.22)$$

$$\frac{V_{dc}}{2}(S5 - S2) = V_{cn} + V_{no} \quad (2.23)$$

Expressing the Equations above in terms of modulation signals and making use of conditions

$$\frac{V_{dc}}{2}(M1) = V_{an} + V_{no} \qquad (2.24)$$

$$\frac{V_{dc}}{2}(M3) = V_{bn} + V_{no} \qquad (2.25)$$

$$\frac{V_{dc}}{2}(M5) = V_{cn} + V_{no} \qquad (2.26)$$

where M is called the modulation signal, which can be any sine or cos term(in accordance to Fourier series) depending on the control we want to implement. The more general fundamental component for M is given as

$$M = m_{\alpha}\cos(wt - \alpha) \qquad (2.27)$$

And $m_{\alpha}$ is called the modulation index which can vary from 0 to 1 and for values of $m_{\alpha}$ less than „1‟ a linear modulation range is supposed to exist and for values of $m_{\alpha}$ greater than „1‟ it is operated in the over modulation range.

Then adding the valide state equation above which is equal to;

$$\frac{V_{dc}}{2}\{(S1 + S3 + S5) - (S6 + S4 + S2)\} = V_{an} + V_{bn} + V_{cn} + 3V_{no} \qquad (2.28)$$

As we know the balanced voltages $V_{an} + V_{bn} + V_{cn}$ =0 and making use of the conditions from Equations above the Equation becomes

$$\frac{V_{dc}}{6}(2S1 + 2S3 + 2S5) = V_{no} \qquad (2.29)$$

Substituting for Vno then each phase voltage becomes

$$\frac{V_{dc}}{3}(2S1 - S3 - S5) = V_{an} \qquad (2.30)$$

$$\frac{V_{dc}}{3}(2S3 - S1 - S5) = V_{bn} \qquad (2.31)$$

$$\frac{V_{dc}}{3}(2S5 - S1 - S3) = V_{cn} \qquad (2.32)$$

Then the RMS value can be calculated as follws

$$V_{RMS} = V_{ratio}V_{dc} \qquad (2.33)$$

whre, Vratio is different for the type of applying control techniques which is the basic parameter.

### 2.3.2 Sinusoidal pulse widith Modulation in Three-Phase Voltage Source Inverters

As in the single phase voltage source inverters PWM technique can be used in three-phase inverters, in which three sine waves phase shifted by 120°with the frequency of the desired output voltage is compared with a very high frequency carrier triangle, the two signals are mixed in a comparator whose output is high when the sine wave is greater than the triangle and the comparator output is low when the sine wave or typically called the modulation signal is smaller than the triangle. The output voltage from the inverter is not smooth but It‟s a discrete waveform and so it is more likely than the output wave consists of harmonics, which are not usually desirable since they deteriorate the performance of the load, to which these voltages are applied[16].

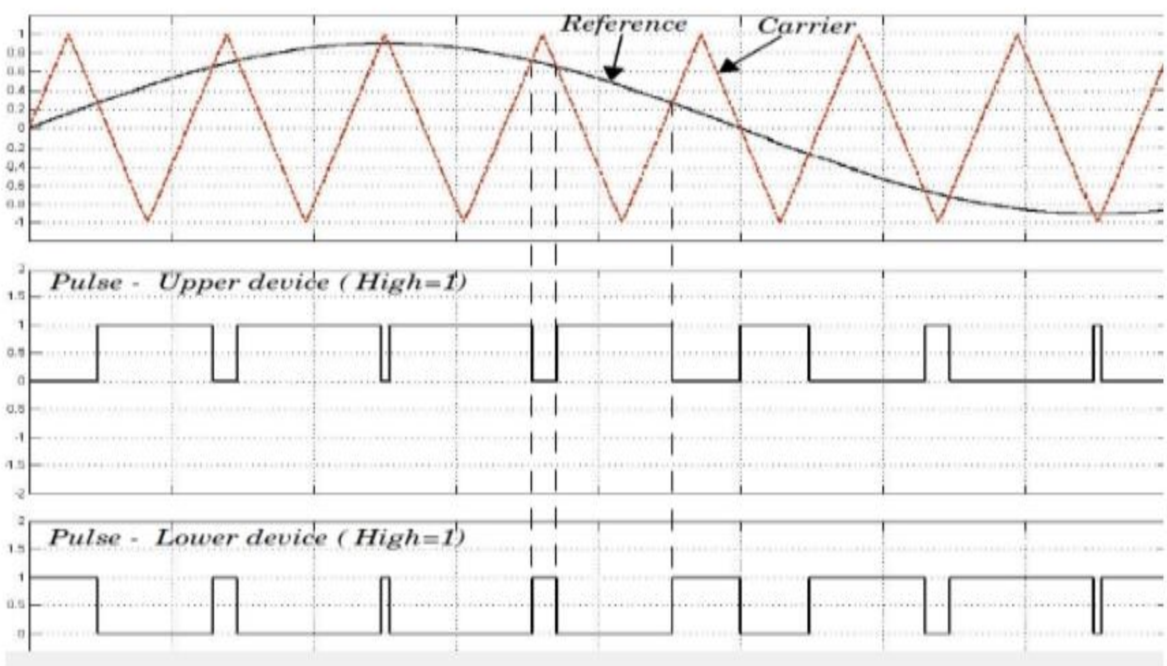


Figure 2. 11 PWM illustration by the sine-triangle comparison method

This signal is internally generated by phase-shifting the original reference signal by180 degrees. For a three-phase bridge, three reference signals are required to generate the six pulses. The reference signals can also be internally generated by the PWM generator. In this case, specify a modulation index, a voltage output frequency, and phase.

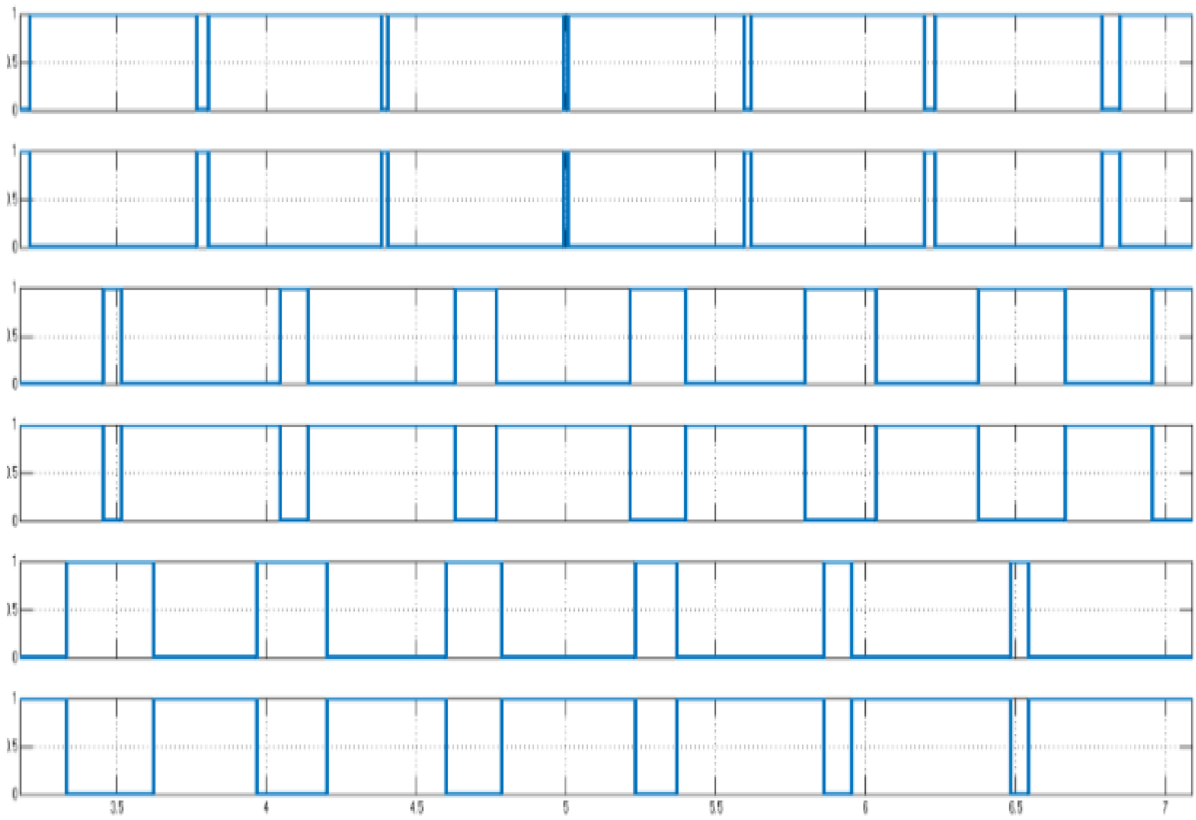

Figure 2. 12 pulse generated by 2-level PWM in Three-Phase VSI

### 2.3.3 Six Step Voltage Source Inverter

Three-phase bridge inverters are most commonly used in ac motor drives and generalpurpose ac supplied. The circuit for the six-step VSI is as shown in Figure below, which consists of three half-bridges, which are mutually phase-shifted by 1.5 π angle [17].

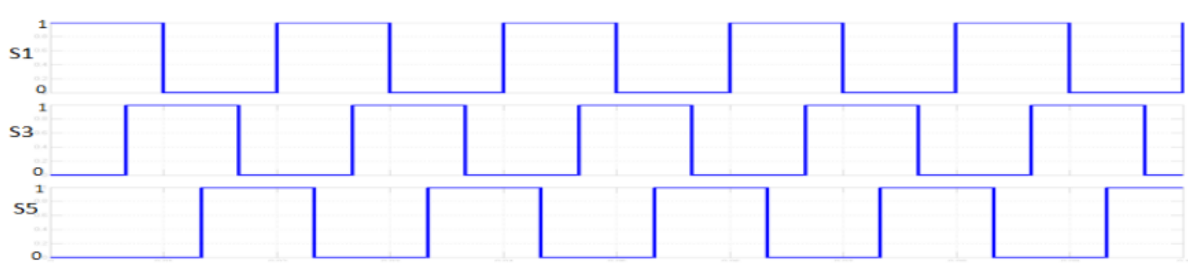


**a)**

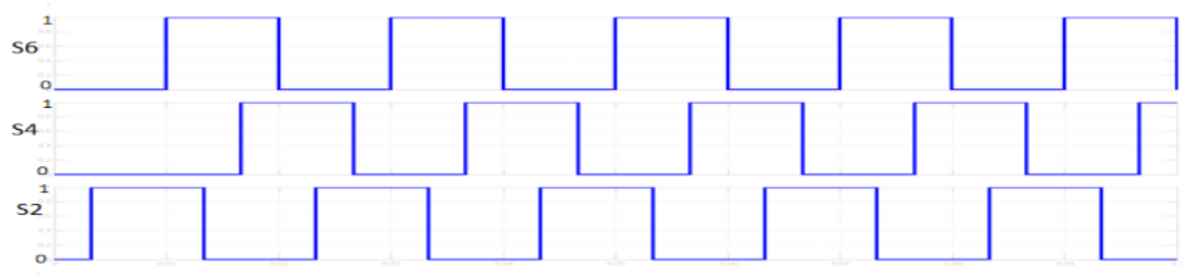


**b)**

Figure 2. 13 180° mode Generation of the switching signals for (a) top devices, (b) bottom devices

The square wave phase voltages with respect to the fictitious dc center tap can be expressed using Fourier series as,

$$V_{an} = \frac{2V_{dc}}{\pi}[\cos wt - \frac{1}{3}\cos 3wt - \frac{1}{5}\cos 5wt - \cdots] \quad (2.34)$$

$V_{bn}$ is Shifted by 120 degree

$$V_{bn} = \frac{2V_{dc}}{\pi}[\cos(wt - 120°) - \frac{1}{3}\cos 3(wt - 120°) - \frac{1}{5}\cos 5(wt - 120°) - \cdots \quad (2.35)$$

$$V_{cn} = \frac{2V_{dc}}{\pi}[\cos(wt + 120°) - \frac{1}{3}\cos 3(wt + 120°) - \frac{1}{5}\cos 5(wt + 120°) - \cdots \quad (2.36)$$

The line voltages can thus be obtained from the phase voltages as

$$V_{ab} = V_{an} - V_{bn} \quad (2.37)$$

$$V_{ab} = \frac{2\sqrt{3}V_{dc}}{\pi}[\cos(wt + 30°) - \frac{1}{3}\cos 3(wt + 30°) - \frac{1}{5}\cos 5(wt + 30°) - \frac{1}{7}\cos 7(wt + 30°) - \cdots \ldots \quad (2.37)$$

$$V_{bc} = V_{bn} - V_{cn} \quad (2.39)$$

$$V_{bc} = \frac{2\sqrt{3}V_{dc}}{\pi}[\cos(wt - 90°) - \frac{1}{3}\cos 3(wt - 90°) - \frac{1}{5}\cos 5(wt - 90°) - \frac{1}{7}\cos 7(wt - 90°) - \cdots \ldots \quad (2.39)$$

$$V_{ca} = V_{cn} - V_{an} \quad (2.40)$$

$$V_{ca} = \frac{2\sqrt{3}V_{dc}}{\pi}[\cos(wt + 150°) - \frac{1}{3}\cos 3(wt + 150°) - \frac{1}{5}\cos 5(wt + 150°) - \frac{1}{7}\cos 7(wt + 150°) - \cdots \ldots \quad (2.40)$$

The fundamental of the line voltages is $\sqrt{3}$ times that of the phase voltage, and there is a leading phase-shift of $\frac{\pi}{6}$.

The line voltages waves as shown in below have a characteristic six step wave shape and thus the name for this inverter. The characteristic harmonics in the wave form are 6n ±1, n is being an integer.

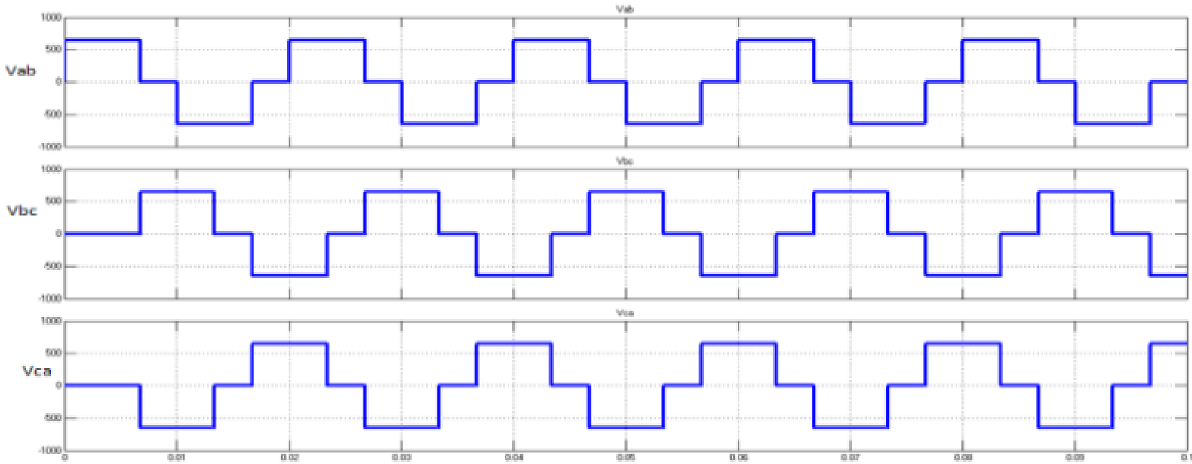


Figure 2. 14 180° conduction mode six step inverter line voltage (Vab, Vbc & Vca)

The three-phase fundamental as well as the harmonic components are balanced with a mutual phase-shift angle of $\frac{2\pi}{3}$.

Now from the above equation the Line-to-line peak voltage value is

$$V_p = \sqrt{3}[\frac{2}{2\pi}\int_0^{\frac{2\pi}{3}}(V_{dc})^2\, d(wt)]^{\frac{1}{2}} \quad (2.41)$$

$$V_p = \sqrt{3}\frac{V_{dc}}{2} \times m \quad (2.42)$$

where Vp is peak voltage and m is modulation indeix.

## 2.4 Output Filters for photo voltaic system

The output of the full bridge inverter is connected to a low pass filter to supply a pure sinusoidal output voltage to the load. The factors such as efficiency, voltage and current harmonics constraints, weight, volume and cost must be taken in to account when selecting the optimal filter design [14]. Also, the saturation of the inductor core should be avoided [18]. There are various filters topologies of sine wave inverter. These topologies include L filter, LC filter and LCL filter.

### 2.4.1 L-filter

L-filter filter has super performance in terms of voltage to current conversion but the damping of the high frequency (HF) noise is weak.

### 2.4.2 LC filter

The LC filter has good performance in terms of current to voltage conversion and noise damping but the filter capacitor may be insecure to line voltage harmonics, which result in large currents.

### 2.4.3 LCL filter

The LCL filter has the same good properties with the L and the LC filters. Moreover, the damping of high frequency noise is better due to the extra inductance, and the capacitor is no more exposed to line voltage distortion. On the other hand, LCL can sometimes cost more than other topologies and is inherently unstable due to resonance [14]. For reducing oscillations and unstable conditions of the LCL filter, a damping resistor (Rd) is placed in series with the filter capacitor. Damping resistor is reliable, but it increases the losses and decreases the efficiency of the system, but the benefits of LCL filter over other types of filter are the reasons that made this filter are used in the proposed inverter circuit.

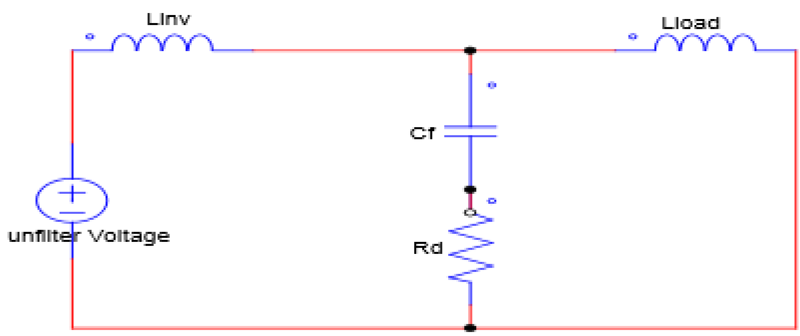


Figure 2. 15 LCL-filter

There are some important factors that should be considered when design LCL filter which comprise such as: Inverter output ripple current, Inverter to load inductor ratios and filter capacitance maximum power variations.

## 2.5 MPPT Controller algorithms

Several MPPT algorithms have been proposed for PV power systems in recent years, to locate the MPP and increase the system efficiency. The MPPT algorithms may be divided into two types, which are indirect control or "quasi tracking techniques" and direct control or "true tracking techniques" [19]. In the indirect control techniques, the MPP is calculated either by measuring the voltage and current of the PV array, the solar insolation, or by the use of mathematical functions obtained from empirical data. Therefore, these techniques are incapable of tracking the MPP with varying irradiation and temperature. The indirect control techniques are look-up table technique, constant voltage technique, fractional open-circuit voltage and fractional short-circuit current. However, the true tracking techniques have the ability to find the optimum operating point even under changing atmospheric conditions, because they do not rely on previous knowledge of or calculated data from the PV array V-I characteristics. The true tracking techniques are the perturbation and observation (P&O) technique, incremental conductance (INC) technique. In the tracking process one or two variables are used for calculating the MPP. The fractional open-circuit voltage and fractional short-circuit current use only one variable, either the PV array output voltage or current respectively, though the P&O and INC methods need both variables to determine the MPP.

### 2.5.1 Simple panel load matching

The simple panel load matching technique is one of the simplest techniques to operate a PV array close to its maximum power point. In this technique the optimum operating point of the PV array is determined either by a series of measurements under average operating conditions or theoretical calculation. The load is designed to produce the values of PV voltage and current corresponding to the MPP [20].

- ❖ This method has the advantages of simplicity and no additional circuit is used, therefore, the power loss between the panel and the battery is reduced and the risk of component failure is kept low for the whole system.
- ❖ However, the system does not take into consideration the changes of solar irradiation or temperature.

### 2.5.2 Load switching technique

In this configuration different panels are connected in series and parallel in an appropriate manner to form a PV array. Then, the PV array is connected to a number of controllable battery cells connected in series to fulfill the load matching process as illustrated in Fig 2.5.2.

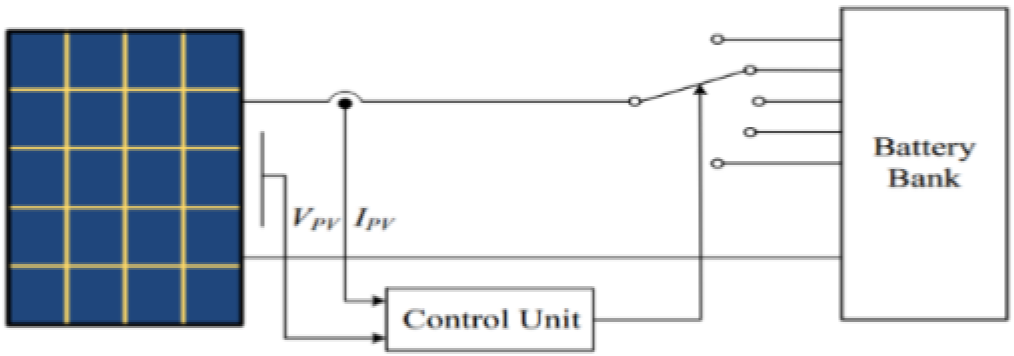


Figure 2. 16 Schematic block diagram of the load-switching method

The group of batteries is used to store the energy produced by the PV array. The control unit detects the output of the solar array in real time, finds out the optimum operating point, and maintains operation as close as possible to this by switching the battery connection.

This technique has the drawbacks that it requires extra switching circuits and wiring, and the stepwise, switched operating voltage cannot guarantee accurate tracking of MPP, Moreover; it is difficult to keep an equal charge level on all the battery cells, hence degrading battery life in the long term.

### 2.5.3 Constant voltage method (CV)

If the PV system is implemented without a battery to tie the bus voltage to an approximately constant level, a simple control scheme of the constant voltage method can be applied as presented in [9]. In this method the feedback of the PV voltage is compared with a fixed reference voltage and the resultant signal adjusts the duty ratio of the DC-DC converter to keep the operating point of the PV array at the MPP or close to it. The reference voltage is set to be equal to the VMPP of the characteristic PV array or to another calculated best fixed voltage.

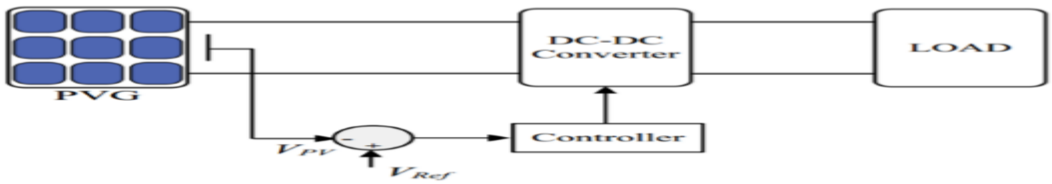


Figure 2. 17 Voltage feed back MPPT method with constant voltage reference

This technique has the drawback that it does not correct for environmental variation such as change in irradiation and temperature it fixes the reference voltage to a best fixed voltage value and holds it constant under any operating condition instead of following the MPP [15].

### 2.5.4 Perturb and observe (P&O) algorithm

The perturb and observe algorithm considered to be the most commonly used MPPT algorithm, among the other techniques because of its simple structure and ease of implementation. It is based on the concept that on the power-voltage curve, the change in the PV array output power is equal to zero ($\Delta PPV = 0$) on the top of the curve. The P&O operates by periodically perturbing (incrementing or decrementing) the PV array terminal voltage or current and comparing the corresponding output power of PV array. If the perturbation in terminal voltage leads to increase in the PV power ($\Delta Ppv > 0$) the perturbation should be kept in the same direction, otherwise the perturbation is moved to the opposite direction. The perturbation cycle is repeated until reaching the maximum power at($\Delta Ppv = 0$).

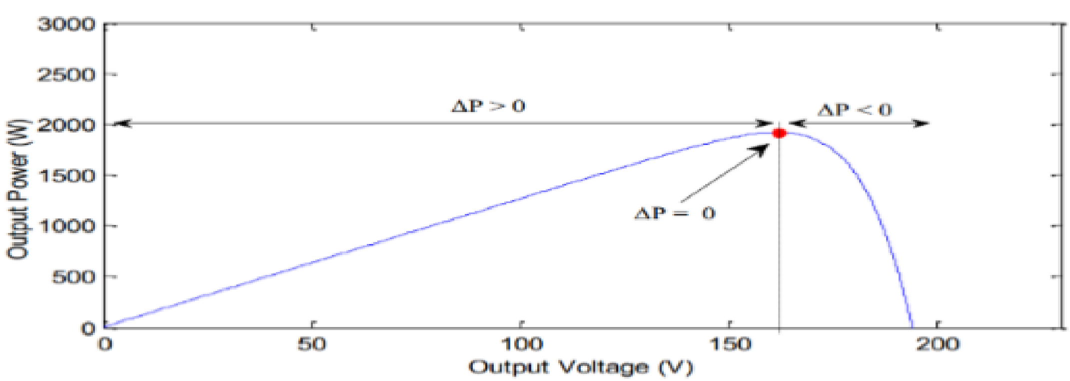


Figure 2. 18 perturbs and observes technique

The advantages of this technique are simplicity, ease of implementation and it does not require a previous knowledge of the PV array. On the other hand P&O will not stop perturbing when the MPP is reached and will oscillate around it resulting in some unnecessary power loss.

### 2.5.5 Intelligent control techniques

#### 2.5.5.1 Fuzzy logic Control

Fuzzy logic is implemented in a control system to emulate human-like decisions in control. FL techniques have been widely used in a wide range of engineering applications due to their heuristic nature associated with simplicity and effectiveness for both linear and nonlinear systems [21]. It can be implemented in software, hardware or a combination of both. Fuzzy sets are considered as the brain of the fuzzy control system which in turn is responsible for converting analog input values into a scale of 0 to 1. Fuzzy logic control uses human expert knowledge to make control decisions. Fuzzy logic can be used in the treatment of unknown systems to model imprecise data and experience knowledge. The fuzzification block is responsible for converting the numerical input variables to linguistic variables in accordance with the membership functions. The Fuzzy inference is the process of formulating the mapping from a given input to an output using fuzzy logic. The defuzzification block converts the linguistic output from the inference engine to numerical output values using the membership function. Fuzzy rule base refer to a set of pre-defined instructions which link the different values of crisp values with different subsets of fuzzy output space [22].

The inputs to the fuzzy control are the error in the power and the change of error the output is the duty cycle variable that controls the pulse width generation block.

The error is given by the following equation. [23]

$$E(k) = \frac{P(K)-P(k-1)}{V(k)-V(k-1)} \qquad (2.43)$$

The change in error is given by

$$CE(k) = E(K) - E(K-1) \qquad (2.44)$$

Fuzzy systems are suitable for uncertain or approximate reasoning, especially for a system with a mathematical model that is difficult to derive. And fuzzy logic allows decision making with estimated values under incomplete or uncertain information.

Most of the time the drawback of the fuzzy systems are not take experience from the previous data and If the input parameters to be controlled increases, fuzzy logic controller will not be useful as effective rules cannot be determined.

### 2.5.3 Artificial Neural Network

Artificial neural networks are one of machine learning techniques which have been developed as generalizations of mathematical models of biological nervous systems. The learning capability of an artificial neuron is achieved by adjusting the weights in accordance to the chosen learning algorithm. The most widely-used neural network for prediction is the single hidden layer feed-forward network. The ANNs operate like a black-box model. It does not require detailed information about the system. They effectively learn the relationship between the input and the output variables by making use of trends in previously recorded data. Also ANNs have the ability to work with highly nonlinear relationships, can work with numerical or analogue data, are relatively robust in terms of finding best-fit solutions, and the user does not require sophisticated mathematical knowledge [22]. The non-linear variation of output voltage and current with solar radiation levels are mainly due to aging and load current. To predict this, artificial neural network using the back propagation theorem is trained. The relationship between input and output variables are studied from their previously recorded data. The ability to handle large and complex systems with many interrelated parameters is done using ANN. These trained data are used to approximate an arbitrary input-output mapping of the system. Since the solar insolation is varying, the corresponding reference voltage (Vref =Vmpp) for the feed forward loop also changes which is estimated.

Table 2. 3 Characteristics of different MPPT techniques

| MPPT technique | Convergence speed | Implementation complexity | Periodic tuning | Sensed parameters |
|---|---|---|---|---|
| Perturb & observe | Varies | Low | No | Voltage |
| Incremental conductance | Varies | Medium | No | Voltage,Current |
| Fractional Voc | Medium | Low | Yes | Voltage |
| Fractional Isc | Medium | Medium | Yes | Current |
| Fuzzy logic control | Fast | High | Yes | Varies |
| Neural network | Fast | High | Yes | Varies |

## 2.6 Grid Synchronization

To achieve power flow between the renewable resource and the utility network, the injected current needs to be synchronized with the grid voltage and current. Different algorithms are used for grid synchronization. The main purpose of these algorithms is to obtain the phase information of grid voltages[47]. Transformation from natural reference frame to stationary or synchronous reference frame may be required to make this possible. Zero crossing method, Filtering of grid voltages and PLL are the methods that are used for grid synchronization. Among these three, PLL is the most widely used method[46].

### 2.6.1 Phase Locked Loop

APLL is a closed-loop feedback structure that sets fixed phase relationship between its output phase and the phase of a reference. It tracks the phase changes that are within the band width of the PLL[45].PLL provides good rejection of harmonics and other disturbances. It is implemented in synchronous reference frame.shows the basic structure of PLL (a filter may be added to this so that negative sequence may be filtered out so that better performance can be achieved during asymmetrical grid faults)

# CHAPTER THREE

# MODELLING AND DESIGN OF MAXIMUM POWER POINT TRACKING FOR ENERGY EFFICIENCY OF PV SYSTEM

## 3.1 Photovoltaic system design

The complete schematic diagram of the proposed system is depicted in Fig.3.1 It consists of the following main stages before getting the pure Ac powers for the purpose of PV panel based on the energy efficiency of PV system connected to grid.

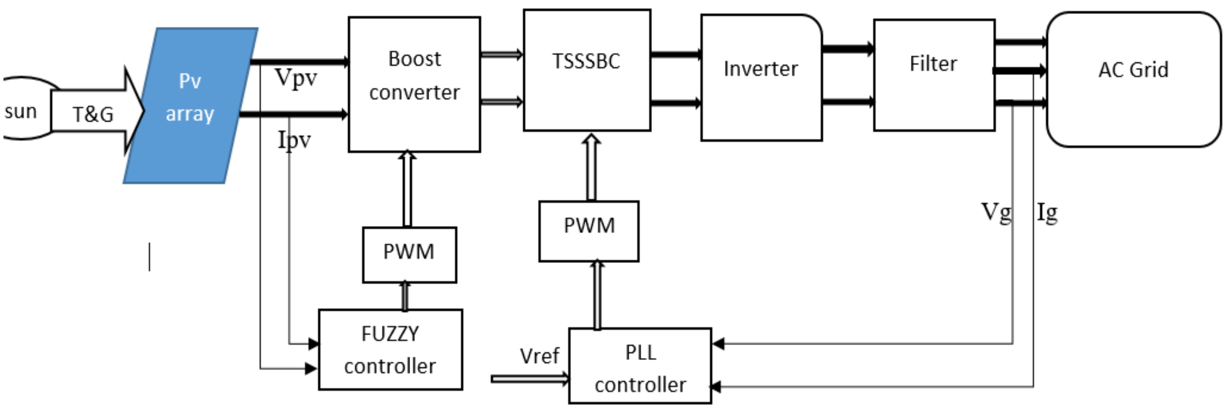


Figure 3. 1 schematic diagram of the proposed model

### 3.1.1 Photovoltaic cells

Photovoltaic cells are the basic components of photovoltaic panels. Most are made from silicon even though other materials are also used; Solar cells take advantage of the photoelectric effect: the ability of some semiconductors to convert electromagnetic radiation directly into electrical current. The charged particles generated by the incident radiation are separated conveniently to create an electrical current by an appropriate design of the structure of the solar cell. Polycrystalline silicon Consists solely of crystalline silicon grains, separated by grain boundaries, Main advantage over amorphous Si: mobility of the charge carriers can be orders of magnitude larger and Material shows greater stability under electric field and light-induced stress.

When placed in the dark, a photovoltaic cell behaves like a p-n junction diode under no voltage excitation. And when the structure of p-n is exposed to the sunlight, Photons with sufficient energy are absorbed by the semiconductor and form hole-electron pairs, if these mobile charge carriers reach the vicinity of the junction before they recombine, the electric field in the depletion region will push the holes into the p-side and push the electrons into the n-side. Hence, the p-side accumulates more holes and the n-side accumulates more electrons.

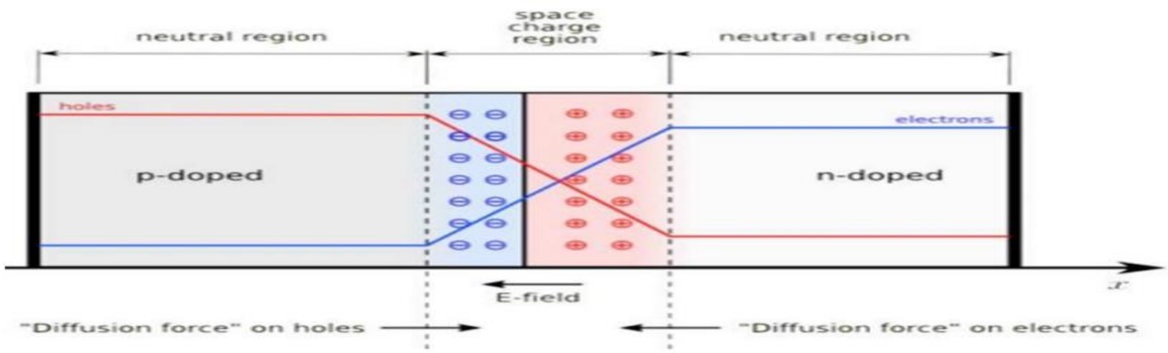


Figure 3. 2 Hole-electron pairs created by photons in p-n junction of PV cell

This separation of charge creates an electric field at the junction which is in opposition to that already existing at the junction, hence a weaker net electric field which increases the diffusion current. When the cell terminals are connected to an external circuit, the lightgenerated electrons are provided an external path, while the holes remain stuck in the p-type semiconductor. Herein, the electrons will flow out of the n-side through the connecting wire to the load, and then recombine with holes that are waiting on the p-side to complete the circuit.

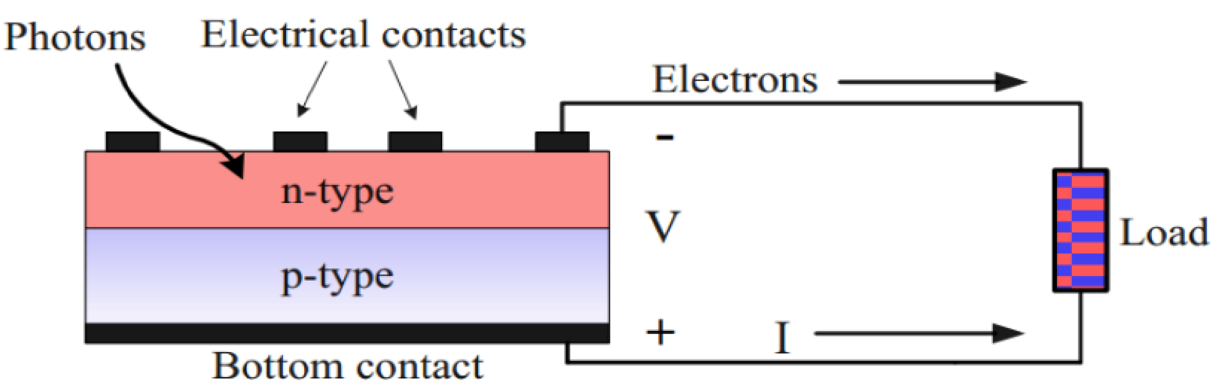


Figure 3. 3 connecting solar cells with a load and conducting current

This shows how the current in the external circuit is generated. Both sides of the junction are attached with metallic contact in order to collect the electrical current induced by the photons received on one side.

The purpose of this paper is to present a brief introduction to the behavior and functioning of a PV device and write its basic equations, without the intention of providing an in-depth analysis of the PV phenomenon and the semiconductor.

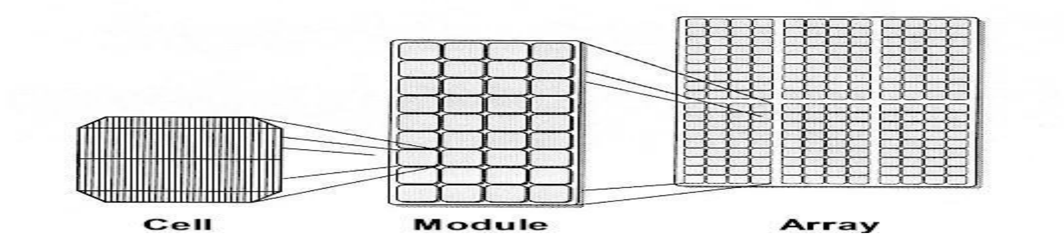


Figure 3. 4 Photovoltaic Hierarch

## 3.1.4 Basic Types of PV cells

Photovoltaic cells are manufactured in different forms; each has its uses and benefits compared to others. The most famous PV types are

- **Mono-crystalline (single crystalline) cells** are cut from a single crystal of silicon, see Fig 3.5 They are basically a slice of crystal which makes them very smooth in texture. Mono-crystalline cells are the most efficient, but also the most expensive to produce.

Figure 3. 5 Mono-crystalline PV cell

- **Polycrystalline (multi-crystalline) cells:** are made from a slice cut from a block of silicon, unlike Mono- these cells consist of a large number of crystals. (See Figure 3.6). Photovoltaic solar panels made from these types of cell are slightly less efficient but also slightly cheaper than mono-crystalline cells.

Figure 3. 6 Poly-crystalline PV cell.

- **Amorphous cells**: are manufactured by placing a thin film of amorphous (non crystalline) silicon onto a wide range of surfaces.(see Fig 3.7). Amorphous cells are the least efficient type of Photovoltaic solar panels but also the cheapest. They form flexible PV panels.

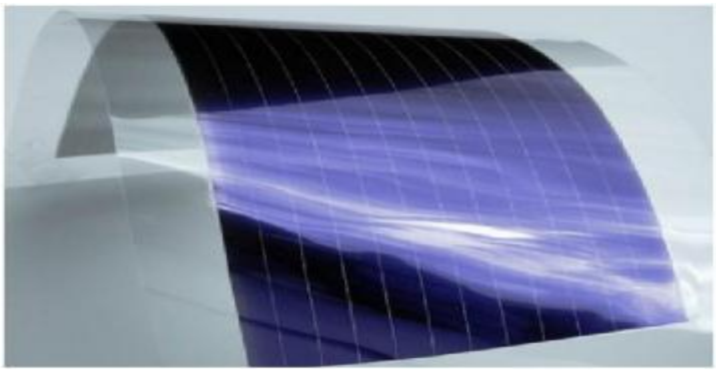

Figure 3. 7 Amorphous PV cell.

## 3.2 Simple solar cell modeling

A simple solar cell model for a photovoltaic cell consists of a real diode in parallel with an ideal current source. The ideal current source delivers current in proportion to the solar flux to which it is exposed.

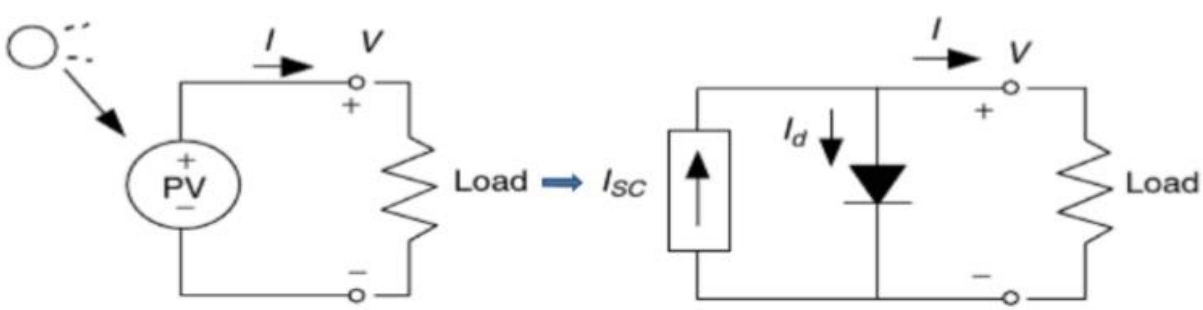


Figure 3. 8 simple equivalent circuit of PV cell

The short circuit current Isc is defined as the current that flows when the terminals are shorted together. This is equal to the magnitude of the ideal current source and the open-circuit voltage Voc is defined as the voltage across the terminals when the loads are left open.

$$I = Isc - Id \quad (3.1)$$

Then applying Shockley diode equation

$$I = Isc - Is(e^{\frac{qVd}{nkT}} - 1) \quad (3.2)$$

Where q is the electron charge ($1.602 \times 10^{-19}$ C), k is Boltzmann‟s constant ($1.381 \times 10^{-23}$ J/K), and T is the junction temperature (K), n is ideality factor a common value for n is 1.2 for Silicon mono and 1.3 for Silicon poly, 1.3 for AsGa, and 1.5 for CdTe. (I) load current, (Is) dark saturation current and (Id) is diode current.

The open-circuit voltage can be found by setting the load current to zero:

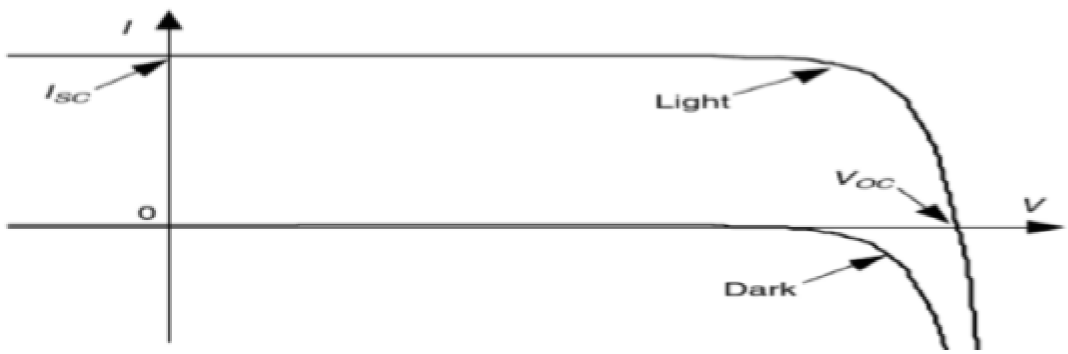


Figure 3. 9 open circuit and short circuit

If the light-generated carriers are prevented from leaving the solar cell, the forward bias of the junction increases to a point where the light-generated current is exactly balanced by the forward bias diffusion current, and the net current is zero. The resulting voltage at the cell terminals under this condition is called the open-circuit voltage (Voc).

$$Voc = \frac{nKT}{q} ln(\frac{Isc}{Is} + 1) \quad (3.3)$$

## 3.3 General solar cell Modeling

Addition of series resistance Rs and parallel resistance Rsh, the current –voltage equation becomes non-explicit but a general PV cell equation is drive. And used to control the parameters that makes difficult to produce the desired out puts.

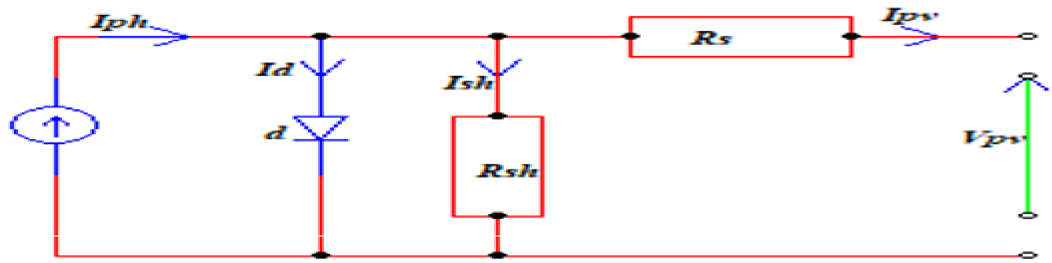


Figure 3. 10 Equivalent circuit of a general solar cell

Apply Kirchhoff law to the above equivalent circuit

$$Ipv = Iph - Id - Ish \quad (3.4)$$

$$Vpv = Vd - IpvRs \quad (3.5)$$

$$Ish = (\frac{Vpv+Ipv \times Rs}{Rsh}) \quad (3.6)$$

$$Id = Is[\exp^{\left(\frac{q.Vpv}{n.K.T}\right)} - 1] \quad (3.7)$$

The saturation current Is also depends on the temperature according to the following expression:

$$Is = Irs.(\frac{T}{Tn})^3.\exp[\frac{q.Ego}{n.k}\left(\frac{1}{Tn} - \frac{1}{T}\right)] \quad (3.8)$$

Where n is diode ideality factor, K is Boltzmann‟s constant, Tn is nominal temperature in kelvin (298.15K) and Irs is the cell reverse saturation current in ampere at nominal temperature Tn and Ego is the band-gap energy of the semiconductor used in the cell. In eq. (3.8) saturation current is dependent on change of temperature.

$$Irs = \frac{Isc}{[\exp(\frac{q.Voc}{n.Ns.K.T}) - 1]} \quad (3.9)$$

The photovoltaic current is linearly dependent on the irradiance (G) and is also influenced by the temperature T according to the following equation

$$Iph = [Ip'n + Ki(T - Tn)]\frac{G}{Gn} \quad (3.10)$$

Iph’n is the photovoltaic current generated at nominal conditions (T = 298.15 K and G=1000 W/m²), and Ki, coefficient of variation of current as a function of temperature.

$$Iph,n = \frac{Rsh+Rs}{Rsh} \times Isc,n \quad (3.11)$$

where Isc,n is the rated short-circuit current under nominal conditions of temperature and irradiation.

Then from the above equations Current Ipv generated by the panel is expressed as a function of Rs and Rp resistors, voltage and currents and as follows:

$$Ipv = Iph - Is\left[exp^{(\frac{q(Vpv+Ipv.Rs))}{n.k.T}} - 1\right] - [\frac{Vpv+Ipv \times Rs}{Rsh}] \quad (3.12)$$

Where Isc is the short-circuit current and Voc open circuit voltage at nominal temperature 25o C and Ki is the temperature coefficient of short circuit current.

In practical applications the solar cells are connected in series strings which are then connected in parallel to produce the required voltage and current. Then finally practical pv panel models with parallel and series solar cells are:

$$Ipv = Np\{Iph - Is\left[exp^{(\frac{q(Vpv+Ipv.Rs))}{n.k.T.Ns}} - 1\right] - Ish\} \quad (3.13)$$

## Determination of shunt and series resistors

The output of photovoltaic panel depends on the shunt and series resistance that the panels made off. The module voltage which the current begins to drop rapidly becomes progressively lower as series resistance (Rs) increases; this impact at low voltage is not significant for typical values of Rs. Since $Vd = V + IRs$ is still low. Similarly Shunt resistor (Rsh) the low value of shunt resistance (Rsh) leading to higher power loss indicates processes defect or device degradation, this impact more sever at low irradiance. When taking a look at the formula for the maximum power output, that makes the peak of the mathematical P–V curve coincide with the experimental peak power at the (Vmp, Imp) point. This requires several iterations until Pmax,m=Pmax,e. Each iteration updates Rs and Rsh toward the best model solution.

$$Pmax,m = Vmp\left\{Iph + Is\left[exp\left[\frac{q}{kT}\frac{Vmp+Rs\times Imp}{n.Ns}\right] - 1\right] - \frac{Vmp+Rs\times Imp}{Rsh}\right\} = Pmax,e \quad (3.14)$$

From equation (3.14) shunt resistance becomes;

$$Rsh = \frac{Vmp(Vmp+RsImp)}{\left\{VmpIph-VmpIs\exp\{\frac{(Vmp+RsImp)}{nNs}\frac{q}{KTn}\right\}+VmpIs-Pmax,\}} \quad (3.15)$$

Imp and Vmp are respectively current and voltage of photovoltaic panel at maximum power point. Pmax,m is maximum power deduced via model identification procedure and Pmax,e is the experimental maximum power indicated by the panel manufacturer under nominal conditions.

Table 3. 1Polycrystalline PV module specifications at standard test conditions.

| No | Model | KC200G(Data sheet) | Modeling value |
|---|---|---|---|
| | Cell type | Polycrystalline silicon(156mm×156mm) | |
| **1** | Maximum power(Pmax) | 200.143W | 200.143W |
| **2** | Current at maximum power (Imax) | 7.61A | 7.61A |
| **3** | Voltage at maximum power (Vmax) | 26.3V | 26.3V |
| **4** | Open circuit Voltage (Voc) | 32.9V | 32.9V |
| **5** | Short circuit current (Isc) | 8.21A | 8.21A |
| **6** | I photovoltaic(Ipv) | 8.211A | 8.2A |
| **7** | Diode ideality constant (n) | 1.3 | 1.3 |
| **8** | Parallel resistance (shunt resistance)(Rsh) | 415.405 Ω | 415.405 Ω |
| **9** | Series resistance (Rs) | 0.221Ω | 0.221 Ω |
| **10** | Electric charge(c) | 1.6*10^-19c | 1.6*10^-19c |
| **11** | Short circuit current of cell(Ki) | 0.0032 | 0.0032 |
| **12** | *Boltzmann's constant(K)* | 1.38*10^-23 J/K | 1.38*10^-23 J/K |
| **13** | Band gap energy of the semiconductor(Ego) | 1.1ev | 1.1ev |
| **14** | Number of cell connected in series(Ns) | 54 | 54 |
| **15** | Number of cell connected in parallel(Np) | 1 | 1 |

| | | | |
|---|---|---|---|
| **16** | Solar irradiation(G) | 1000W/M^2 | 1000W/M^2 |
| **17** | Nominal temperature(Tn) | 298K | 298K |
| **18** | Tempreture(minimum)(T) | 25℃ | 25℃ |

### 3.3.1 Module I-V characterstics

Solar cells naturally exhibit a nonlinear I-V and P-V characteristics which vary with the solar irradiation and cell temperature. The output voltage reduces acutely with the raise in temperature whereas the current at the output terminal rises slightly; overall there is a net devaluation in power. With increase in irradiance, increase in the output current occurs greatly, subsequently results in increase in the output power.

The main electrical characteristics of a PV cell or module are summarized in the relationship between the current and voltage produced on a typical solar cell I-V characteristics curve. The intensity of the solar radiation (insolation) that hits the cell controls the current (I), while the increases in the temperature of the solar cell reduces its voltage (V).

Solar cell I-V Characteristics Curves are basically a graphical representation of the operation of a solar cell or module summarizing the relationship between the current and voltage at the existing conditions of irradiance and temperature are shown in fig 3.11

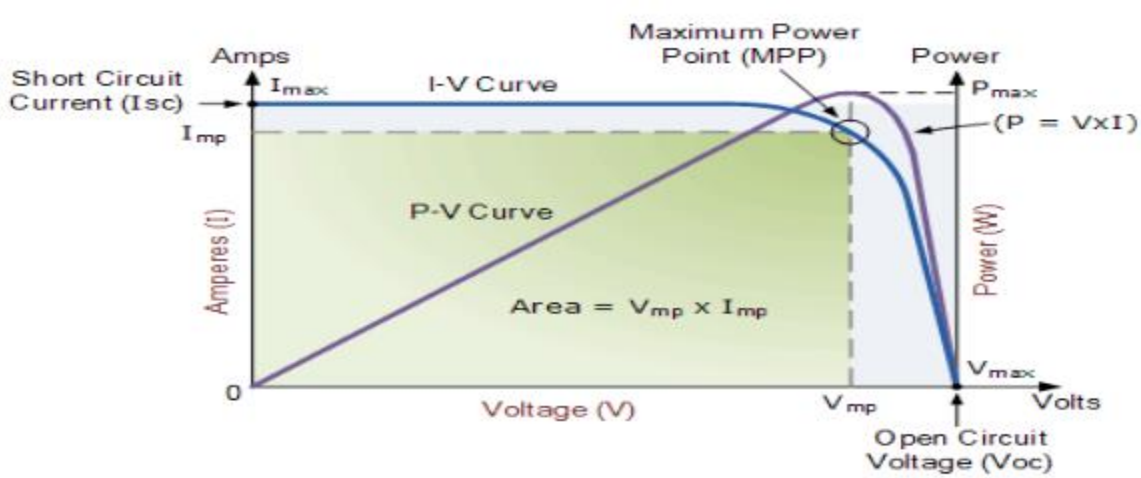


Figure 3. 11 solar cell I-V characteristics curve

The above graph shows the current-voltage (I-V) characteristics of a typical silicon PV cell operating under normal conditions. The power delivered by a solar cell is the product of current and voltage (I x V). If the multiplication is done, point for point, for all voltages from short-circuit to open-circuit conditions, the power curve above is obtained for a given radiation level. Then the span of the solar cell I-V characteristics curve ranges from the short circuit current ( Isc) at zero output volts, to zero current at the full open circuit voltage Voc . In other words, the maximum voltage available from a cell is at open circuit, and the maximum current at closed circuit.

Of course, neither of these two conditions generates any electrical power, but there must be points somewhere in between were the solar cell generates maximum power. The MPP of a solar cell is positioned near the bend in the I-V characteristics curve.

### 3.3.2 Factors that affecting Solar PV System Performance

Understanding these factors will help us to make accurate predictions for controlling them and smart decisions on how to eliminate those problems as much as possible. There are many factors affect the photovoltaic systems.

### Irradiance

Irradiance is a measure of the amount of sunlight falling on a given surface. The higher the irradiance on a solar cell, the more energy a cell will produce. It is obvious that as the irradiation level increases the PV output voltage and current increases with it. In general, the increment in the irradiation level leads to a theoretical increment in the maximum power voltage when there is no change in the cell temperature. On the other hand, the short circuit current ISC depends totally and linearly on the irradiance level therefore the maximum power current is changed as shown below. However, the total energy received by the system from the sun remains relatively constant from year to year. The angle of the sun, passing clouds, hazy weather, and air pollution can affect irradiance levels.

a) 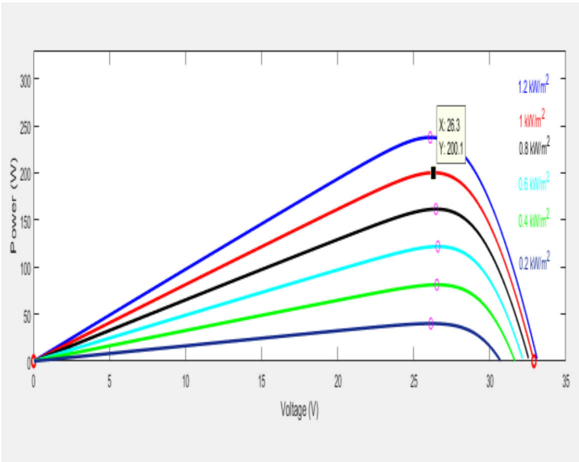

b) 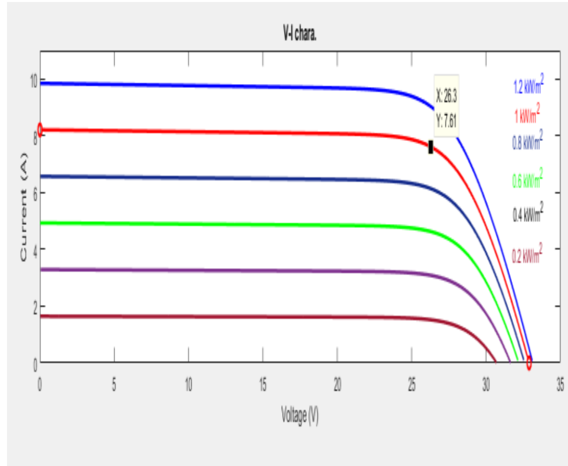


Figure 3. 12 (a) V-P (b) V-I characteristics at constant ambient temperature (STD)

## Temprature

As temperature increases, the band gap of the intrinsic semiconductor shrinks, and the open voltage (Voc) decreases following the p-n junction voltage temperature dependency of seen in the diode factor circuit . Solar cells therefore have a negative temperature coefficient of Voc.[15]

As temperature increases, again the band gap of the intrinsic semiconductor shrinks meaning more incident energy is absorbed because a greater percentage of the incident light has enough energy to raise charge carriers from the valence band to the conduction band. A larger photocurrent results; therefore, Isc increases for a given insolation, and solar cells have a positive temperature coefficient of Isc [15].

In general as the temperature increases with a fixed irradiation level it results in a slight increase in the short circuit current Isc, because the band gap energy decreases and more photons have enough energy to create electron-hole pairs. On the other hand, the increase of temperature have an obvious reduction in the PV panel output power due to the drop in the open circuit voltageVoc and the fill factor; therefore the module efficiency is reduced [15].

a) 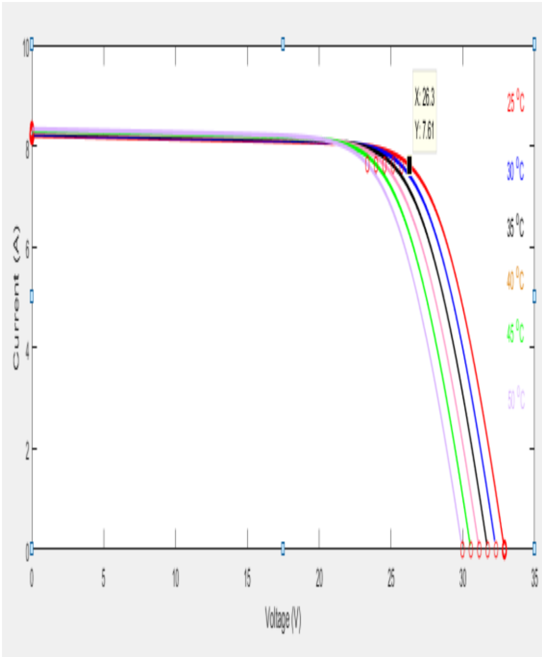

. b) 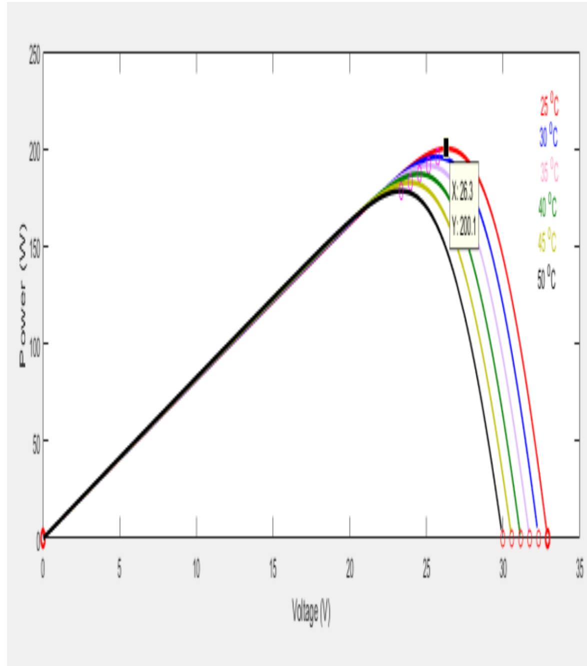


Figure 3. 13 (a) V-I characteristics (b) V-P characteristics of PV module at fixed irradiance level

### 3.3.3 Photovoltaic arrays

In general a single solar cell generates very low output power. Therefore, the photovoltaic cells are connected in particular configurations so as to form an array which is called a photovoltaic module. The modules consist of group of cells connected in series and parallel to provide the desired output power and voltage In addition to that, for a photovoltaic system a group of several PV modules are connected in parallel and series in form of PV array to generate the required voltage and current values for the system. When two or more solar modules are wired in series, the same current flows through each module and the output voltage is the sum of the voltages generated by each modules. the other hand when two or more solar modules connected in series the same voltage would have across each modules and the output current is the sum of each generated current. In addition to this to determine the construction of PV panel the following parameters are basic [27].

## Maximum Dc voltage of PV systems

The maximum DC voltage commonly is a safety relevant limit for sizing a PV system. All components (modules, inverters, cables, connections, fuses, surge etc.) have a certain maximum voltage they can withstand or handle safely. If this voltage gets exceeded, damage or even worse harm can result. From an economic point of view, a high voltage makes sense, by causing lower investments (fewer strings) and higher earnings (lower losses and mostly higher efficiencies). So the challenge is to size a PV system with the highest possible and safe DC voltage. In this case the required voltage to generate frome the PV panel is 289.3volt.

## Open Circuit Voltage of a PV module

On the datasheet of a PV module the open circuit voltage is specified most times at STC. (Standard Test Conditions) defining the irradiation at 1000W/m² and a cell temperature at 25°C) As the voltage correlates mainly with the cell temperature, also a temperature coefficient is specified, either in V/°C or %/°C. This is an inverse correlation, meaning the highest voltage occurs with the lowest cell temperature. Naturally also irradiation is necessary to produce voltage and power. So the voltage shows also a non-linear dependency from the irradiation, meaning at low irradiations also the voltages will be low. Modern PV Modules have an efficiency of 15% to 20% of the sun shine. While this percentage is converted into electricity the bigger "rest" (80% - 95%) of the irradiation is mostly converted into heat, meaning the PV cell (module) gets heated-up quite quickly. As a matter of fact, with irradiation (at daytime) the cell temperature always will be higher than the ambient temperature.

**Defining the minimum cell temperature for calculating Voc,max With STC values**

For the design of a photovoltaic system, the cell temperature limits established on the international market are minimum 25 °C and maximum 50 °C. Commonly these temperatures are used with the STC values of a module for the calculation of the extreme voltages. As the voltage of a PV cell (module) has a high dependency on its temperature but also a dependency on the irradiation (especially at low irradiation levels) and further the cells own temperature has a high dependency on the irradiation, the Minimum Cell Temperature can be chosen higher than the Minimum Ambient Temperature. Taking into account, that the lowest day temperatures are higher, modules are mounted on roofs where the surrounding air temperature is higher (heated up from the building, less dissipation of heat) and so on, even a higher difference between the lowest Minimum Ambient Temperature and the lowest Minimum Cell Temperature can be assumed.

## Calculating the maximum arising open circuit voltage (Voc, max)

The most established and easiest way to calculate the maximum dc voltage (maximum open circuit voltage) is to use the STC value from the datasheet with a certain estimated lowest occurring cell temperature.(from datasheet temperature Coefficient (Voc=-0.355%/°C ) and Temperature Coefficient of (lsc= 0.06%/°C). As a matter of fact, STC (1000W/m²) doesn"t take into account the influence from the irradiation. Lower voltage at lower irradiation.

$$Voc,max = Voc,stc[v] + Voc,stc[v](\frac{Tcell,min(°C) - Tstc(°C) \times Tc,Voc[\%/°C]}{100}) \quad (3.16)$$

## Determine the size of module in the strings and number of strings

As described, calculating maximum DC Voltage with a lower ambient temperature enables sizing the strings and more flexibility, which reduces investment costs and leads to higher yields. When building a PV system with sizing strings often the number of strings can be reduced and therefor the costs for inverter, cabling, mounting and supporting systems, connections, fuses, and so on can be saved. With less cabling (and other current carrying components) also the energy losses are reduced.

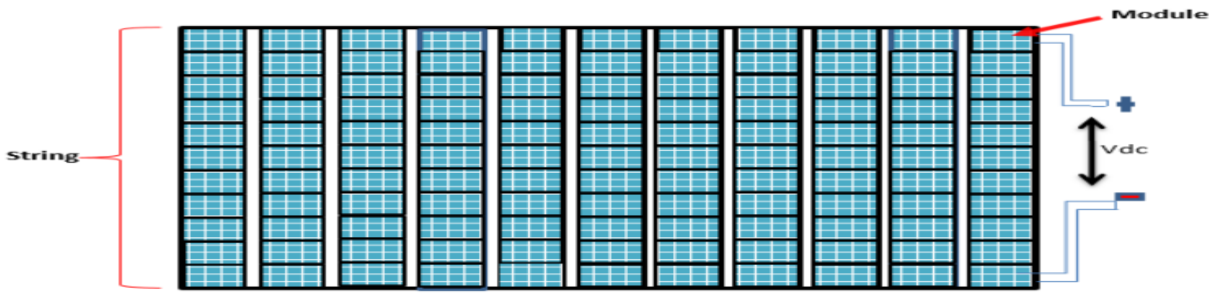


Figure 3. 14 The proposed real PV array series parallel structure

Now we can calculate the number of required strings for the system using the above equation and the desired output power. It requires eleven strings with eleven modules to generate the desired power which is 24.22kW. The proposed array has shown in the following figure and the calculated value of the array is listed in Table 3.2

Table 3. 2 The proposed module and array value

| Parameters | Modeled module value | Proposed array | Unit |
|---|---|---|---|
| Maximum power (Pmax,) | 0.200143 | 24.22 | kW |
| Open circuit voltage (Voc) | 32.9 | 361.9 | V |
| Short circuit current (Isc) | 8.21 | 90.31 | A |
| Maximum current (Imax) | 7.61 | 83.71 | A |
| Maximum voltage (Vmax) | 26.3 | 289.3 | V |
| Number of cells (Ns) | 54 | 6534 | - |

## 3.4 Design of DC-DC boost converter

DC-DC converters are used to interface the photovoltaic module with the inverter, in order to ensure the photovoltaic module is always operating at the maximum power point. This is done by controlling the converter duty ratio (D) with maximum power point tracking algorithms (MPPT). When the converter is operating at steady-state condition, the duty ratio, D

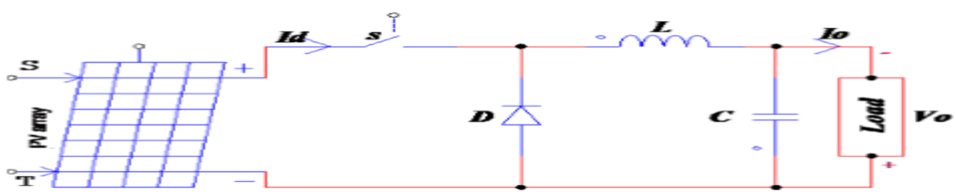


Figure 3. 15 Proposed Boost converter

The boost converter is used in this circuit which steps up the input voltage giving a steady output voltage but one which is always greater than the input voltage. The inductor, capacitor, load resistance & MOSFET values must be worked out for this circuit to be built. Determining a value for the output voltage is a key step in finding the value of components required and as shown the following table 3.3.

Table 3. 3 Boost converter parameters.

| | |
|---|---|
| Power rating (Pmax) | 24.22kW |
| Input voltage range (Vin=Vpv) | 289.3V |
| Output voltage (Vdc=Vout) | 500V |
| Max, input current (Ivp = Pmax/Vin) | 83.71A |
| Max. load current =Pmax/Vout | 48.4A |
| Switching frequency (fs) | 20KZ |
| Vout ripple (ΔVout) | 1%-50% |
| $I_{in}$ ripple ($\Delta I_{in}$) | 20%-40% |
| Inductance (L) | $6.75\times 10^{-4} H$ |
| Output capacitance (C) | $40.69\mu F$ |
| Duty (D) $= 1 - \frac{V_{in}}{V_{out}}\eta$ | 0.42 |
| Load resistance($R_{load}$) $= \frac{{V_{out}}^2}{P_{max}}$ | 10.3Ω |

## 3.4.1 Three-Stage Soft-Switching Boost Converter

Based on the working of single switch soft switching boost converter (SSSSBC), the three-stage soft switching boost converter (TSSSBC) has been developed and analyzed with eight modes. Figure shows the equivalent circuit diagram for various modes of operation of SSSSBC. For TSSSBC,the same is applicable with aphase shift of 120° for the MOSFETgate pulse in each arm. The formula for $i$ L($t$ ), $i\ L\ r\ (t\ )$,$V\ C\ r\ \ (t\ )i_{L(t),}$, and $V\ C\ a\ \ (t\ )$ during various modes of operation are summarized in Table.By introducing soft-switching technique, the switching loss is minimized. Hence, the total loss is minimized with the TSSSBC.Figure below Equivalent circuit diagram of

SSSSBC for various modes of operation.The circuit diagram for three-stage soft-switching boost converter (TSSSBC) is shown in Figure below. In the proposed TSSSBC, the three main inductors ($L$ 1, $L$ 2, and $L$ 3) and resonant inductors($L$ $r$ 1,$L$ $r$ 2,and $L$ $r$ 3)of reduced magnitudes (1/3rd of the original values) are considered. Driving pulses for the three switches were phase shifted by120∘. By introducing soft-switching technique, the switching loss is minimized. Hence,the total loss is minimized with the TSSSBC.

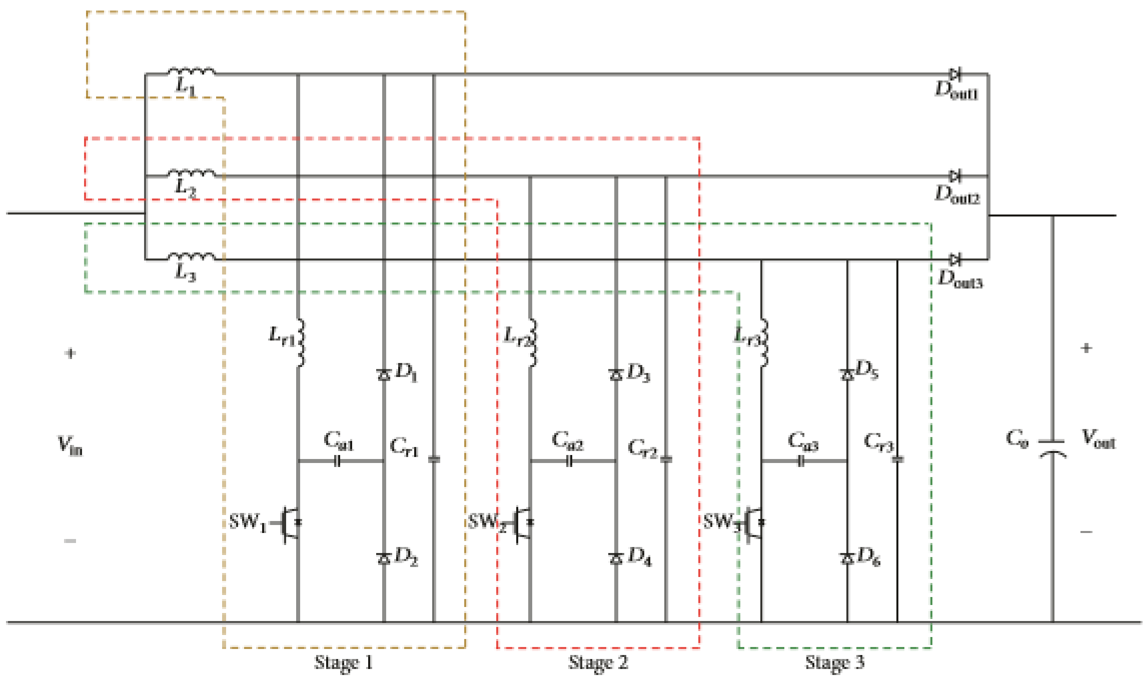


Figure 3. 16 Circuit diagram for three-stage soft-switching boost converter.

The inductor, capacitor, load resistance & MOSFET values must be worked out for this circuit to be built. Determining a value for the output voltage is a key step in finding the value of components required and as shown the following table.

The specification of active and passive elements used in this work based on the design equation is tabulated in Table3.4

Table 3. 4 Specifications of the components.

| Parameters | symbol | Value | Unit |
|---|---|---|---|
| Main inductor | $L_1, L_2, L_3$ | 187.6 | $\mu H$ |
| Resonant inductor | $L_{r1}, L_{r2,} L_{r3}$ | 6 | $\mu H$ |
| Auxiliary capacitor | $c_{a1}, c_{a2,} c_{a3}$ | 15.5 | nF |
| Resonant capacitor | $c_{r1}, c_{r2,} c_{r3}$ | 405 | $nF$ |
| Out put capacitor | $c_o$ | 10 | $\mu F$ |

### 3.4.2 DC Link Design

In many applications the solar converter is separated into two general components. The first component is the DC/DC converter which has the main task to ensure the required minimum DC input voltage of the second component, the DC/AC converter. The latter has to feed the power into the AC induction load which here is a three phase system. These two components are connected by a DC link capacitor to smooth the DC link voltage. An easy to use method to appreciate a minimal capacity of the capacitor bank is linked between the boost converter and the inverter [28]. This method of calculating a minimal capacity of the DC link capacitor depends on the expected maximum input power step and the definition of a limit of allowed voltage deviation. A widely-used limit is a deviation of ten percent of the DC link voltage at any step-on and step-off load response. The expected maximum input power step is equal to the solar panel power at the maximum power point (MPP).

### 3.4.3 Three phase full-bridge inverter design and interfaceing

The boost converter are step-up the photovoltaic output voltage of the PV array from 289.3volt (Natural) to 500volt (step up) DC outputs to feed the inverter, but the desired goal is to produce (400 ±5%)V AC in ordered to take the PV system of the ground .

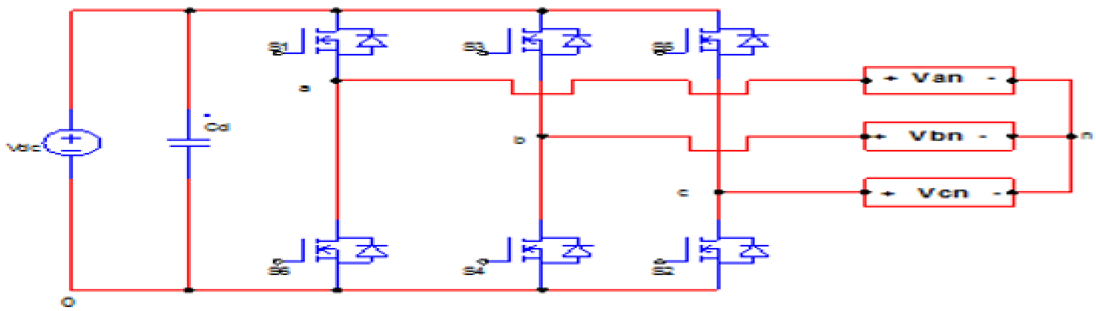


Figure 3. 17 The proposed three phase full bridge PWM inverter

### 3.4.1 Photovoltaic Array – Inverter Interface

Totally 121 multi-crystalline silicon types, 54-cells PV modules series parallel combination is conducted in the previous topic to design 24.22kw power generator PV arrays.

#### Nominal power

The maximum power generated by the investigated PV array is 27.04kW at an irradiation of 1200 W/m2, and an ambient temperature of 25°C. This operating point is however very seldom reached. The nominal power for the inverter is therefore selected to 27.04kW / 1.2 which is 22.533kW, with the capability of operating at 120% power during short time [30].

#### Starting power

The inverter should be able to invert even small amounts of DC power into AC power. In other words, the inverter must be able to operate at very low irradiation. The European efficiency is the weighted average of efficiencies down to 5%. Thus, the inverter should be able to operate at 5% or less of the nominal power, which is 1.35kW.

#### Open circuit voltage

The worst-case open-circuit voltage across the investigated PV array is estimated to 361.9V at 1000 W/m2, and a cell temperature of 25 °C. Thus, the inverter must withstand at least 361.9V without being damaged, so that 300 V inverter is selected.

#### Maximum Short Circuit Current

The maximum short-circuit current generated by the investigated PV array is 90.2A. A maximum current of 100A is therefore chosen.

## Over Voltage Protection

The inverter must be capable to withstand over-voltages caused by nearby lightning, etc. It is recommended to use a surge arrestor (Metal Oxide Varistor) with an inception voltage of 1.2 time nominal voltage [31].

The inception- and inclination-voltage should therefore be higher than 300V times 1.2 which is equal to 360V.

## 3.4.2 Inverter – load interface

The Output Ac voltage (Vrms) is calculated as;

$$V_{LL-convr} = m\frac{Vdc\sqrt{\frac{3}{2}}}{2} \quad (3.17)$$

$$V_{LL-convr} = 0.6124 * \mathrm{m} * Vdc \quad (3.18)$$

where: $Vdc$ is output voltage of the boost converter, and „m" is modulation index we had seen about modulation index in chapter two.

Table 3. 5 Specifications of three phase H-bridge inverter

| | |
|---|---|
| Nominal Power rating | 22.533kW |
| Input voltage, Vout of the boost converter(Vdc) | 500V |
| Modulation index(m) | 0.84 |
| Output Ac voltage(Vrms) | 257.21V |
| Output Ac current(Irms) | 48.44A |
| Frequency Ac out put | 50Hz |
| PWM frequency | 20kHz |
| DC link capacitor (CDc_link) | 200 μF |

## 3.4.3 LCL low pass filter design

Even if the LCL filter is selected, it is inherently unstable [32]. This is seen by the peak in the transfer-function around the resonant frequency, must be added to make the filter more stable. This can be done in several ways either by introducing a resistor in series with the filter capacitor, or by adding a resistor in parallel with the load connected inductor or to include a circuit, made up around a resistor and a capacitor in series, in parallel with the filter capacitor. But in this thesis it chosen introducing a resistor in series with the filter capacitor due to its simplest.

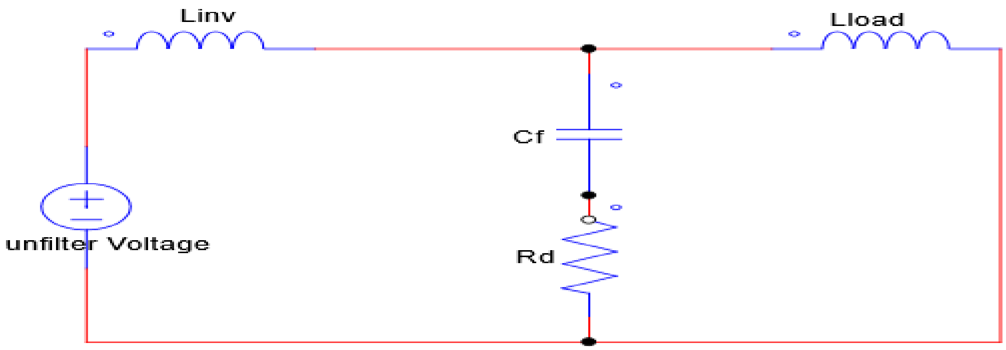


Figure 3. 18 LCL proposed Filter

The output ripple current ($\Delta I_L$) in the design of Linv was assumed up to 10% of the rated output current of the inverter ($I_{inv}$).

$$\Delta I_L = 10\% I_{inv} \quad (3.19)$$

A simplified formula for the LCL filter parameters with damping resistance may have discussed and analysis through the following equations, to calculate the inverter side inductance ($L_{inv}$), load side inductance ($L_{load}$), filter capacitance ($C_f$) and the damping resistance ($R_d$).

First calculating filter parameters is founding Linv, which is given as

$$L_{inv} = \frac{V_{inv-peak}}{16 \times f_s \Delta I_l} \quad (3.20)$$

Where $V_{inv-peak}$ is the peak output voltage of the inverter which is equal to the output of the boost converter input to the inverter. The output ripple current ($\Delta I_l$) in the design of Linv was assumed up to 15% of the rated output current of the inverter (Iinv). The load side inductance (Lload) is given by some Constance (R) multiply by the inverter side inductance.

$$L_{load} = R \times L_{inv} \quad (3.21)$$

The constant (R) is called relation factor which represents the ratio between Linv and Lload. The voltage drop across the inductor filter (Linv+Lload) must be less than 3% of the inverter output voltage (Vinv) [33].

$$I_{inv(max)} \times 2\pi \times f \times L < 0.03 V_{inv} \quad (3.22)$$

Where, $I_{inv(max)}$is the max inverter current (rms), f is the output frequency(50 Hz) and (L≈Linv+Lload). The capacitance of the filter ($C_f$) is limited to less than 10% of the base capacitance ($C_b$) that is given by:

$$C_f = 10\% C_b = 0.1 \frac{P_{inv}}{2\pi f V_{inv}^2} \tag{3.23}$$

Whre Pinv is the rated output power of inverter.and the design of the filter capacitance adopts the fact that the max power factor variation acceptable by the grid in case of grid tied inverter should be exceed 10 % [34]. Then the value of the Rd ought to be one third of the impedance of the filter capacitor at the resonant frequency (f0). The values of f0 and Rd are given by:.

$$f_o = \frac{1}{2\pi}\sqrt{\frac{V_{inv}+L_{load}}{L_{inv}\times L_{load}\times C_f}} \tag{3.24}$$

$$R_d = \frac{1}{3}\left(\frac{1}{2\pi f_o C_f}\right) \tag{3.25}$$

And assume the two inductor ratio is 0.8 which is constant R.and apply the given equations to calculate Table 3.6 parameters.

Table 3. 6 LCL filter specification

| Parameters | Specification |
|---|---|
| $L_{inv}$ | $173\mu H$ |
| $L_{load}$ | $138.4\mu H$ |
| $C_f$ | $30.8\mu f$ |
| $R_d$ | 0.5Ω |

# CHAPTER FOUR

# DESIGN OF CONTROLLERS FOR ENERGY EFFICIENCY OF PV SYSTEM

## 4.1 Fuzzy logic controller

Fuzzy logic is work based on a mathematical model which deals with uncertainty and imprecise, ambiguous, noisy, or missing input information. It compares an analog input signal to a predetermined logic variable membership function or fuzzy sets that correspond to values in the range 0 and 1. It is implemented in a control system to emulate human-like decisions in control. Essential characteristics of Fuzzy logics are listed below [35]:

- In fuzzy logic, exact reasoning is viewed as a limiting case of approximate reasoning.
- Knowledge is interpreted a collection of elastic or, equivalently, fuzzy constraint on a collection of variables and in FL everything is a matter of degree.
- Interface is viewed as a process of propagation of elastic constraints. And any logic system can be fuzzified.

The two main characteristics of fuzzy systems that i prefer to apply in my thesis are:

- Fuzzy systems are suitable for uncertain or approximate reasoning, especially for a system with a mathematical model that is difficult to derive.
- Fuzzy logic allows decision making with estimated values under incomplete or uncertain information.

### 4.1.1 Fuzzy logic controller structure

The fuzzy logic controller consists of four components: fuzzification interface, knowledge base, interface engine, and defuzzification interface.

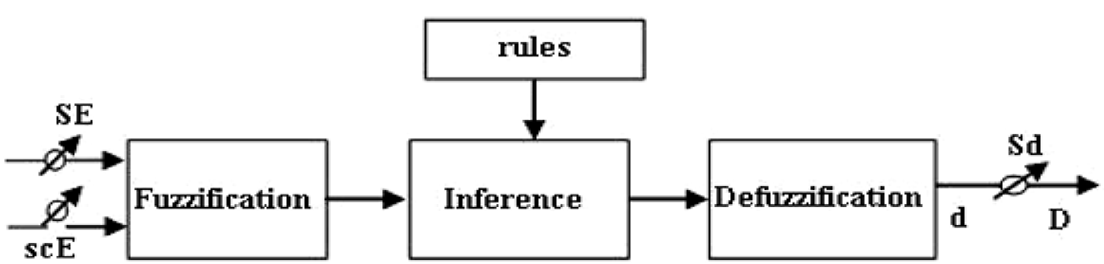


Figure 4. 1 General diagram of a fuzzy controller

The fuzzifier transforms crisp inputs into the fuzzy subsets to obtain degrees of memberships and represent them with linguistic variables, which in turn are used to activate rules. The fuzzy inference engine process those data to obtain the desired output. The defuzzifier converts those fuzzy outputs to crisp variables to complete the desired fuzzy logic control objectives. Every fuzzy set can be represented by its membership function. In practice the membership functions can have a number of different shapes depending on the designer interest. They can be triangular, trapezoidal, Gaussian, bell-shaped, sigmoidal or S-curve. Some of them are shown below. Trapezoidal or triangular membership functions are usually used in systems that require significant dynamic variation in a short period of time. A Gaussian or S -curve membership function is always selected if the system requires very high control accuracy [36].

### 4.1.2 Knowledge Base

It is the heart of the fuzzy control system. It is the inference basis for fuzzy control. The knowledge base defines all relevant language control rules and parameters.

The derivation of fuzzy control rules can be performed in not mutually exclusive, and it is necessary to combine them to obtain an effective system [37].

- ❖ Expert experience and control engineering knowledge: the fuzzy control rule is based on information obtained from the controlled system.
- ❖ Operators‟ control actions: observation of human controller‟s actions in terms of input-output operating data.
- ❖ Based on the fuzzy model of process: linguistic description of the dynamic characteristics of a process.

The number of base rules can be defined based on the number of membership in the fuzzy set and the inputs.

### 4.1.3 Fuzzy interface procedure

Among several techniques for performing the fuzzy interface process the Mamdani method and Takagi-Sugeno_Kang (TSK) method are the most commonly used methods in fuzzy controllers.

Mamdani method is usually more popular for most control engineering applications due to its computationally more efficient and has better interpolative properties than the other interface methods [38]. Mamdani fuzzy logic uses the linguistic variables to describe the process states and uses these variables as inputs to control rules. The terms of the linguistic variables are fuzzy sets with certain shape. Mamdani fuzzy logic usually uses the trapezoidal or triangular fuzzy set but other shapes are possible. The fuzzy interface process of the Mamdani method can be formed in four steps [39]: Fuzzification, rule evaluation, aggregation of the rule outputs and defuzzification.

**Fuzzification**; Fuzzification is the first step in fuzzy logic processing, in which the crisp quantities are converted to fuzzy inputs. The transformation process of fuzzy values is represented by the membership function. As an example if we have two inputs input 1 and input 2 firstly, take the crisp inputs, input 1 and input 2, and determine the degree to which these inputs belong to each of the appropriate fuzzy sets.

**Rule evaluation**; in this step the fuzzified inputs are applied to the antecedents of the fuzzy rule, then applying the fuzzy operator to fuzzy rule that has multiple antecedents to resolve the antecedents to a single number between 0 and 1. The fuzzy operator (AND or OR) is used to obtain this signal number. If the OR fuzzy operation is used, thus the classical fuzzy operation union is used or Maximum is used.

**Defuzzification**; The Defuzzification is the last step in the process of the fuzzy inference, and its reverse of the fuzzification process. The output of the fuzzy inference process result from the combination of the control inputs and it is still linguistic variable. However, the final output of the fuzzy control has to be a crisp number.

Hence the defuzzification process is needed to convert the fuzzy output back to the crisp output to be available for real application controllers. Among several defuzzification techniques, Mean of maximum method (MOM), Height method (HM) and Centre of gravity method (COG) are the most common techniques.

**Mean of maximum method (MOM)** :The MOM defuzzification strategy computes the average value of all the control actions whose membership functions reach the maximum.

$$MOM = \sum_{j=1}^{l} \frac{w_j}{l} \quad (3.26)$$

Where; wj is the support value when the membership function reaches the maximum value $\mu z$ (wj), and l is the number of support values.

**Height method (HM)** is can only be applied when the output membership function is an aggregated union result of symmetrical functions [36].

$$z = \frac{\sum_{j=1}^{n} w_j.\mu(w_j)}{\sum_{j=1}^{n} \mu(w_j)} \tag{3.26}$$

**Centre of gravity method (COG)** is the most widely used defuzzification technique in real applications. The advantage of COG method is the defuzzified values tend to move smoothly around the output fuzzy region. The COG technique is a basic general defuzzification technique that computes the value of the abscissa of the center of gravity of the area below the membership functions.

$$z = \frac{\sum_{j=1}^{n} w_j.\mu_z(w_j)}{\sum_{j=1}^{n} \mu_z(w_j)} \tag{3.27}$$

where n is the number of quantization levels of the output.

### 4.1.4 Fuzzy logic controller for Energy efficiency of PV system

The variation of solar radiation and ambient temperature are the most important factor in the MPPT of PV system. It is changing periodically and nonlinearly, hence FLC based MPPT is proposed to solve the problem and to deliver the maximum available power of the PV array to the load. A schematic of the photovoltaic array used to investigate the fuzzy logic controller performance is shown in Fig 4.3.

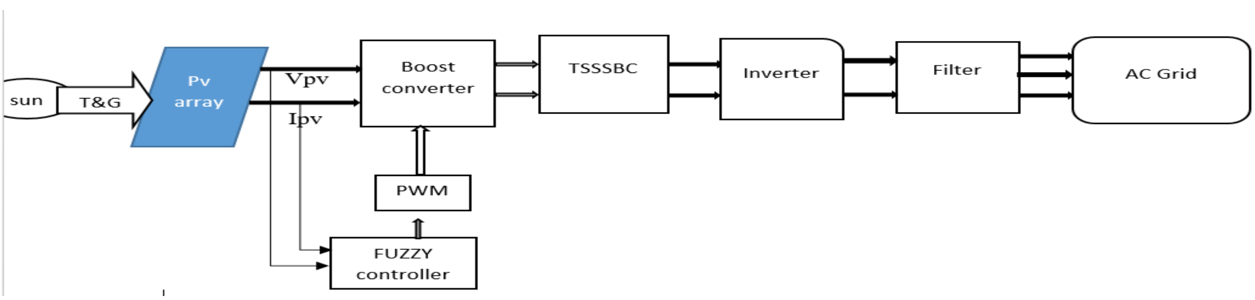


Figure 4. 2 Schematic diagram of the proposed FLC MPPT based Energy Efficiency of PV system.

**Operation of Fuzzy logic controller in the MPPT based Energy Efficiency of PV system**

It is introducing to determine the operating point corresponding to maximum power for different insolation levels and temperature. A fuzzy logic controller has been proposed to adjust the boost converter duty ratio which adapts online the PV array output voltage to maximize the output power.In the fuzzification stage, numerical input variables are calculated or converted into linguistic variables based on subsets called membership function the proposed FLC has two input variables and one output variable as shown above. The input variables of the fuzzy logic controller are current variation (Ipv) and voltage variation (ΔVpv) at sampling instant k. The output variable is the duty ratio (D) of the boost converter. The input variables Ipv and ΔVpv are expressed by the following Equations

$$I_{pv}(k) = G_I\{\frac{P_{pv}(k)-P_{pv}(k-1)}{V_{pv}(k)-V_{pv}(k-1)}\} \tag{3.28}$$

$$\Delta V_{pv}(k) = G_V\{V_{pv}(k) - V_{pv}(k-1)\} \tag{3.29}$$

And the crisp value of the output variable ΔD (k) is computed by;

$$D(K) = D(k-1) + G_D\Delta D(K) \tag{3.30}$$

$G_I$, GV and GD are scaling factors used to normalize the Ipv(k), ΔVpv (k) and ΔD (k) respectively. The scaling factors play an important role in optimizing performance and can be chosen using trial and error. D (k) is the final output signal sent to the system. The membership functions of the both inputs and output variables are represented by symmetric triangular functions and defined normalized range of (-1, 1) for input 1, (-1, 1) for input 2 and (-1, 1) for output.

The membership functions of the input variables Ipv and ΔVpv, and the output variable sets which are assigned for fuzzy sets have the same shape. The membership function of both inputs and output variables are assigned seven sets, including positive big (PB), positive medium (PM), positive small (PS), zero (Z), negative big (NB), negative medium (NM) and negative small (NS) and the class range arrangement is listed in appendix (C).

The fuzzy control rules have been set up using a set of IF-THEN statements that contain all information for the controlled parameters. The fuzzy control rule includes 49 rules as described in Table (4.1). These rules are used for the control of the boost converter such that the maximum power is achieved at the output of the PV array.

The fuzzy rules are designed to incorporate the following considerations keeping in view the overall tracking performance.

- ❖ If a positive variation in the generated voltage is accompanied with a positive variation of PV array output power, then the duty cycle ratio should be increased. Otherwise if the variation of PV array output power is negative, then duty cycle ratio should be decreased.
- ❖ If the generated voltage variation is zero or sufficiently close to zero which means that its maximum is reached, then there should be no change in the duty cycle ratio.
- ❖ If a negative variation in the generated voltage is accompanied with a positive variation in PV array output power, then the duty cycle ratio should be decreased. Otherwise if the variation of PV array output power is positive, then duty cycle ratio should be increased.

Table 4. 1 fuzzy rule base table

| **ΔVpv/Ipv** | **NB** | **NM** | **NS** | **Z** | **PS** | **PM** | **PB** |
|---|---|---|---|---|---|---|---|
| NB | NB | NB | NB | NB | NM | NS | Z |
| NM | NB | NB | NB | NM | NS | Z | PS |
| NS | NB | NB | NM | NS | Z | PS | PM |
| Z | NB | NM | NS | Z | PS | PM | PB |
| PS | NB | NS | Z | PS | PM | PB | PB |
| PM | NS | Z | PS | PM | PB | PB | PB |
| PB | Z | PS | PM | PB | PB | PB | PB |

In the defuzzification stage and inference mechanism the output of fuzzy logic control is converted from linguistic variables to numerical variables. The inference mechanism determines the matching degree of the current fuzzy input with respect to each rule and the controller has to resolve the conflict between different rules being obeyed at the same time and decides which rules are to be obeyed according to the input field. Then the obeyed rules are combined to form the control actions. The method of dfuzzifcation used for this is called Centre of Gravity (COG) or centroid. The idea of (COG) is to find the variable value of the center of gravity of the composite membership function for the fuzzy value.

## 4.2 Phase-Locked Loop Controller

The PLL is designed to control the phase difference and other harmonic distortion. The phase of generated signals of solar system is automatically adjusted to match the phase of an input signals of the grid. Block diagram of the phase-locked loop (PLL) considered in this work to enhance the performance of the system under consideration is shown in Fig 4.4.

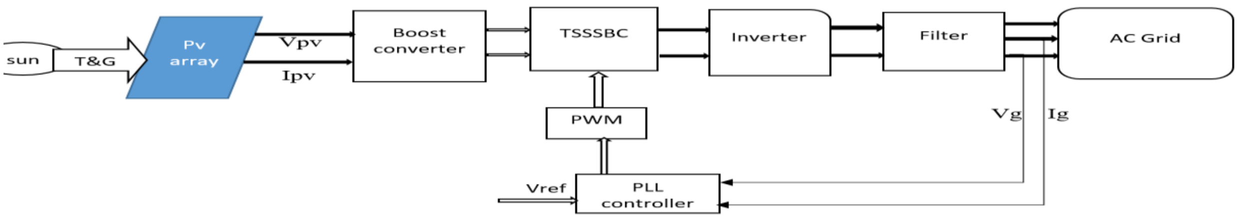


Figure 4. 3 Schematic diagram of the proposed PLL based Energy Efficiency of PV system.

A PLL is a closed-loop feedback structure that sets fixed phase relation ship between its output phase and the phase of a reference. It tracks the phase changes that are within the band width of the PLL. A PLL comprises several components, namely, phase or phase-frequency detector, charge-pump current, loop filter, voltage-controlled oscillator,and frequency divider.

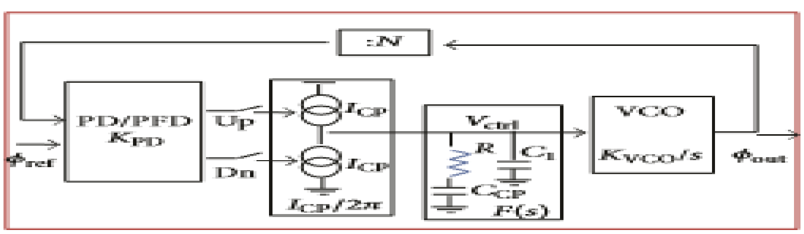


Figure 4. 4 Block diagram of phase-locked loop.

The open-loop transfer function canbe written as

$$H_{open}(s) = \kappa_{PFD}.\frac{I_{cp}}{2\Pi}.F(s).\frac{k_{VCO}}{s} \quad (3.31)$$

where $\kappa_{PFD}$ is the phase-frequency detecto rgain, $F(s)$ is the loop filter transfer function,and $k_{VCO}$ is the transfer gain of the VCO. The closed-loop transfer function from the input phase to the output phase is a low-pass filter. This low-pass behavior of a PLL is desirable because it rejects input noise frequencies higher than the PLL bandwidth. Similarly, the closed-loop transfer function from the VCO control voltage, $V$ctrl,to the out put phase is a band pass filter.It rejects internal noise coupled in to $V$ctrl with in the PLL band width.Filtering out noise sources by the closed-loop behavior of the PLL forms the baseline for jitter analysis. Noise of the PLL's output clock can be optimally filtered by adjusting the loop bandwidth and peaking in frequency response based on the dominant noise source. The loop bandwidth and peaking are adjustable by varying loop parameters.

# CHAPTER FIVE

# SIMULATION STUDIES AND ANALYSIS OF RESULTS

This chapter describes how the MATLAB/SIMULINK models of the proposed PV power systems are implemented to test and verify the functionality of the proposed MPPT controllers. PV system is simulated in MATLAB, with an AC Gird to demonstrate the feasibility and performance of the proposed artificial intelligence controller based on MPPT of PV system. Used two controller, Fuzzy Logic Controller and PLL controller.

## 5.1 Photovoltaic System modelling using Simulink

The system design is modeled and simulate using MATLAB R2016a /SIMULINK. The modelled system consists mainly of PV array model, DC/DC boost converter(BC,TSSSBC) model used to interface PV output to the inverter to track the maximum power of the PV array, DC/AC three phase PWM inverter model used to interface with the AC Gird, LCL low pass filter to supply a pure sinusoidal output voltage to the Gird.

The PV model simulator was implemented in MATLAB/SIMULINK as shown in the appendix (A).

The PV array used in the simulation is a 24.22kW power that eleven strings with eleven modules of 200.143W power. Or 11x11 elements are combined to generate the desired power at standard conditions specified at irradiation of (G = 1000kW/m2) and temperature of (T =25℃).

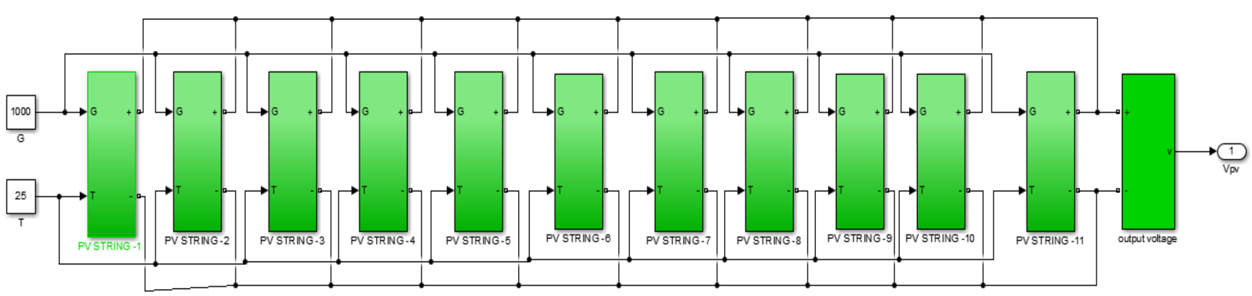


Figure 5. 1 Connection of Eleven PV strings in parallel

In fig 5.1 series parallel connections are applied, first a 200.143W PV module are designed to build a strings which consists eleven series modules, then constrict the PV array or PV panel by connecting 11 PV strings in parallel as the designed calculated values.

Totally one hundred and twenty one modules are implemented to get the PV power that used to generate 24.22kW for the required purpose.

The PV panel Simulink block has been masked in the embedded form as follow. The temperature T and isolation G are fed to the Embedded MATLAB Function and the outputs are the current and voltage produced by the panel.

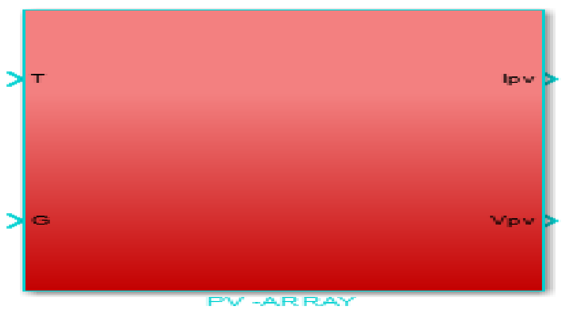


Figure 5. 2 Embedded PV Array or PV panel SIMULINK model.

Table 5. 1 The proposed module and array value

| Parameters | Modeled Module value | Module value Proposed array Value | Unit |
|---|---|---|---|
| Maximum power (Pmax,) | 0.200143 | 24.22 | KW |
| Open circuit voltage (Voc) | 32.9 | 361.9 | V |
| Short circuit current (Isc) | 8.21 | 90.31 | A |
| Maximum current (Imax) | 7.61 | 83.71 | A |
| Maximum voltage (Vmax) | 26.29 | 289.3 | V |
| Number of cells (Ns) | 54 | 6534 | - |

The voltage to current , voltage to power and voltage to power relation curve of the simulated model is used to know the influence of temperature and irradiation change on the output characteristics of the PV panel.

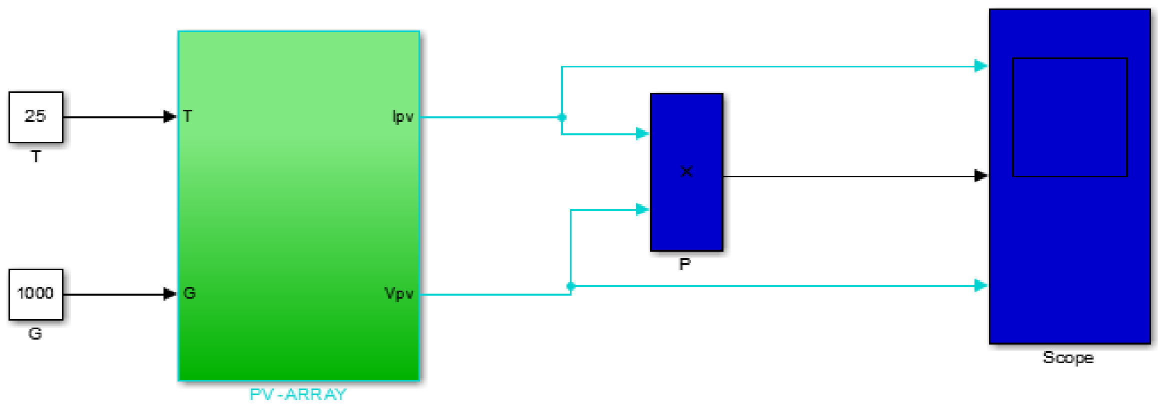


Figure 5. 3 Simulink model for data collecting system of PV array

The output of the PV array is recorded in different level of irradiation (1200, 1000, 800, 600, 400 & 200) w/m2 at 25℃, as well as different environmental temperature (50, 45, 40, 35,30 & 25) at standard values for afar region value of temperature and irradiation level and the result of the characteristics curves are shown in figures below.

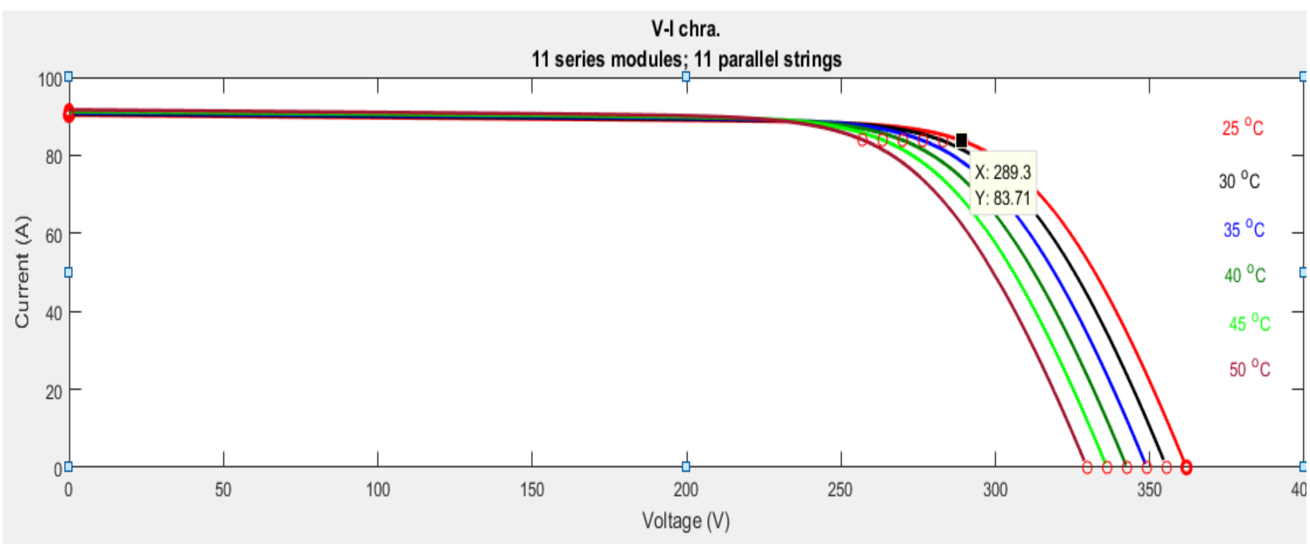


a).V-I characteristics

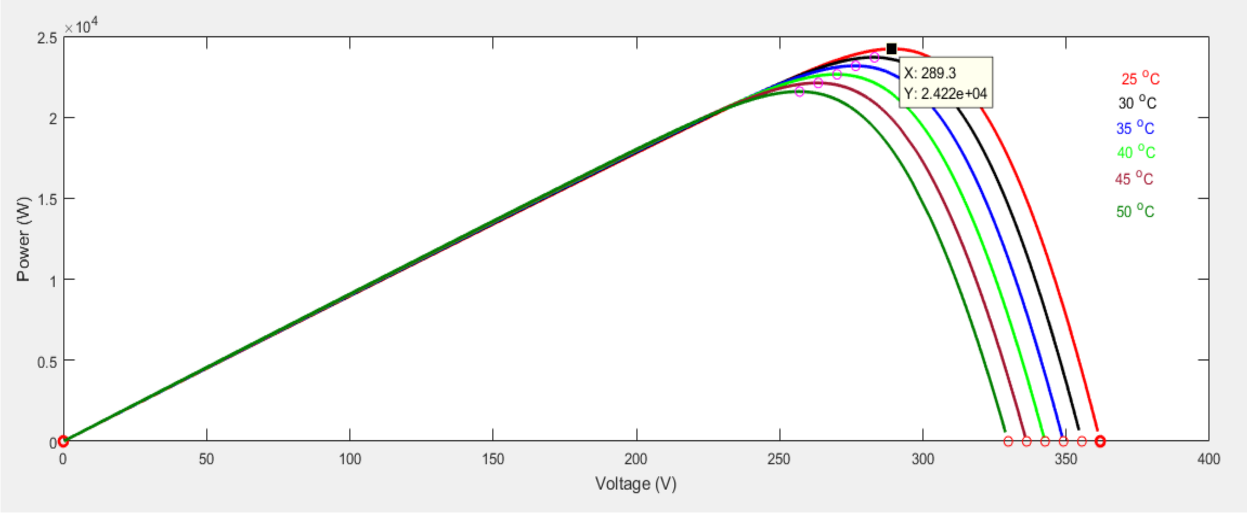


b).V-P characteristics

Figure 5. 4 V-I and V-P characteristics of the PV array at standard irradiation level.

In the fig.5.4 the effect of temperature clearly shown on current voltage and power, as temperature increased the voltage becomes less on the contemporary the generated current is increased. To get the maximum power the output current and voltage has been maximum, this phenomena occurs during the low value of temperatures.

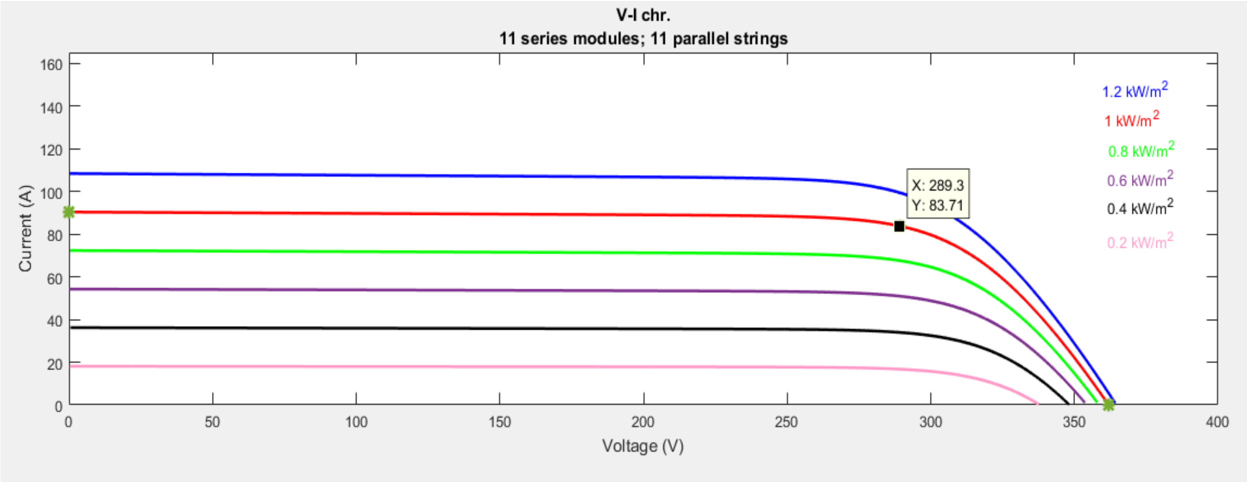


a). V-I characteristics

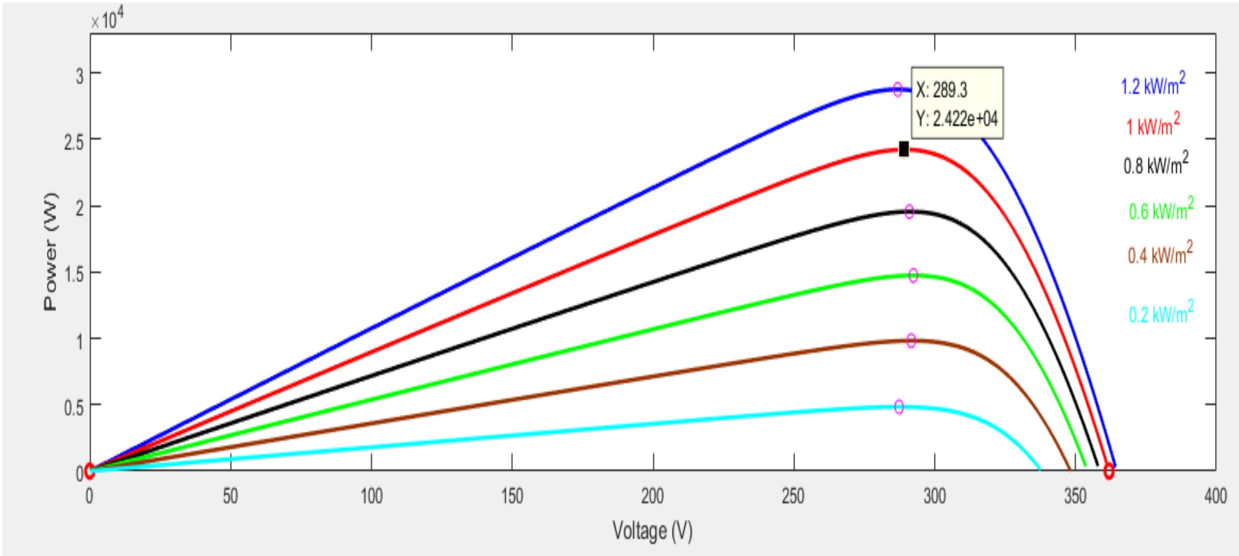


b). V-P characteristics

Figure 5. 5 V-I and V-P characteristics of PV array at standard temperature

In fig 5.5 the effect of irradiation at standard level of temperature is displayed. The irradiation had directly relationship with current and voltage, as the irradiation increased the current also increased and the voltage had slowly increased.

### 5.1.1 Boost converter modelling

The boost converter is conducted in MATLAB and simulated using SimPower Systems blocks and the circuit diagram is depicted in Fig. 5.6. The converter consists of MOSFET switch and freewheeling diode. Additionally, input filter and output capacitor is included. The inductor is responsible for reducing the output current ripple; the larger the value of the inductor, the smaller the value of the ripple and the Capacitor responsible to minimize harmonic.

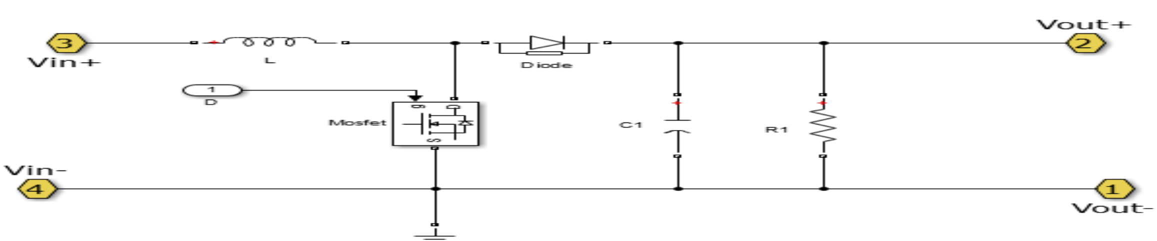


Figure 5. 6 Simulation model of DC-DC Boost converter

The model can be masked by the SIMULINK and simplified into Single block.

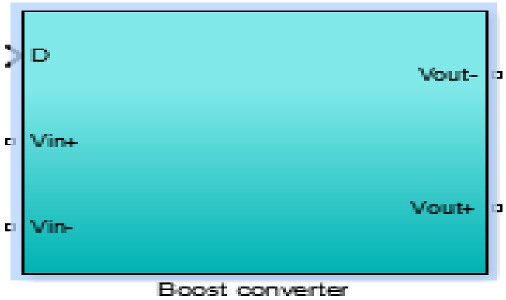


Figure 5. 7 Boost converter one block representation

There are three inputs and two outputs in the boost converter block, the inputs are the duty cycle(D) from the PWM block and Vin- , Vin+ are the input negative and positive voltage from the PV panel respectively. The outputs are Vout+, Vout- the positive and negative output voltage is the voltage to be generate from PV panel.

### 5.1.2 Three-Stage Soft-Switching Boost Converter Modelling

The Three-Stage Soft-Switching boost converter is conducted in MATLAB and simulated using SimPower Systems blocks and the circuit diagram is depicted in Fig. 5.8. The converter consists of MOSFET switch and The values of the inductor and the capacitor for auxiliary resonant circuit of TSSSBC are chosen so as to design the resonant frequency to be less than the switching frequency.The main inductor rating is 33% of the actual inductor rating used in a single stage boost converter. The boost converter, interleaved boost converter,and the three-stage boost converter are simulated for the same input voltage and switching frequency and the performances of the three converters. The inductor is responsible for reducing the output current ripple, introducing soft-switching technique, the switching loss is minimized. Hence, the total loss is minimized with the TSSSBC.

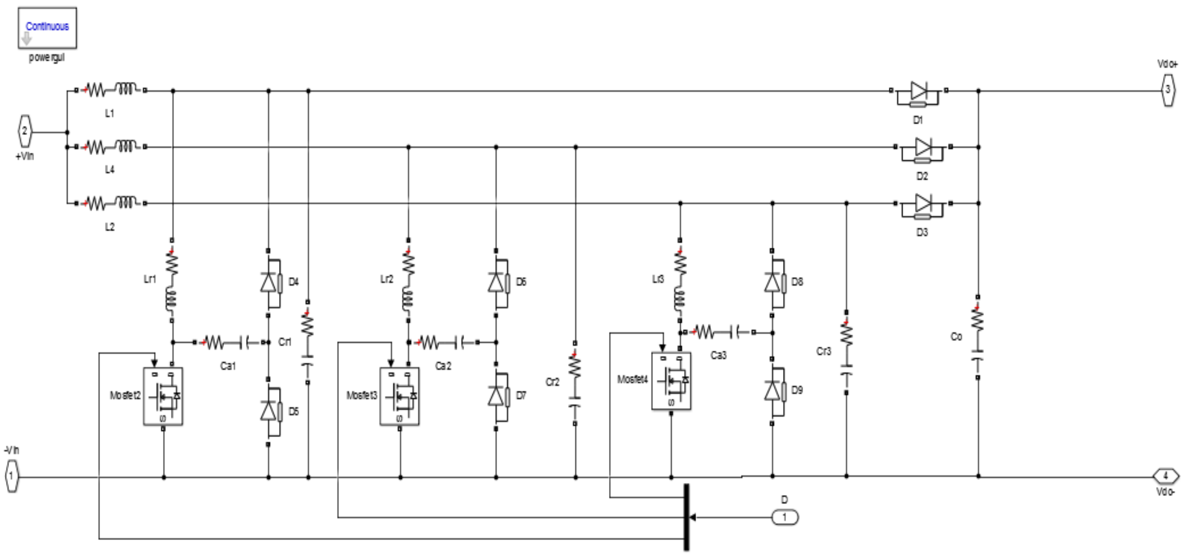


Figure 5. 8 Simulation circuit of three-stage soft-switching boost converter

The model can be masked by the SIMULINK and simplified into only one block

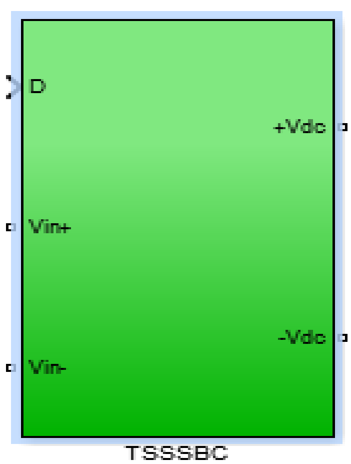


Figure 5. 9 TSSSBC one block representation

There are three inputs and Two outputs in the TSSSBC block, the inputs are the duty cycle(D) from the PWM block and Vin- , Vin+ are the input negative and positive voltage from the boost converter respectively. The outputs are Vdc+, Vdc- the positive and negative output voltage .

### 5.1.2 DC to AC converter modelling

In chapter two the inverter topology simulation result is mentioned detail, but in this circuit three phase full-bridge inverter takes the output of the TSSSBC as the input and the gate signal which is generated by two level PWM generator, finally it inverts the input DC voltage in to Ac voltage to drive the energy efficiency of PV system.

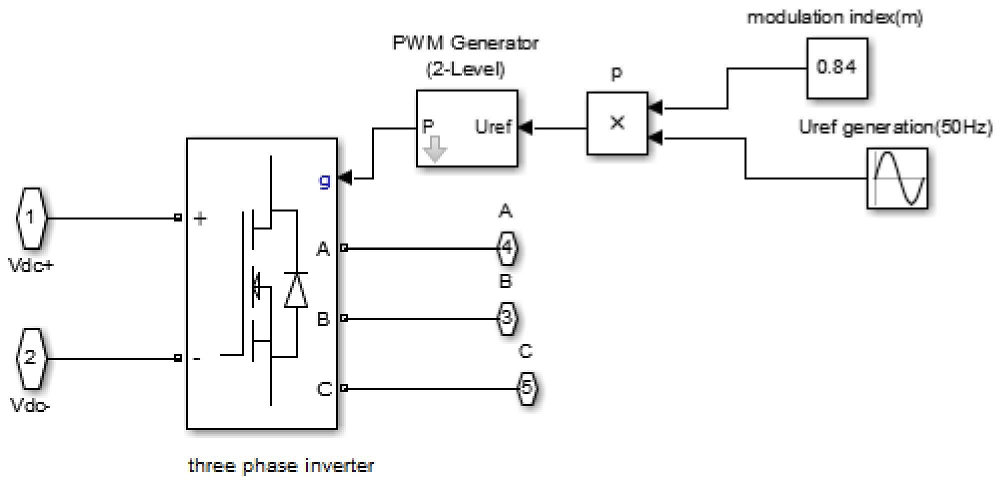


Figure 5. 10 Simulink models of three phase inverter

### 5.1.3 LCL Low pass filter modelling

The output of the full bridge inverter is not pure sinusoidal ac voltage this responsibility is taken to account for the low pass filter which is minimize the harmonic of the output voltage to supply a pure sinusoidal output voltage to the load. The inverter contains the input side and output side inductor, filter Capacitor and resistor with the appropriate scale.

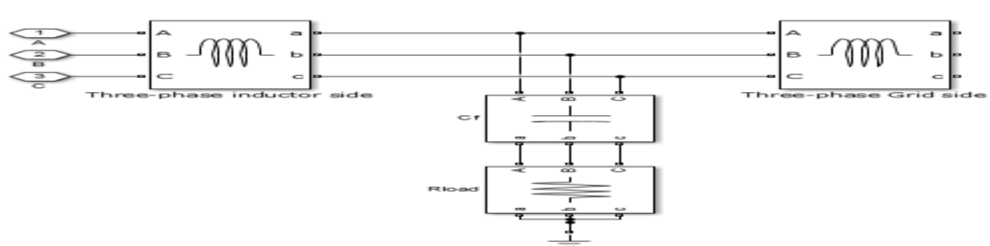


Figure 5. 11 Simulink model of LCL filter

## 5.2 Simulink Model of controllers for Energy efficiency of PV system

In this thesis artificial intelligence and PLL controlling method had been practice, those are fuzzy logic controller and PLL controller.

### 5.2.1 Fuzzy logic controller simulink model for Energy efficiency of PV system

The control model is shown in Fig. 5.12. The fuzzy control rule has been completed in MATLAB FIS as discussed in chapter five section two. The detailed design of the Fuzzy Interface system (FIS) editor, Membership Function Editor and Rule Editor are as shown in the Appendix (C). The FLC uses the PV array Current Ipv and the output voltage Vpv as input signals and produces duty cycle ratio D as a control signal for the boost converter.

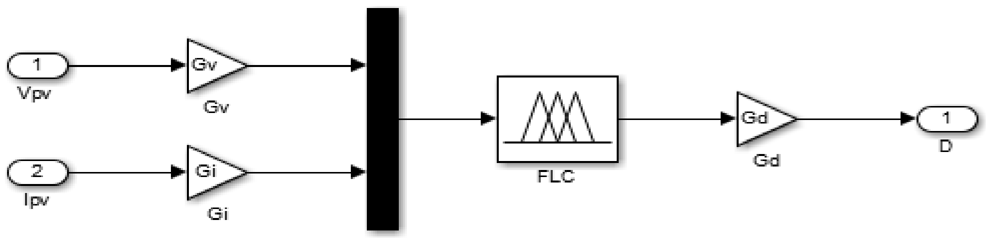


Figure 5. 12 SIMULINK block of fuzzy logic controller

Table 5. 2 Fuzzy logic controller parameter

| Fuzzy logic controller parameter | Scale |
|---|---|
| The scaling factor of the PV array output current variation (Gi) | 0.003122 |
| The scaling factor of the PV array output variation (Gv) | 0.14517 |
| The scaling factor the duty ratio variation (GD) | 1 |

### 5.2.1 Phase-Locked Loop Controller simulink model for Energy efficiency of PV system

The control model is shown in Fig. 5.13.The PLL control rule has been completed in MATLAB. The detailed design of Phase-Locked Loop, phase detector (PD), loop filter (LF) and voltage controlled oscillator VCO .The PLL uses the Grid current Ig and the Grid voltage Vg as input signals,reference voltage Ur and produces duty cycle ratio D as a control signal for the TSSS boost converter.

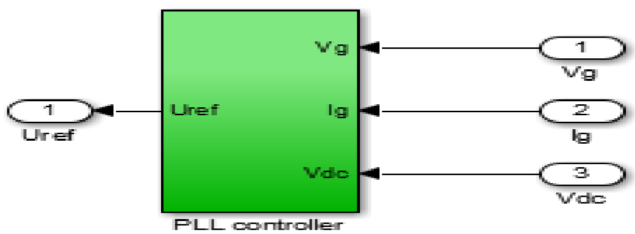


Figure 5. 13 SIMULINK block of phase locked loop controller

Table 5. 3 phase locked loop parameter

| phase locked loop parameter | Scale |
|---|---|
| Kpd | 0.1 |
| Kp | 0.5 |
| Ki | 1 |
| Kvco | 1 |
| Vref | 500 |

## 5.3 Energy efficiency of PV system with and without controllers

The MATLAB\SIMULINK software is used for simulation of the energy efficiency of photovoltaic system. The system was simulated to verify the functionality and performance of the proposed FLC based MPPT and to quantify how the proposed controllers contribute to an increase in the system efficiency with each algorithms to connect the PV array system to the AC grid. The device was used to clear flickers on the lines such as phase difference, harmonics. So, synchronizing the solar PV array system with the utility grid using PLL has given a better result.The effectiveness of the proposed methods to handle weather condition changes especially the change of solar irradiation and temperature change is evaluated through different levels of solar irradiation and temperature levels.The total Simulink block of the system is shown in Fig 5.14.

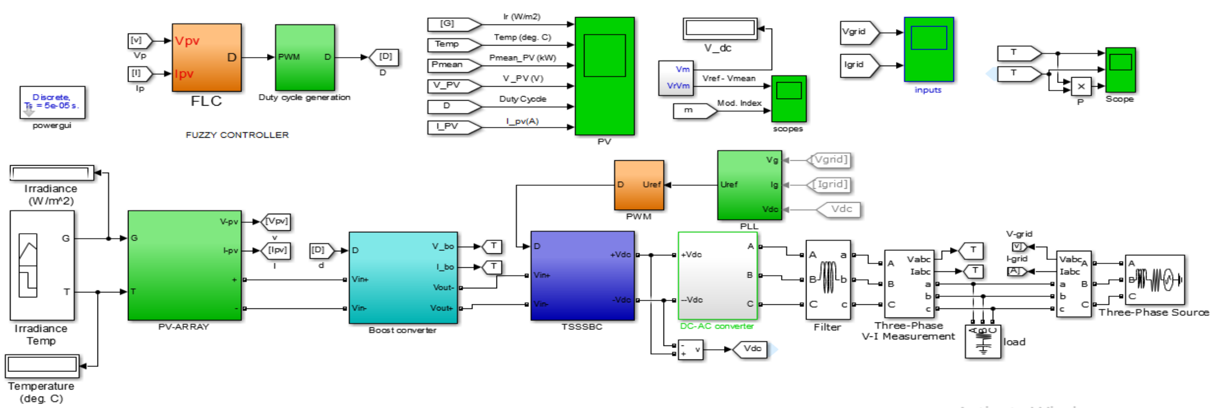


Figure 5. 14 General Simulink model of the PV systems

To test the performance and response of each controller for the PV system three conditions had applied.

First, slow and rapid changes in solar insolation using the three proposed MPPT controllers at standard temperature (25℃) and the insulation was started from 1000w/m2 and then changed from 1000w/m2 to 600 w/m2 and 600 w/m2 to 400W/m2 at the time division of 0.5s, 1.0s 1.5s respectively

The second division was both temperature and solar irradiation level is varied randomly, the insulation continues from 200W/m2 raised to 1200W/m2 and then from 1200W/m2 to 800W/m2, from 800W/m2 to 1000W/m2 with the temperature (35℃, 50℃ and 25℃) at the time division of 2.0s, 2.5s and 3.0s respectively.

The final division was slowly and rapid change in temperature at standard insulation (1000W/m2) and the temperature changes starting from the previous division up to 35℃ and then from 35 ℃ to 45℃, finally tend to 25℃ at a time of 3.5s, 4.0s and 4.5s respectively.

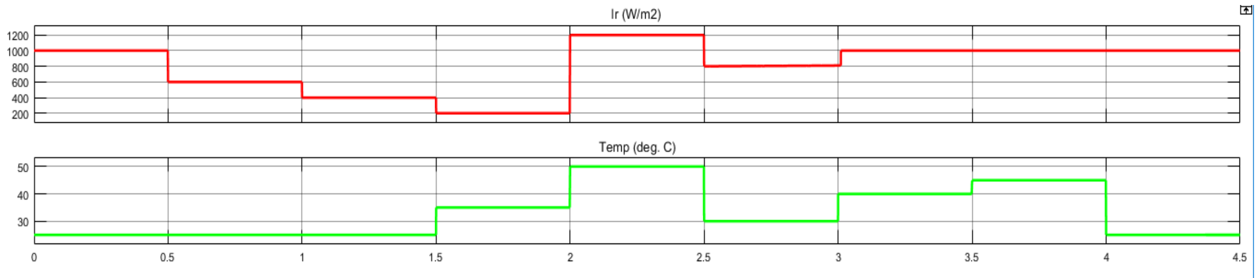


Figure 5. 15 Different level of solar irradiation and temperature values for testing system performance

### 5.3.1 Energy efficiency of PV system simulation without any controller

In this PV system, the PV array has been connected to the 24.22kW Ac grid without controller at the MPP duty cycle (Dmp) to the boost converter using PWM generators. The system was subjected to a sudden change in solar irradiation and temperature. The simulation results for these systems are shown in the following figures which are the PV array output current, voltage, power and the three phase ac voltage and current. The simulation waveforms show that connected system is operating far from the maximum power point at some irradiation and temperature levels . Fig. 5.16 and Fig. 5.17 illustrates that the PV array current and voltages are far from the optimum level. As a result of this, the system deviates from the maximum operating power all the time as shown in Fig. 5.18. The system is operating at a power point much less than the maximum power point and the three phase output voltage and current wasn‟t smooth and the optimum value is not achived. The result obtained from the simulated grid connected solar PV array model without PLL was not quite clear as displayed by the waveforms. Based on observation, the system output is distorted by flickers. Therefore, it clearly shows that, both the solar PV array system and the utility grid are not having same characteristics. Therefore, some of the energy will be dissipated, hence, the systems is operating at a relatively poor efficiency or even not work, for various insolation and temperature levels.

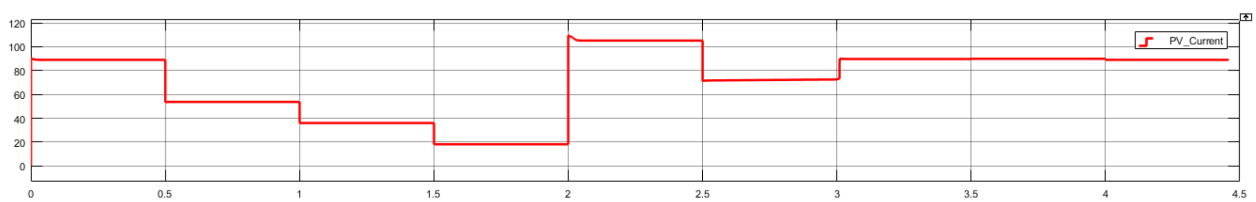


Figure 5. 16 PV array output current at different environments

The generated 90.31A Ipv current is boosted to different level of amperes .The output boost current from zero to 0.5s and from 3s to 4.5s has been near to the optimum relative to other time intervals.

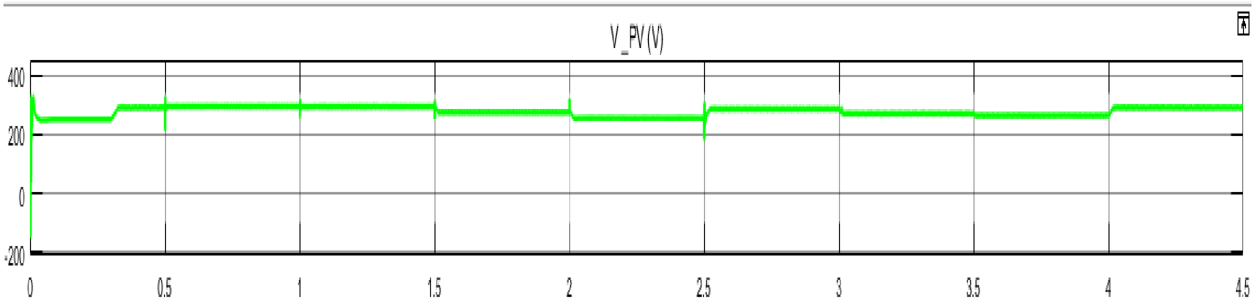


Figure 5. 17 PV array output voltage at different condition.

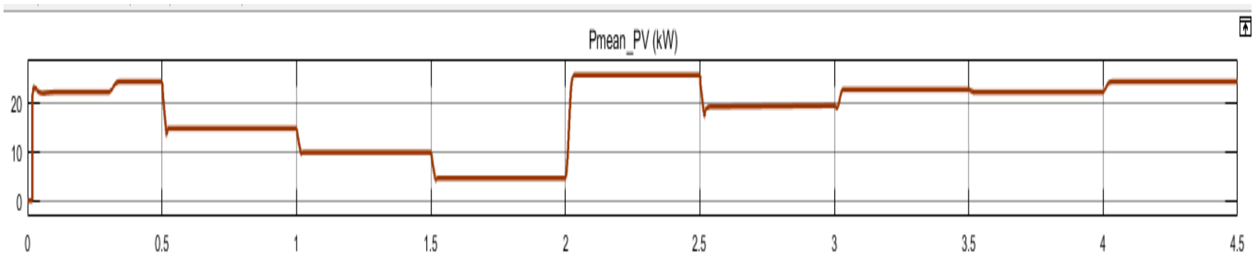


Figure 5. 18 The PV panel output power in direct connection systems

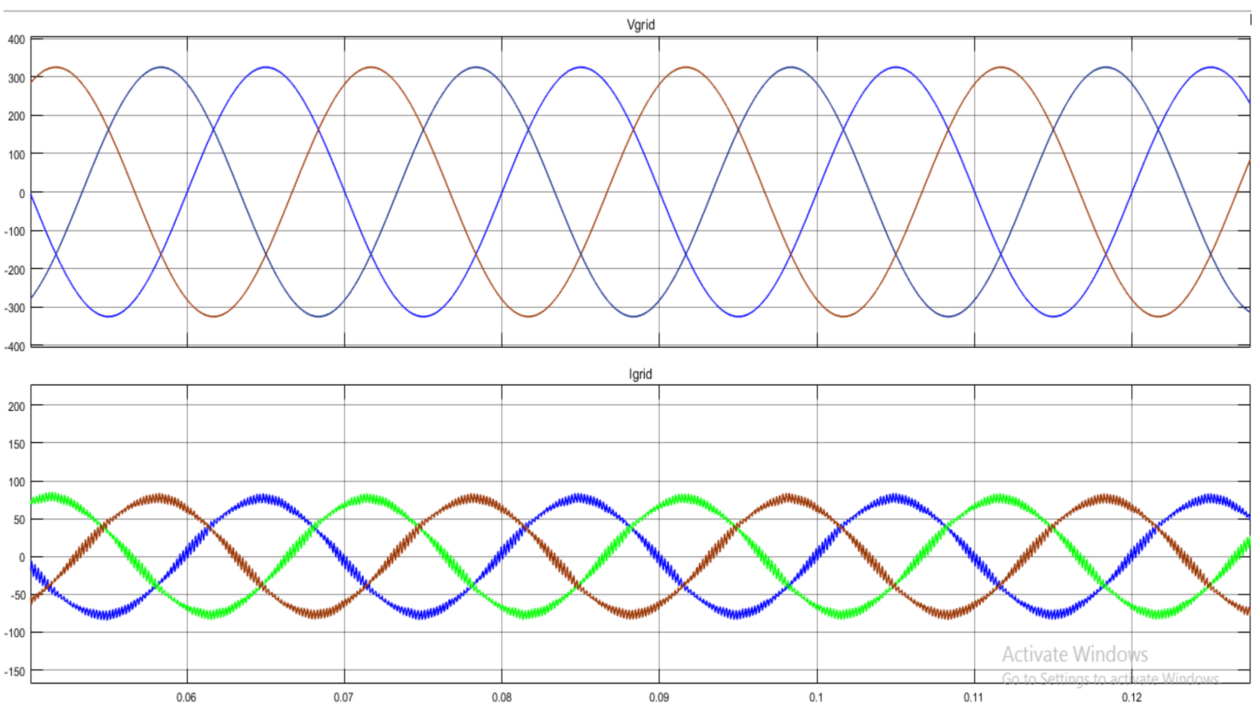

Figure 5. 19 The output three phase voltage and current of the PV system at different conditions

As we seen in figure 5.19 the three phase Ac output voltage and current is not good to use for the required purposes as well as any Ac equipment due to its harmonic output properties. The output result clearly indicated that the synchronization was unbalanced due to the absent of PLL. Therefore, due to the poor result obtained from the system PLL is needed in the system to clear the distortions on the lines.

### 5.3.1 Energy efficiency of PV system simulation using fuzzy logic and Phase locked loop controller

The seven class two input one output fuzzy logic system simulation results are listed below. In Fig.5.20 the fuzzy output signal is shown. When the Temperature and irradiation level is change to adjust the boost converter by sending optimum duty cycles. The fuzzy system is better than the direct connections but it requires expert designer to design the fuzzy class ranges as the system wants.

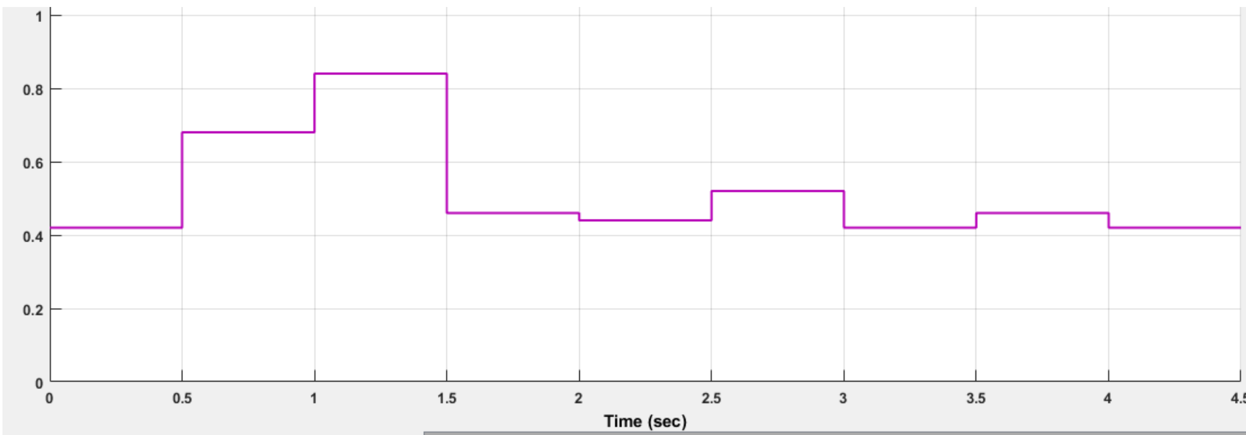


Figure 5. 20 Duty cycle signal output of FLC for different level of temperatures and irradiations

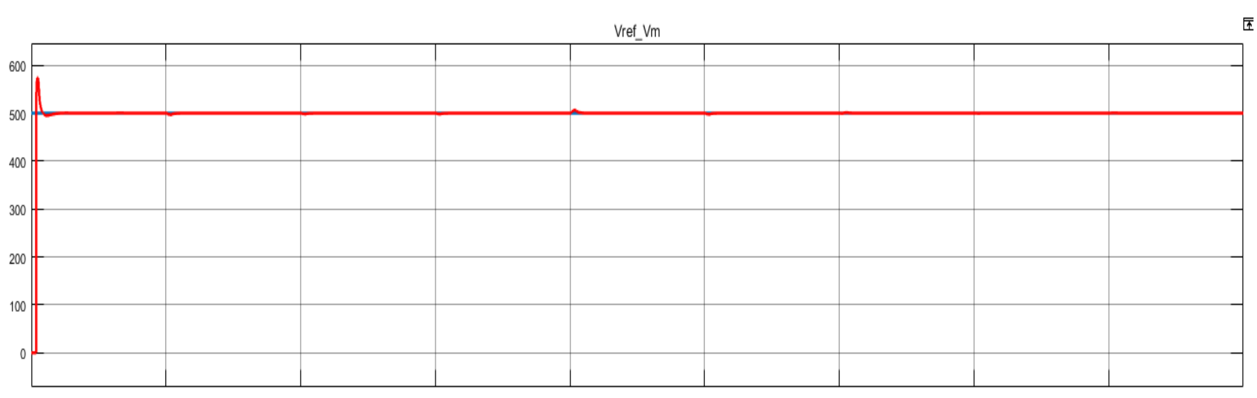


Figure 5. 21 Boost output voltage based on FLC PV systems.

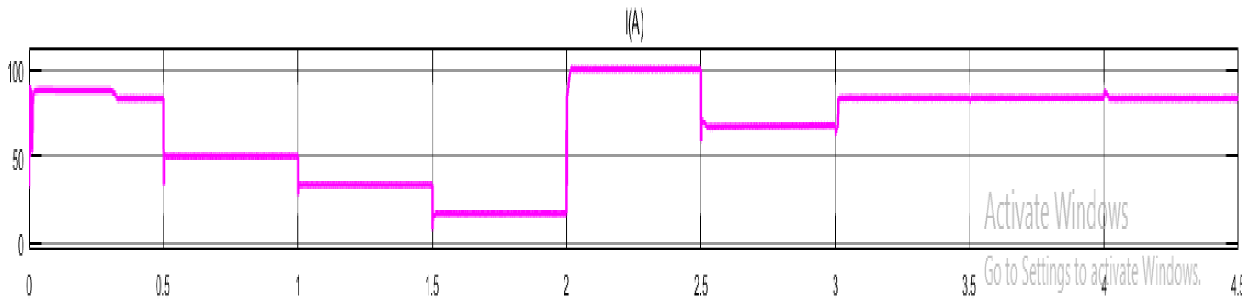


Figure 5. 22 Boost current based on FLC and Direct connection PV systems

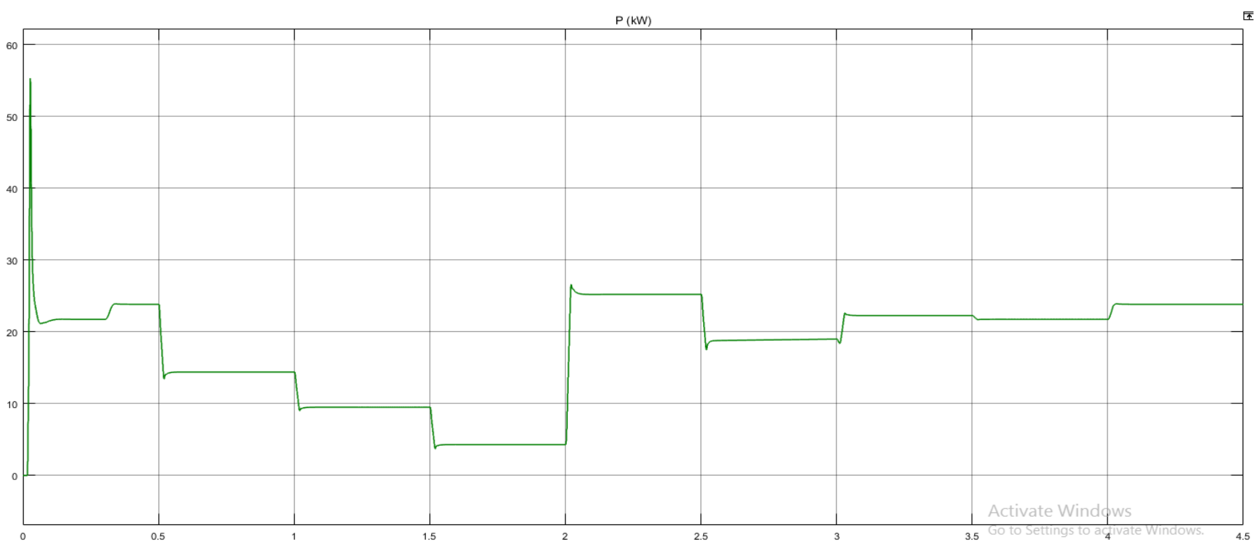


Figure 5. 23 Output power in KW based on FLC PV systems

The selection of Phase lock loop was due to its high degree of immunity and insensitivity to disturbances, harmonics, unbalance and sags. the three phase AC output voltage had some harmonic in a time of environmental changes occurred. The soft-switching region of the three-stage converter is increased with the proposed phase-locked loop leads to a reduction in the ripple content, rating of components, and switching losses. The phase-locked loop is used in the cascaded three-stage converter to extend the soft-switching region to minimize the losses.

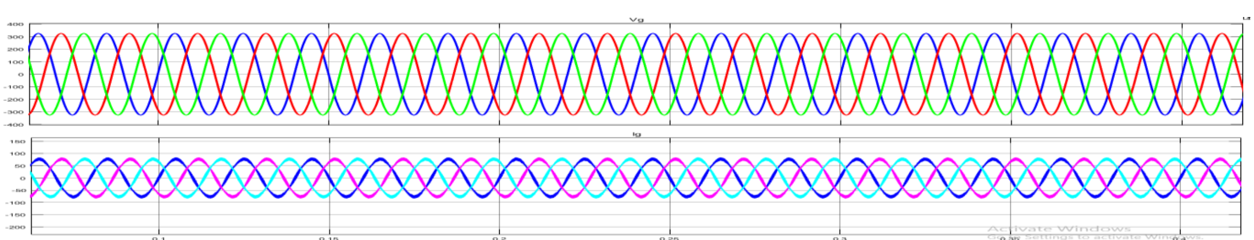

Figure 5. 24 Three phase output voltage based on PLL controller

## 5.4 Performance analysis of controllers

The analysis of the MPPT technique are carried out to show the performance of each technique in the same condition. In order to the performance of the controller in tracking of the maximum power for each controller for the same level of solar irradiation and temperature. Generally the controllers tried to track MPP,all controllers are better than direct connecting PV systems. On the other hand we have to compared the proposed MMPT controller performances with the direct connected systems. The direct system onece connected with the best or the desired output signal at the MPPT which is (**D$_{mppt}$ =0.42**) and vary the environmental conditions.

Table 5. 4 The controller output at different level of environmental condition

| Irradiation | G (W/m$^2$) | 1000 | 800 | 400 | 1000 | 1200 |
|---|---|---|---|---|---|---|
| Temperature | T(°C) | 25 | 25 | 35 | 40 | 45 |
| Direct | Calculated(D) | 0.4288 | 0.5048 | 0.7492 | 0.4416 | 0.4260 |
| | Output signal | 0.42 | 0.42 | 0.42 | 0.42 | 0.42 |
| | Error e (%) | 0.0088 | 0.0848 | 0.3292 | 0.0216 | 0.0060 |
| | Efficiency(η %) | 99.6 | 84.08 | 59.58 | 96.85 | 94.89 |
| FLC | Output signal | 0.4241 | 0.4635 | 0.7248 | 0.4370 | 0.3943 |
| | Error e (%) | 0.0047 | 0.0413 | 0.0244 | 0.0046 | 0.0317 |
| | Efficiency(η %) | 99.7 | 99.6 | 99.3 | 98.8 | 98.7 |

The output signal from the controller fed to the boost controller is used to adjust the output voltage and current , and tried to maintain the output voltage to be 500volt Dc to fed the inverter.

Table 5. 5 Performance compression of Fuzzy logic controller and direct connection

| Irradiation | G (W/m$^2$) | 1000 | 800 | 400 | 1000 | 1200 |
|---|---|---|---|---|---|---|
| Temperature | T(°C) | 25 | 25 | 35 | 40 | 45 |
| Direct | Efficiency(η %) | 99.6 | 84.08 | 59.58 | 96.85 | 94.89 |
| | Avarage Efficiency (η %) | 87 | | | | |
| FLC | Efficiency(η %) | 99.7 | 99.6 | 99.3 | 98.8 | 98.7 |
| | Avarage Efficiency (η %) | 99.2 | | | | |

# CHAPTER SIX

## CONCLUSIONS,RECOMMENDATIONS AND FUTUIRE WORKS

## 6.1 Conclusions

The cascaded converters with intelligent control techniques are developed to track the maximum power from the photovoltaic (PV) system. Mathematical model of PV array is developed and the same is used for simulation.The main focuses of this research was how to improve the total system efficiency by implementing an efficient MPPT techniques to transfer the maximum available power tothe load especially under rapidly changing atmospheric conditions which was temperature and irradiation.The thesis reviewed and discussed some existing MPPT controller methods and illustrated the advantages and disadvantages of each individual MPPT technique tracking performance and showed their ability to track the MPP under rapidly changing weather conditions. The efficient of MPPT controller proposed were analyzed and developed in more depth using system simulations to clearly show improvements. For the system which operates with MPPT based FLC the time response for tracking the MPP is faster.

The simulation results were divided into three parts for each controller algorithm to show the effect of environmental changes. In the first part the PV system is feeding a variable irradiation at standard temperature to test the performance of controller in a time of shadow occurred. Second the PV system fed both temperature and irradiation are varied and test the performance and efficiency of controller. And then make Irradiation constant and show the effect of temperature on PV output characteristics and test the effect of the controller.

The results showed that the directly connected the energy efficiency of PV system without MPPT has poor efficiency due to the mismatching between the PV array and the Ac load. Whereas, the system with the proposed MPPT techniques utilizes the available PV array energy. The proposed MPPT techniques were able to track the MPP deliver maximum power to the Grid with high efficiency under the dynamic and steady-state conditions. Based on the simulated result the efficiency have been 99.2% for FLC respectively, whereas the same without any controller is found to be 87%. So that the results confirm that the proposed MPPT methods have the potential to significantly increase the total efficiency of the PV system. The developed model is efficiently used for tracking the maximum power using FLC. The ripple content is minimized and the soft-switching regionis increased by embedding PLL. With this arrangement, better transient response is achieved and efficiency of 99.2% is obtained. The synchronizer (PLL) was connected to the system to clear disturbances on the lines. The results obtained from the simulated system are the same frequency, amplitude, and phase angle, which indicated that the designed grid-connected solar photovoltaic system have succeeded in tackling the problem of power supply in the study area.

## 6.2 Recommendations

In this work, simulation models were developed and used to the performance of the MPPT techniques and also the PLL controller. However, practical hardware tests at a representative power level and under the typical climatic conditions of an application need to be conducted to verify the simulation results. The simulation results achieved in this work will hopefully incentivize future investigations involving building prototype models to test experimentally the developed MPPT techniques and PLL controller for the energy efficiency of PV system, and the proposed controller shows better peroformance than the direct connections so it ought to apply this controller in practical maners for the energy efficiency of PV system.

## 6.3 Suggestions for future work

The ac load used in the current work is equal to the required calculated load from standard tables but for future improvement design and model an AC of PV system with its sized parameters.

In the current PV system, the boost converter is used as an interface to enable the MPPT process. Future research could investigate some other converters such as buck-boost along with the proposed MPPT techniques to improve flexibility in the choice and configuration of PV array connection. And instead of two level inverter three level inverter will smooth the output three phase voltages.

# 7. References

[1]. S. Kaur, "Clean energy with super grid!," IETE Technical Review, vol. 30, pp. 364–366, 2013.

[2]. T. Esram and P. L. Chapman, "Comparison of photovoltaic array maximum power point tracking techniques," IEEE Transactions on Energy Conversion, vol. 22, no. 2, pp. 439– 449, 2007.

[3]. M. A. G. De Brito, L. Galotto, L. P. Sampaio, G. De AzevedoMelo, and C. A. Canesin, "Evaluation of the main MPPT techniques for photovoltaic applications," IEEE Transactions on Industrial Electronics, vol. 60, no. 3, pp. 1156–1167, 2013.

[ 4]. S. Jain and V. Agarwal, "Comparison of the performance of maximum power point tracking schemes applied to single-stage grid-connected photovoltaic systems," IET Electric Power Applications, vol. 1, no. 5, pp. 753–762, 2007.

[5]. S.-T. Kim, T.-H. Bang, and S.-C. Lee, "Real-time maximum power point tracking method based on three points approximation by digital controller for PV system," Journal of Electrical Engineering and Technology, vol. 9, no. 5, pp. 1447–1453, 2014.

[6]. J. Cubas, S. Pindado, and A. Sanz-Andr ´ es, "Accurate simulation ´of MPPT methods performance when applied to commercial photovoltaic panels," *Scientific World Journal*, vol. 2015, Article ID 914212, 16 pages, 2015.

[7] .N. Femia, G. Petrone, G. Spagnuolo, and M. Vitelli, "Optimization of perturb and observe maximum power point tracking method," *IEEE Transactions on Power Electronics*, vol. 20, no.4, pp.963–973,2005.

[8]. A. K. Abdelsalam, A. M. Massoud, S. Ahmed, and P. N. Enjeti, "High-performance adaptive Perturb and observe MPPT technique for photovoltaic-based micro grids," *IEEE Transactions on Power Electronics*, vol. 26, no. 4, pp. 1010–1021, 2011.

[9]. R. Leyva, P. Artillan, C. Cabal, B. Estibals, and C. Alonso, "Dynamic performance of maximum power point tracking circuits using sinusoidal extremum seeking control for photovoltaic generation," *International Journal of Electronics*, vol. 98, no. 4, pp. 529–542, 2011.

[10] Yun Tiam Tan, Daniel S. Kirschen, and Nicholas Jenkins, “A Model based PV Generation suitable for stability analysis”, IEEE trans. on energy conv., vol.19, no.4, pp. 748-755, Dec 2004.
[11] E. Koutroulis E, K. Kalaitzakis, and NC. Voulgaris, “Development of a microcontroller based photovoltail maximum power point tracking control sytem”, IEEE trans. on Power Electronics, vol. 16, pp. 46-54, 2001.

[12] Abdulhadi Varnham, M. Abdulrahman, Al-Ibrahim, S. Gurvinder, Virk, and Djamel Azzi, “Soft computing model based controllers for increased photovoltaic plant efficiencies”, IEEE trans. on energy conv., vol. 22, no. 4, pp. 873-879, Dec. 2007.

[13] Weidong Xiao, Zeineldin, H.H., and Peng Zhang, "Statistic and Parallel Testing Procedure for Evaluating Maximum Power Point Tracking Algorithms of Photovoltaic Power Systems," Photovoltaics, IEEE Journal of , vol.3, no.3, pp.1062,1069, July 2013.

[14] X. Weidong and W. G. Dunford, "A modified adaptive hill climbing MPPT method for photovoltaic power systems," in Power Electronics Specialists Conference, PESC, /IEEE 35th Annual, 2004.

[15] T. Tafticht, et al., "A new MPPT method for photovoltaic systems used for hydrogen production," COMPEL: The International Journal for Computation and Mathematics in Electrical and Electronic Engineering, vol. 26, pp. 62-74, 2007.

[16] N. Mohan and T. M. Undeland, Power electronics: converters, applications, and design: Wiley-India, 2007. [10] H. Sira-Ramirez and R. Silva-Ortigoza, Control Design Techniques in Power Electronics Devices, Power Systems Series: Springer-Verlag London, 2006.

[17] R. F. Coelho, et al., "A study of the basic DC-DC converters applied in maximum power point tracking," in Power Electronics Conference,. COBEP '09. Brazilian, 2009.

[18] J. M. Enrique, et al., "Theoretical assessment of the maximum power point tracking efficiency of photovoltaic facilities with different converter topologies," Solar Energy, vol. 81, pp. 31-38, 2007.

[19] E. Duran, et al., "Comparative analysis of buck-boost converters used to obtain I-V characteristic curves of photovoltaic modules," in Power Electronics Specialists Conference, PESC/IEEE, pp. 2036-2042, 2008.

[20] A. Oi, "Design and simulation of photovoltaic system,"Master Thesis, California ,2009.

[21] R. C. Neville, Solar energy conversion: the solar cell: Elsevier Science, 1995.

[22] O. Ojo, P. Kshirsagar, “Concise Modulation strategies for four leg voltage source inverter,” Conference Records Power Electronics Specialists Conference, vol. 1, pp. 238243, 2002.

[23] Kjær, S. B. . Design and Control of an Inverter for Photovoltaic Applications. Aalborg Universitet: Institut for Energiteknik, Aalborg Universitet, 2005.

[24] M. L. a. C. Greenwood, "Green investing: Towards a clean energy infrastructure," World Economic Forum USA Inc, Polytechnic State University, January 2009.

[25] V. Salas, et al., "Review of the maximum power point tracking algorithms stand-alone photovoltaic systems," Solar Energy Materials and Solar Cells, vol. 90, pp. 1555-1578, 2006.

[26] W. Xiao, "A modified adaptive hill climbing maximum power point tracking (MPPT) control method for photovoltaic power systems," Master Thesis The University of British Columbia, 2003.

[27] M. veerachary, et al., "Feedforward maximum power point tracking of PV systems using fuzzy controller," Aerospace and Electronic Systems, /IEEE Transactions on, vol. 38, pp. 969-981, 2002.

[28] Mohamed E. El Telbany, Ayman Youssef, Electronics Research Institution Computer and Systems Department, 4th International Conference on Artificial Intelligence with Applications in Engineering and Technology, 2014.

[29] S. A. Kalogirou, "Artificial intelligence for the modeling and control of combustion processes: a review," Progress in Energy and Combustion Science, vol. 29, pp. 515-566, 2003.

[30] M. Figueiredo and F. Gomide; "Design of Fuzzy Systems ", /IEEE Transactions on Neural Networks, Vol. 10, no. 4, pp.815-827, 1999.

[31] N. Argaw, R. Foster and A. Ellis Renewable Energy of pv system ,Applications in Rural, National Renewable Energy Laboratory, Villages, pp.19-26, July 2003.

[32] H. Pollock and J. Flower, “New-method of power control for series-parallel load resonant converters maintaining zero-current switching and unity power factor,” /IEEE Transactions on Power Electronics, vol. 12, no.1, pp. 103-115, January 1997.

[33] Fathi A O Aashoor A thesis submitted for the degree of Doctor of Philosophy Department of Electronic and Electrical Engineering University of Bath, May 2015.

[34] B. Wittig, W.-T. Franke, F.W. Fuchs Institute of Power Electronics and Electrical Drives Christian-Albrechts-University of Kiel, D-24143 Kiel, Germany, 2007.

[35] Professor, Ph.D., Frede Blaabjerg (IET), Associate Professor John K. Pedersen (IET), Aalborg University Institute of Energy Technology, , pp.30, August 2005.

[36] Utility aspects of grid connected photovoltaic power systems, International energy agency – photovoltaic power systems programme, IEA PVPS T5-01, 1998,

[37] M. Liserre, F. Blaabjerg, S. Hansen, Design and control of an LCL-filter based threephase active rectifier, /IEEE proc. of the 36th annual industry application conference vol. 1, pp. 299-307, 2001.

[38] H. Knopf, "Analysis, Simulation, and evaluation of maximum power point tracking (MPPT) methods for a solar powered vehicle," Master Thesis, Portland State University, 1999.

[39] Rashid, M. H. Pulse-Width-Modulation Inverters. Upper Saddle River, NJ: PrenticeHall, pp. 237–248, 2004.

[40] R. J. Machado and A. Freitas da Rocha, "A hybrid architecture for fuzzy connectionist expert systems," in Hybrid architectures for intelligent systems, 1992.

[41] Y. Bai, et al., Advanced fuzzy logic technologies in industrial applications: Springer, 2007.

[42] M. Mobaied, "Fuzzy Logic Speed Controllers Using FPGA Technique for Three-Phase Induction Motor Drives," Master Thesis, The Islamic University– Gaza, 2008.

[43] N. S. D'Souza, "Variable perturbation size maximum power point tracking algorithms for photovoltaic systems," Master Thesis, Concordia University, 2006.

[44] I. Iancu, "A Mamdani type fuzzy logic controller," Fuzzy Logic: Controls, Concepts, Theories and Applications, InTech Croatia, Rijeka, pp. 55-54, 2012.

[45] Limkumnerd, S., & Eungdamrong, D. (2007). Mathematical models and simulations of phase noise in phase-locked loops, (February 2007).

[46] Natsheh, E. M., Albarbar, A., & Yazdani, J. (2009). Modeling and Control for Smart Grid Integration of Solar System. Modeling and Control for Smart Grid Integration of Solar/Wind Energy Conversion System, 1–8.

[47] Rafal, K., Jasinski, M., & Kazmierkowski, M. P. (2011). Grid synchronization and symmetrical components extraction with PLL algorithm for grid connected power electronic converters – a review, 59(4). http://doi.org/10.2478/v10175-011-0060-8

# APPENDIX A

## A.1 MATLAB functions and scripts of PV panel

### A.1.1 MATLAB Function of the module specifications

```
%PV panel parameters
Voc=32.9;
Isc=8.21;
Vmp=26.3; % maximum voltage of a module at MPPT
Imp=7.61;  % maximum current of a module at MPPT
Ki=0.0032;
Kv=-0.65;
q=1.6e-19;
K=1.3805e-23;
n=1.3;
Rs=0.221;
Rsh=415.405;
Gn=1000;                % nominal irradation at STD
Tn=298.15;              % nominal temperature
ns=54;                  % no of series cells in a module
np=1;                   % parallel cells in a module
Ns=11;                  %no of series module in a strings
Np=11;                  %n no of parallel strings in an array
Rl=10.3,                % load resistance in a module
Ts=1e-06;               %setling time
Vmpv=Vmp*Ns; % maximum voltage of the PV panel at MPPT
Impv=Imp*Np;  % maximum current ofthe PV panel at MPPT
P_max_panel=Vmpv*Impv;
% Boost converter parameters
Sfb=20000;          % swiching frequence of the PWM generator
V_boost_out=500;        % required boost converter output voltage
I_boost_out=P_max_panel/V_boost_out;    % expected output current of the
boost cnvertor
Vin_max=289.3; % maximum output voltage of the PV array
Vinmax =Vpv at STD Vin_min=100; % expected minimum PV output voltage
out_rI=0.4*I_boost_out*(V_boost_out/Vin_max);    % output repple current
D=1-(Vin_max/V_boost_out)*n;% duty cycle ration t STU
Lb=(Vin_min*D)/(out_rI*Sfb);    %boost converter inductor value
Cb=(I_boost_out*d)/(out_rV*Sfb);    % boost converter capasitor value
RLd=V_boost_out/I_boost_out;  %load resistor
%Invertor parameters
I_inv=48;               % invertor current
V_inv=300;
fn=50;                  % signale generated index frequency
fs=50*33;               % swiching frequence of the 2 leve PWM generator
M=0.84;                 % modulation index
inv_out_rI=0.15*I_inv; %inverter output repple current is up to 15% of the
invertor rated current
P_inv=300*48;                     %invertor rated power
```

```
% LCL Filter parameters
r=0.8;                          %ratio of invertor side and load side inductors
L_inv=V_boost_out/(16*fs*inv_out_rI);   % inverter side three phase inductor
L_Lo=r*L_inv;                     % load side three phase inductor
Pi=3.14;
cb=P_inv/(2*pi*fn*V_inv^2);       % base capacitor
Cf=0.2*cb;                       %filter capacitor
fo=(1/2*pi)*sqrt((L_inv+L_Lo)/(L_Lo*L_inv*Cf)); % resonant freqeuncy
Rd= 1/(3*2*pi*fo*Cf);          %Damping resistance
% FLC parameters
Gi=0.003122;               % current scalling factor
Gv=0.14517;                 % Voltage scalling factor
GD=1;                  % duity ratio scalling factor
```

# APPENDIX B

## B.1 MATLAB simulation of the PV system

```
%PV module of saturation current
```

$$Is = Irs.\left(\frac{T}{Tn}\right)^3.\exp\left[\frac{q.Ego}{n.k}\left(\frac{1}{Tn}-\frac{1}{T}\right)\right]$$

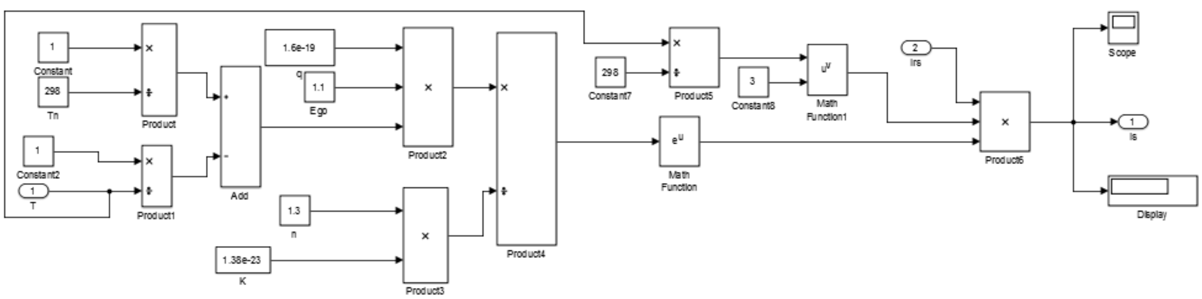


Figure B. 1 simulink model of saturation current

```
%PV module of Reverse saturation current
```

$$Irs = \frac{Isc}{[\exp(\frac{q.Voc}{n.Ns.K.T})-1]}$$

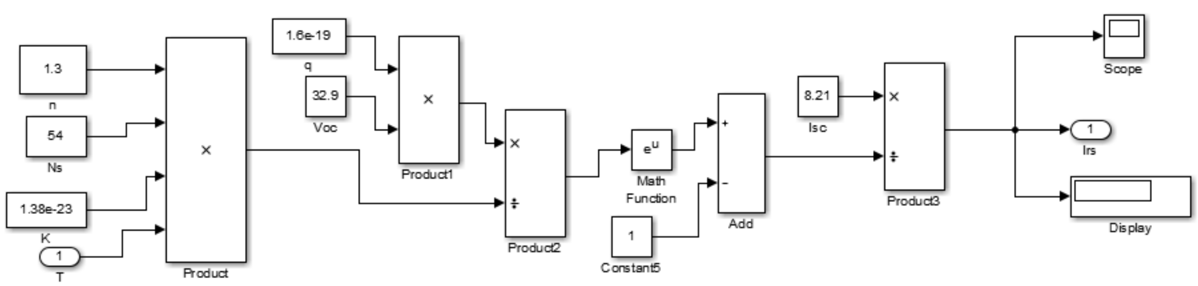


Figure B. 2 simulink model of Reverse saturation current

```
%PV module of photo current
```

$$Iph = [Ip'n + Ki(T - Tn)]\frac{G}{Gn}$$

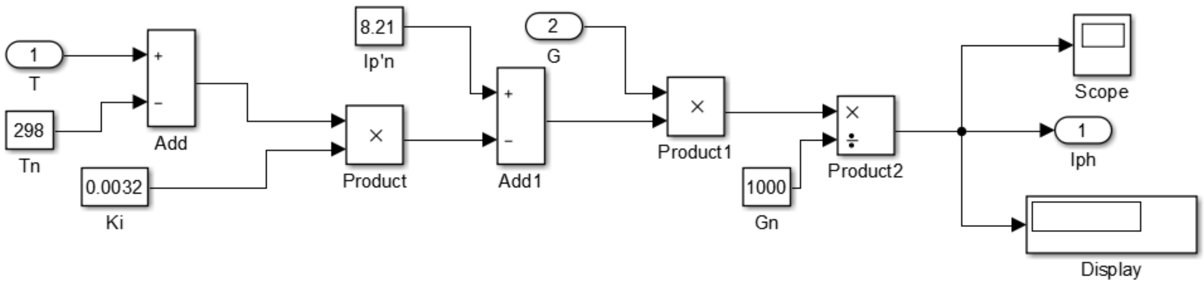


Figure B. 3 simulink model of photo current

```
%PV module of shunt current
```

$$Iph,n = (\frac{v+Rs*Isc,n}{Rsh})\frac{N's}{N's}$$

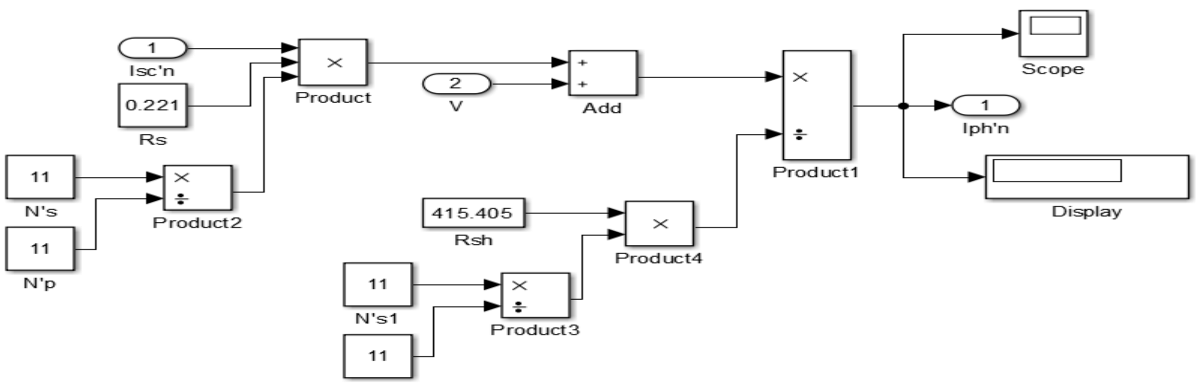


Figure B. 4 simulink model of shunt current

```
%PV module of PV current
```

$$Ipv = Iph - Is\left[exp^{(\frac{q(Vpv+Ipv.Rs))}{n.k.T}} - 1\right] - \left[\frac{Vpv+Ipv\times Rs}{Rsh}\right][\frac{N's}{N'p}]$$

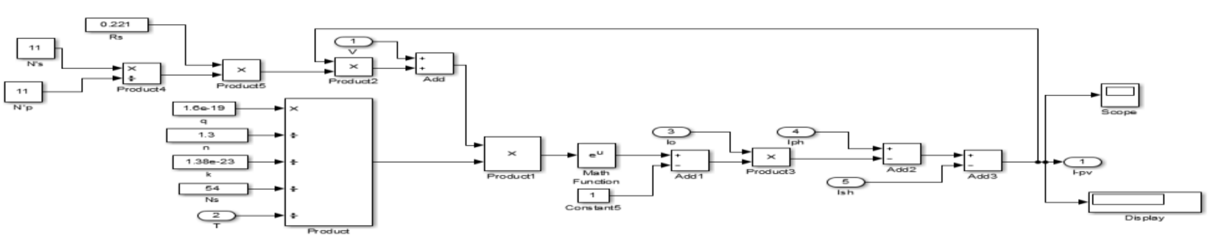

Figure B. 5 simulink model of pv-current

# APPENDIX C

## C.1 Artificial Intelligent MPPT Controllers MATLAB Simulation

### C.1.1 FIS of FLC based MPPT of Energy efficiency of PV system MATLAB SIMULINK

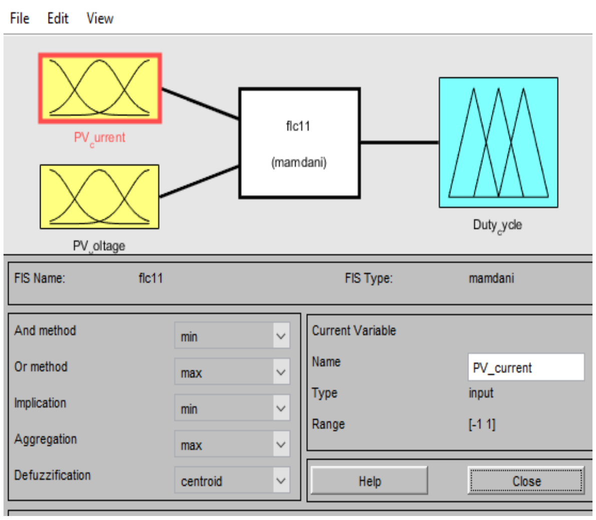


Figure C. 1 FIS editor

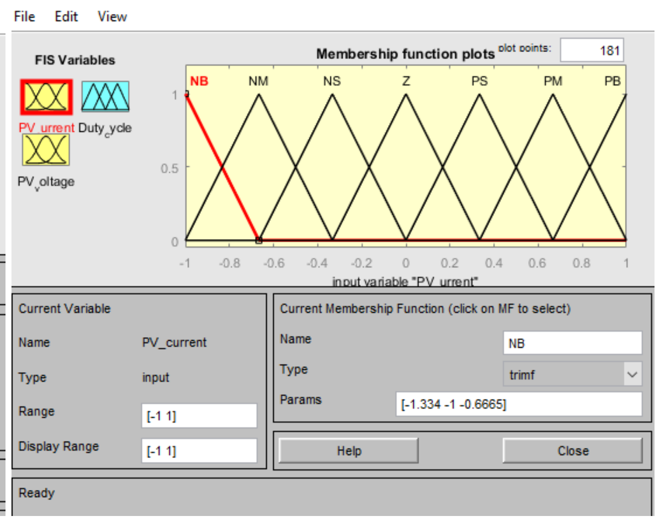


Figure C. 2 membership function editor in put varable PV current(dIpv)

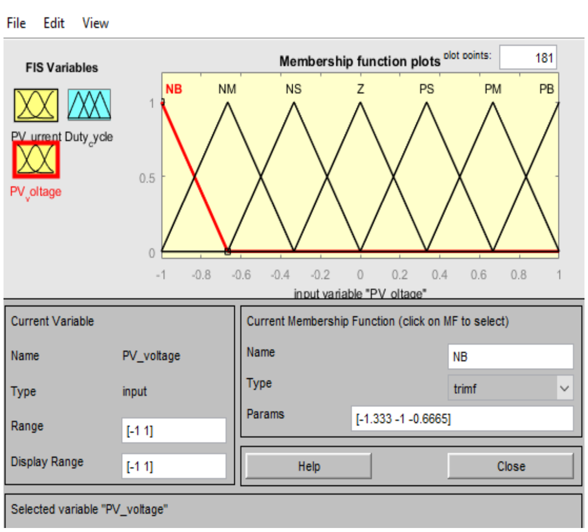


Figure C. 3 membership function editor in put put varable PV voltage(dVpv)

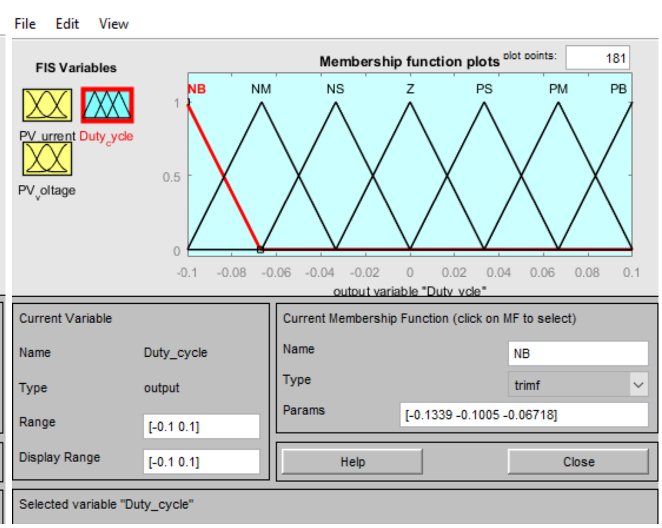


Figure C. 4 membership function editor out varable duty cycle(D)

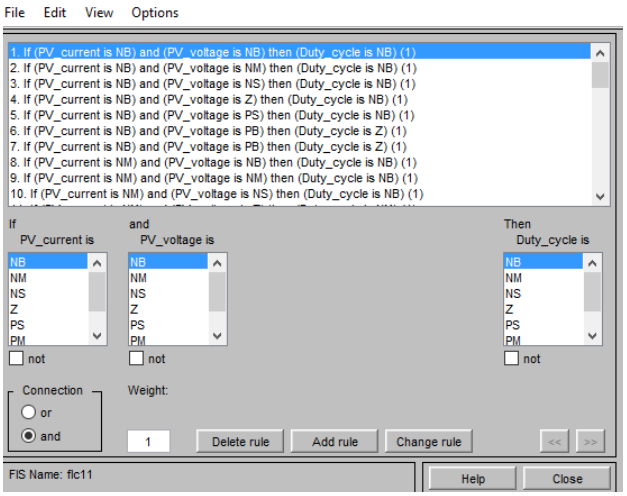


Figure C. 5 Rule- base editor

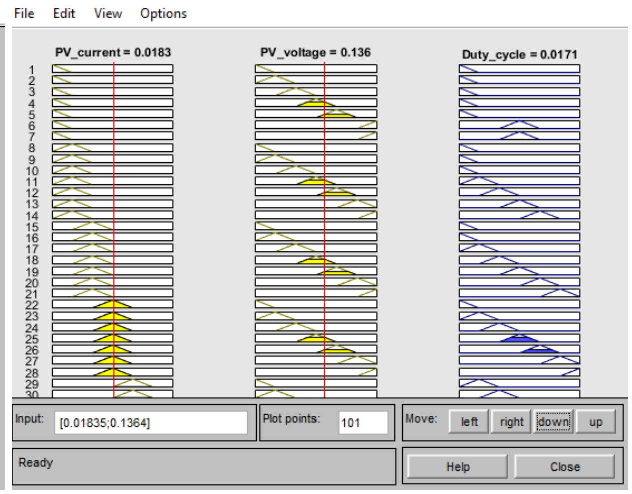


Figure C. 6 Rule viewer

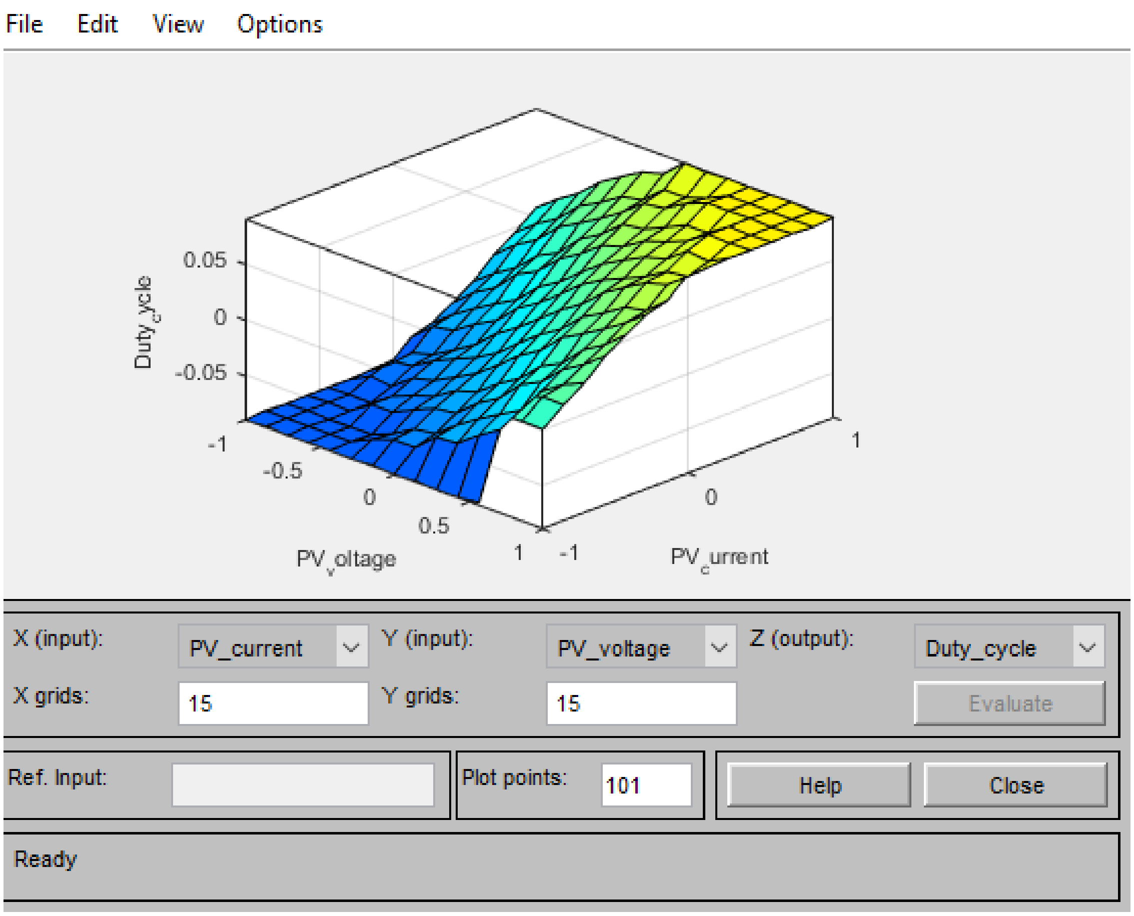


Figure C. 7 3D surface viewer

# APPENDIX D

## D.1 Artificial Intelligent Fuzzy controller Data From Pv Panel.

Table D.1. 1 The data set collected for Fuzzy logic controller

| Ambient Temperature (C) | Solar Insulation (W/m2) | PV Array Current (A) | PV Array Voltage (V) | PV Array Powerr(W) | Duty Ratio (D) |
|---|---|---|---|---|---|
| 25 | 1200 | 87.78 | 307.2 | 27,040 | 0.3856 |
| 25 | 1000 | 83,02 | 290.6 | 24,220 | 0.4288 |
| 25 | 800 | 70.74 | 247.6 | 17,580 | 0.5048 |
| 25 | 600 | 53.48 | 187.2 | 10,060 | 0.6256 |
| 25 | 400 | 35.84 | 125.4 | 4,496 | 0.7492 |
| 25 | 200 | 18.01 | 63.03 | 1,135 | 0.87394 |
| 30 | 1200 | 86.36 | 302.2 | 26,530 | 0.3956 |
| 30 | 1000 | 82 | 287.1 | 23,640 | 0.4258 |
| 30 | 800 | 70.79 | 247.8 | 17,600 | 0.5044 |
| 30 | 600 | 53.64 | 187.7 | 10,070 | 0.6246 |
| 30 | 400 | 35.95 | 125.8 | 4,522 | 0.7484 |
| 30 | 200 | 18.06 | 63.22 | 1,142 | 0.84356 |
| 35 | 1200 | 84.92 | 297.2 | 25,240 | 0.4056 |
| 35 | 1000 | 80.9 | 283.3 | 22,920 | 0.4334 |
| 35 | 800 | 70.75 | 247.7 | 17,520 | 0.5046 |
| 35 | 600 | 53.8 | 188.3 | 10,130 | 0.6234 |
| 35 | 400 | 36.05 | 126.2 | 4,549 | 0.7476 |
| 35 | 200 | 18.11 | 63.41 | 1,164 | 0.87318 |
| 40 | 1200 | 83.47 | 292.1 | 24,460 | 0.4158 |
| 40 | 1000 | 79.76 | 279.2 | 22,340 | 0.4416 |
| 40 | 800 | 70.62 | 247.1 | 17,450 | 0.5058 |
| 40 | 600 | 53.95 | 188.8 | 10,190 | 0.6224 |
| 40 | 400 | 36.16 | 126.6 | 4,576 | 0.7468 |

| | | | | | |
|---|---|---|---|---|---|
| 40 | 200 | 18.17 | 63.6 | 1,156 | 0.8428 |
| 45 | 1200 | 81.99 | 287 | 23,530 | 0.426 |
| 45 | 1000 | 78.56 | 274.9 | 21,590 | 0.4502 |
| 45 | 800 | 70.8 | 248.3 | 17,550 | 0.5034 |
| 45 | 600 | 54.1 | 189.3 | 10,240 | 0.6214 |
| 45 | 400 | 36.27 | 126.9 | 4,603 | 0.7462 |
| 45 | 200 | 18.22 | 63.79 | 1,163 | 0.84242 |
| 50 | 1200 | 80.51 | 281.8 | 22,820 | 0.4364 |
| 50 | 1000 | 77.27 | 270.5 | 20,900 | 0.459 |
| 50 | 800 | 69.89 | 244.6 | 17,090 | 0.5108 |
| 50 | 600 | 54.25 | 189.8 | 10,290 | 0.6204 |
| 50 | 400 | 36.37 | 127.3 | 4,631 | 0.7454 |
| 50 | 200 | 18.29 | 63.98 | 1,184 | 0.84204 |